Proceedings of a symposium sponsored by the Division of Industrial and Engineering Chemistry of the American Chemical Society.

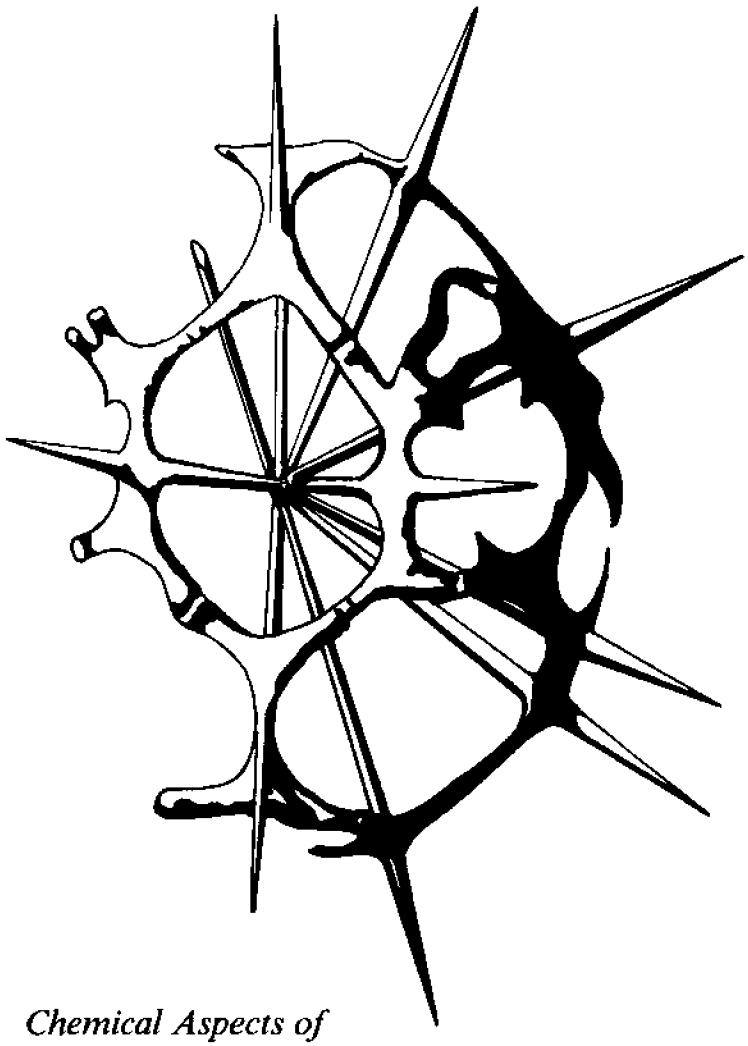

Chemical Aspects of

Regulation of Mineralization

Edited by C. Steven Sikes and A.P. Wheeler

Chemical Aspects of

Regulation of Mineralization

Proceedings of a symposium sponsored by the Division of Industrial and Engineering Chemistry of the American Chemical Society held in New Orleans, September 3-4, 1987.

Editors: C. Steven Sikes and A.P. Wheeler

Administrative Assistant: Jerelyn B. Cox

Library of Congress Catalog Number: 88-51819.

Cosponsors: Mississippi-Alabama Sea Grant Consortium and The Coastal Research and Development Institute of The University of South Alabama

The purpose of the symposium was to provide a forum within a major scientific society for research in academia, government, and industry to discuss recent results within the field of mineralization. Each of the 14 papers in the symposium involved in one way or another the interactions between a mineral phase and organic substances that may regulate the formation of the mineral phase. Minerals considered were principally carbonates, phosphates, and silica. The investigators chose topics that would be described as either basic or applied research. One message that resulted from the symposium was that there often is no clear distinction between basic and applied research.

An additional result was general agreement to hold other symposia at future ACS meetings. The next symposium is scheduled for the ACS annual meeting in April 1989 in Dallas. This symposium is titled, "Surface Reactive Peptides and Polymers", and will include 28 invited presentations about topics ranging from regulation of crystallization to regulation of growth of cells.

Cover: Skeleton of an acantharian, a marine protozoan (pg. 46).

University of South Alabama Publication Services, 1988

MASGP-87-049

This work is a result of research sponsored in part by NOAA, National Sea Grant College Program, U.S. Department of Commerce under Grant #NA85AA-D-SG005, the Mississippi-Alabama Sea Grant Consortium and the University of South Alabama are authorized to produce and distribute reprints for information and governmental purposes notwithstanding any copyright notation that may appear hereon.

CONTENTS

Chemical Aspects of Regulation of Mineralization. C.S. Sikes and A.P. Wheeler, editors, University of South Alabama Publication Services, Mobile, Alabama, 1988.

Physical-Chemical Mechanisms That Affect Regulation of Crystallization

M.M. Reddy

U.S. Geological Survey, Mail Stop 408, Denver Federal Center, Lakewood, Colorado 80225

ABSTRACT

Minerals of biological and geological importance commonly exist as more than one polymorph or hydrate; crystallization of these minerals and polymorphs may have different pathways or mechanisms. Processes by which organisms form minerals can be complicated by the variety of mineral polymorphs and hydrates that may form, transform, and subsequently dissolve during a mineralization reaction and by the presence of the original mineral phase. Rates and mechanisms of mineral formation and transformation are regulated by conditions in solution and at the solution-mineral interface. Thermodynamic factors, such as solution pH, mineral-phase supersaturation, ionic strength, temperature, and the extent of ion association, regulate crystallization. In addition, crystallization processes also may be regulated by the kinetics of the crystallization reaction, which indicates an interfacial rate-determining step. In the example of calcium carbonate, depending on conditions, precipitation from a supersaturated solution results in a variety of mineral polymorphs and hydrates that have varying thermodynamic stabilities and reactivities. When a solution is only slightly supersaturated several common inorganic and simple organic ions decrease the calcite-seeded-crystallization rate. This rate decrease follows a Langmuir adsorption isotherm indicating that the mechanism of this process involves adsorption of these ions at growth sites on the crystal surface.

Introduction

In biological (Wheeler and Sikes 1984; Bills 1985; Lowenstam and Weiner 1985), geological (Spencer *et al.* 1985), environmental and technical processes (Reddy 1978) mineral crystallization has important consequences. However, an area of uncertainty in applying crystal-growth theory to processes occurring in these disciplines is that the crystallization mechanism may not be well characterized. Even though the number of possible mineral phases that will form from a supersaturated solution may be few, several different polymorphs may form, transform, and subsequently dissolve during precipitation. The potential for a variety of different solid phases forming simultaneously or consecutively from a supersaturated solution complicates the interpretation of precipitation data and the description of crystallization mechanisms. Nielsen and Christofferson (1982) propose that the most appropriate way to study and understand mineral formation in solution is by using kinetic techniques. They suggest that insight into mineral-crystallization mechanisms is best developed by a comparison of empirical rate laws and absolute reaction rates with theoretical considerations derived from well-developed hypotheses.

Nancollas (1982) has reported that mixed mineral phases may be caused by formation of one phase on another in metastable, supersaturated solutions. In other mineral systems, a sequence of unstable polymorphs form and subsequently transform in a supersaturated solution (Bills 1985; Lowenstam and Weiner 1985; Ogino *et al.* 1987). For example, for the precipitation of calcium phosphate minerals at ambient temperatures, different calcium phosphate phases (arranged in order of increasing solubility: hydroxyapatite, tricalcium phosphate, octacalcium phosphate, and dicalcium phosphate dihydrate) may form depending on the degree of supersaturation, ionic medium, and pH (Amjad 1987). Slow formation rates for hydroxyapatite cause the formation of less stable polymorphs, such as dicalcium phosphate dihydrate, during spontaneous precipitation of calcium phosphate minerals under physiological conditions. In the example of calcium carbonate, calcite is the stable phase at ambient temperature and pressure, but other less stable polymorphs, such as aragonite, may remain unaltered for extended intervals. Mineralization in biological systems also may involve complex organic matrix-mineral interactions that may affect mineral form and reaction kinetics (Wheeler and Sikes 1984).

Calcium carbonate is a common constituent of hard tissues of many biological organisms, geological materials and sediments in freshwater and saltwater. Because of its presence and importance in these media, the equilibria and kinetics of the heterogeneous reactions of calcium carbonate in aqueous solutions have received extensive study (see for example Reddy and Wang 1980 and references therein). However, many kinetic studies have used solutions of much greater supersaturation than those typical of biological or geological environments; therefore results from such investigations may not be directly applicable to natural mineralization reactions.

This paper presents descriptions of the mechanisms that regulate mineral crystallization and illustrate these mechanisms using specific examples from studies of calcium carbonate. The focus of the experimental results presented will be on mineral-reaction kinetic data obtained in the author's laboratory. A brief discussion of the procedures used to characterize solution composition is presented based on a thermodynamic-solution model. Precipitation reactions in moderately supersaturated and supersaturated solutions, the mechanism of calcium carbonate (calcite) seeded crystallization from a metastable solution, and the effect of inhibitor ions on the rates and mechanism of calcite growth onto seed-crystal surfaces will be reviewed.

Factors Affecting Crystallization Mechanisms

Lattice-ion concentrations in solution substantially affect crystallization mechanisms. The lattice-ion concentrations typically are calculated from measured total-solution concentrations taking into account ion-association and acid-dissociation reactions, and activity-coefficient terms. Typical thermodynamic data used in the calculation of solution composition are presented in Table 1 for the solubility of calcite at 25 degrees Celsius, the solubility of carbon dioxide in water, the dissociation of carbonic acid, the dissociation of calcium carbonate and calcium bicarbonate ion pairs, and the dissociation of water. In the quantitative analysis of data from crystal growth experiments and calculation of supersaturation values, it is important to consider ion pairs as well as unassociated ions. For example,

a calcite-seeded-growth experiment containing a total calcium concentration of 2.6×10^{-4} mole per liter and a total inorganic carbon concentration of 42×10^{-4} mole per liter has substantial concentrations of the calcium carbonate (0.308×10^{-4} moles per liter) and the calcium bicarbonate (0.122×10^{-4} moles per liter) ion pairs (Reddy 1977).

Table 1. Thermodynamic constants at 25° Celcius for the sytem $CaCO_3$ - CO_2 - H_2O

Reaction	log K	Source
$CaCO_3$ (Calcite) = $Ca^{2+} + CO_3^{2-}$	-8.475	Jacobson and Langmuir (1974)
$CO_2 + H_2O = H_2CO_3^*$	-1.466	Harned and Davis (1943)
$H_2CO_3^* = H^+ + HCO_3^-$	-6.351	Harned and Davis (1943)
$HCO_3^- = H^+ + CO_3^{2-}$	-10.330	Harned and Scholes (1941)
$CaHCO_3^+ = Ca^{2+} + HCO_3^-$	-1.015	Jacobson and Langmuir (1974)
$CaCO_3^0 = Ca^{2+} + CO_3^{2-}$	-3.135	Reardon and Langmuir (1974)
$H_2O = H^+ + OH^-$	-14.000	Helgeson (1969)

Solution Supersaturation

Mineral solubility (in convenient units of concentration) plotted as a function of temperature may be divided into zones that are above and below the saturation-concentration curve. In this type of plot (Figure 1), the equilibrium concentration (i.e., the solubility), the subsaturated-solution zone and the supersaturated-solution zone of a thermodynamically stable mineral can be schematically shown as a function of temperature. The solubility of other thermodynamically less stable and, hence, more soluble polymorphic forms of the mineral also can be shown on such a plot. As shown in Figure 1, the polymorphic solubilities decrease as follows: thermodynamically stable phase < unstable anhydrous phase < unstable hydrate phase < unstable amorphous phase.

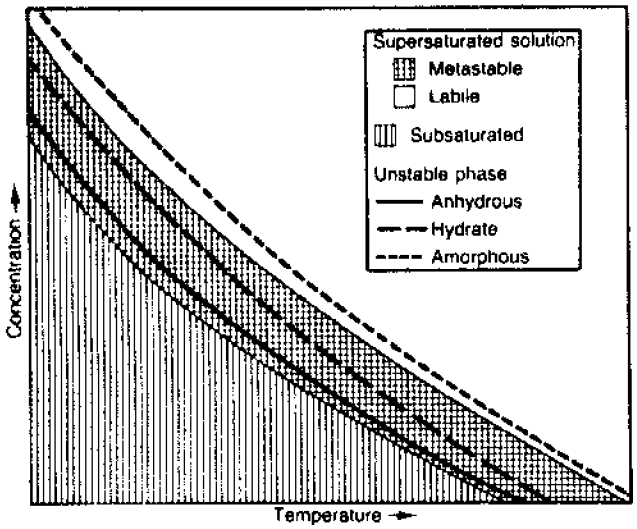

Figure 1. Schematic diagram of dissolved mineral concentration and saturation concentration plotted as a function of temperature (modified from Nancollas and Reddy 1974). Mineral subsaturated- and supersaturated-solution zones in this diagram are defined by the mineral saturation concentration curve. Steady-state solubility saturation concentration curves are shown for three thermodynamically unstable phases of the mineral. The supersaturated-solution zone is further divided into subzones of metastable and labile supersaturated solutions, determined by the induction interval as described in the text.

In the example of calcium carbonate, the thermodynamically stable phase is calcite, and there are two unstable anhydrous phases – aragonite and vaterite. In addition, there are two unstable hydrate phases – calcium carbonate monohydrate and calcium carbonate hexahydrate – and one reported amorphous phase.

Below the saturation-concentration curve in Figure 1 solutions are subsaturated solutions; that is, mineral crystals placed in solutions of this composition will dissolve. Solutions that have a composition on the saturation-concentration curve are in equilibrium, and mineral crystals placed in this solution remain unchanged. If the solution composition is above the saturation-concentration curve shown in Figure 1, the composition is within the supersaturated-solution zone, and mineral will eventually form on crystals placed in this solution.

Supersaturation, Ω_c, is defined as the ion-activity product (i.e. IAP) of the lattice ions of the mineral divided by the thermodynamic solubility product of the mineral (i.e., K_{sp}):

$$\Omega_c = IAP/K_{sp}. \qquad (1)$$

Supersaturation values are of major importance in defining the pathway or mechanism of precipitation reactions in the absence of a solid mineral.

The solution-supersaturation zone is divided into two operational subzones that reflect the time interval required to form a solid phase in solution. These two subzones consist of: 1) metastable supersaturated solutions, and 2) labile supersaturated solutions (Figure 1). In metastable supersaturated solutions, which have supersaturation values less than about 10 in the case of calcium carbonate, nucleation, in the absence of seed crystals, of the stable phase does not occur for extended time intervals (as long as several days in some instances). In labile supersaturated solutions, which have supersaturation values greater than about 20 in the case of calcium carbonate, nucleation occurs within a well-defined time interval during solution formation or shortly thereafter. This well-defined time interval, t_i, is called the induction interval, which can vary from a few seconds to a few hours.

Metastable supersaturated solutions of calcium carbonate can be prepared with small supersaturation values; these solutions are stable for 24 hours or longer. As illustrated in Figure 2 for a metastable supersaturated solution, crystal growth will not commence unless seed crystals are added. In the absence of inhibiting ions, labile supersaturated solutions of calcium carbonate with supersaturation values greater than 100 nucleate within a few seconds, usually during the time of mixing.

Nucleation

Nucleation processes illustrated in Figure 2 generally occur when supersaturation values are greater than about 20. Characteristic values of supersaturation that can be used to measure induction intervals vary among minerals; for calcium carbonate, induction intervals can be measured for supersaturation values that range from about 20 to about 80. A summary of data for calcium carbonate nucleation experiments is shown in Figure 3; particle number, the number of particles formed in

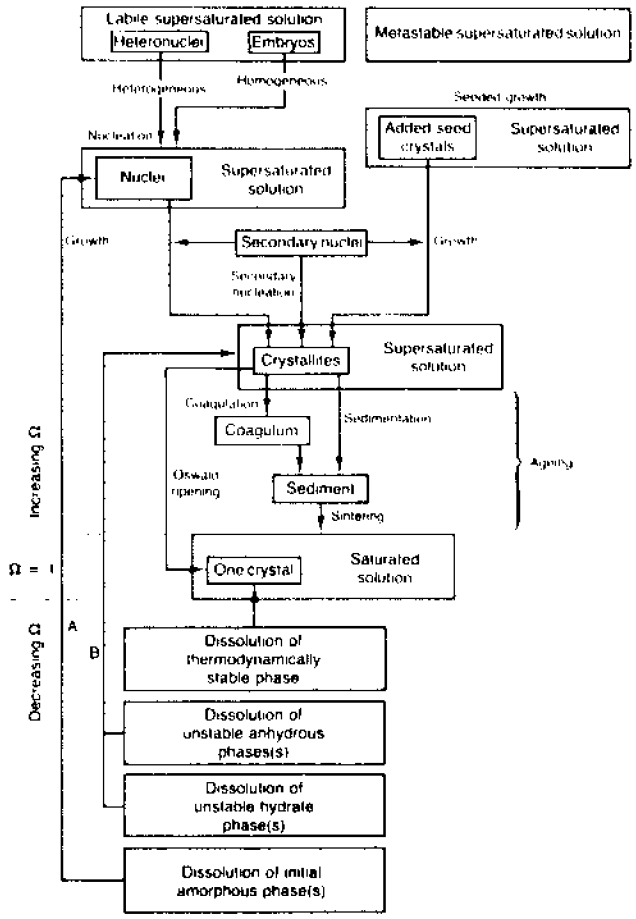

Figure 2. Pathways of mineral formation, transformation, and dissolution in aqueous solutions (modified from Nancollas and Reddy 1974). This diagram is for a hypothetical thermodynamically stable mineral that has three unstable phases that increase in solubility as follows (1) anhydrous phase, (2) hydrate phase, and (3) amorphous phase. As shown in Figure 1, the solubility of the unstable amorphous phase is within the labile-supersaturated-solution subzone; thus, nucleation of the stable phase can occur in solutions containing this phase. The unstable anhydrous and hydrate phases have lesser solubility than the amorphous phase; thus, nucleation of the stable phase does not occur readily in solutions containing these phases.

each milliliter of solution (Figure 3A), and induction interval, in minutes (Figure 3B), are plotted as a function of supersaturation. Scatter in the particle-number and induction-interval results is caused by heterogeneous nucleation on the walls of the reaction vessel and on submicrometer size particulates present in solution. Nucleation rates, expressed as the number of particles produced per milliliter per minute also can be used to evaluate calcium carbonate formation. At less than a critical supersaturation value (a supersaturation value of about 10 for the data shown in Figure 3) nucleation rates are slow.

Calcium carbonate nucleation experiments may not clearly identify processes (that is a direct path in Figure 2 from the supersaturated solution to the solution at equilibrium) that regulate crystal growth. This is difficult because there commonly are one or more unstable phases that form in the initial supersaturated solutions. For calcium carbonate precipitation several investigators (Reddy and Nancollas 1976; Reddy 1986; Ogino *et al.* 1987) have examined the initially formed calcium carbonate precipitate. Scanning-electron-microscopic examination of the initial

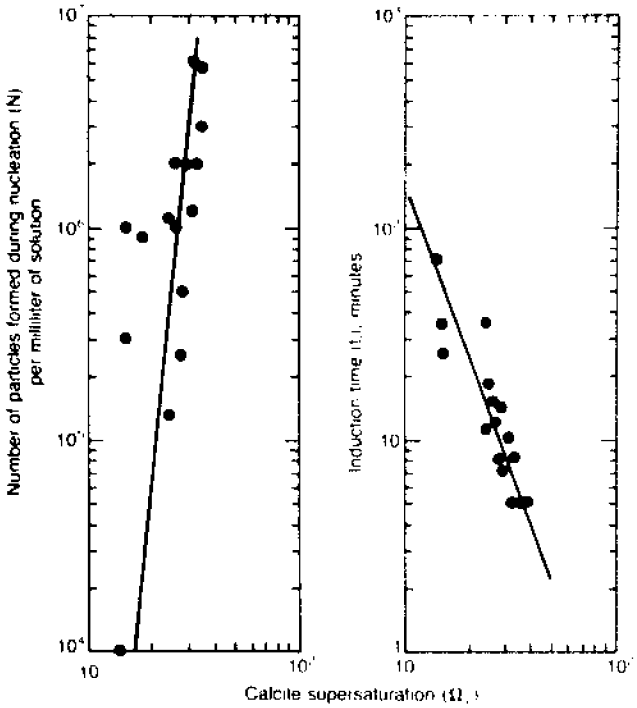

Figure 3. Calcium carbonate nucleation expressed as, A, the number of particles formed during nucleation per milliliter of solution plotted as a function of the supersaturation values of calcite; and B, the induction interval, in minutes, plotted as a function of supersaturation values of calcite (Reddy 1986).

precipitate indicates spherical particles with diameters that range from several tenths of a micrometer to as much as 1 micrometer (Reddy 1986). X-ray diffraction and optical-microscopy measurements indicate that this material is amorphous calcium carbonate.

Ogino *et al.* (1987) recently have published a careful investigation of calcium carbonate precipitation processes in supersaturated solutions. They have identified an amorphous calcium carbonate, that has a solubility product of approximately 10^{-6} (mole per liter)^2, which forms during rapid precipitation from supersaturated solutions and subsequently transforms to a mixture of crystalline polymorphs within minutes. Specifically, this amorphous calcium carbonate transforms either to the unstable polymorphs of vaterite (at low temperatures) and aragonite (at high temperatures) or to calcite; both polymorphs transform to calcite through a dissolution-reprecipitation mechanism. The rate determining step in the dissolution-reprecipitation process is the growth of calcite crystals.

Crystallization

In contrast to spontaneous precipitation experiments, which investigate nucleation and crystal-growth mechanisms in combination (Figure 2), the crystallization mechanism alone can be studied using a seeded-crystal-growth technique (Reddy 1983). During a seeded-growth-experiment, seed crystals are placed in a metastable supersaturated solution. These seed crystals grow at a rate defined by the solution composition. Spontaneous precipitation in solution is avoided; the incorporation of growth units on a crystal surface and the effect of additive ions on the reaction rate can be reproducibly measured.

Calcite seed crystals used in selected seeded-crystal-growth experiments are about 10 micrometers on the edge, and are aged in a seed suspension prior to use (Reddy and Gaillard 1981). Most calcite seed crystals used in experiments described here have uniform surfaces, and are free of irregularities. After addition of the seed crystals to the supersaturated solution, there are changes in the surface morphology of the seed crystals that correspond to new crystal growth (Reddy and Gaillard 1981).

Seeded-crystal-growth experiments can be used to identify interfacial-rate-determining processes, and the effect of additive substances on the crystallization mechanisms. Conditions for a typical calcite seeded-crystal-growth experiment discussed here were: temperature, 25 degrees Celsius; pH, 8.72; total calcium concentration, about 2.6×10^{-4} mole per liter; total carbonate concentration, 42×10^{-4} mole per liter. A relatively small quantity of total carbonate was present as free carbonate ions at this solution pH, and the supersaturation value was 4.6 with respect to calcite.

In seeded-crystal-growth experiments (in the absence of growth inhibitors), crystallization of fresh mineral begins immediately after addition of the seed crystals and is accompanied by a corresponding decrease in solution concentration. Experimental results (Figure 4) illustrate that the total calcium concentration in the solution decreases from 2.6×10^{-4} mole per liter at the start of the experiment to 1×10^{-4} mole per liter at the end of the experiment. During the crystallization reaction, there is a corresponding change in pH of the solution that is plotted as a function of time, in minutes, in Figure 4. The rate of reaction is equal to the slope of the total calcium concentration as a function of time curve at any particular time.

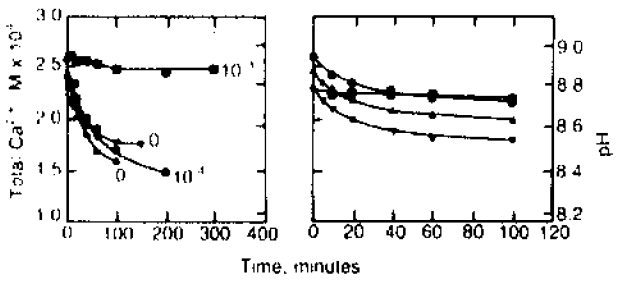

Figure 4. Total calcium concentration and pH of the supersaturated solution plotted as a function of time for seeded crystal growth in the presence and absence of added magnesium ion. Molar concentrations of added magnesium ions are indicated at the end of the curves (Reddy and Wang 1980).

Results of seeded-crystal-growth experiments can indicate the effect of additive ions, such as magnesium ions, on the crystallization process. The change in solution calcium concentration as a function of time for seeded crystallization in the presence (upper curves) and absence of magnesium ions (lower curve) is plotted in Figure 4. As magnesium ion concentration increases from 10^{-4} to 10^{-3} mole per liter, there is a concomitant decrease in the calcite-crystal-growth rate.

A number of rate equations have been proposed for the analysis of calcite crystallization kinetics (Reddy 1977; Smallwood 1977; Reddy et al. 1981; Inskeep and Bloom 1985; Compton and Daly 1987; House and Donaldson 1986; House 1987). In these mathematical expressions, the rate of crystal formation, which is the change in crystal mass with time, is related to a product of terms; each term in the rate equation corresponding to a process or factor that regulates the crystallization reaction. These terms are: (1) the crystallization rate constant k, which is a kinetic factor; (2) the surface area term, s; and (3) a term for the chemical driving force, which is related to the difference between the actual solution concentration and the equilibrium value for the mineral being crystallized. This term for the chemical driving force is raised to a power greater than unity (to the second power in the example of a parabolic rate law, Nielsen 1981) in crystal-growth processes that have a surface-reaction-rate determining step.

Nielsen (1987) has classified the mechanisms that control the growth rate of electrolyte crystals in aqueous solutions. Linear kinetics originate when crystal-growth rates are controlled by transport through the solution or by adsorption at the crystal surface. Conversely, parabolic kinetics originate when the crystal-growth rates are controlled by the integration of growth units at kinks on the crystal surface.

For the growth of calcite seed crystals at pH 8.8 and fixed ionic strength, the change in total calcium ion concentration with time follows a rate expression of the form:

$$dN/dt = -k\, s\, N^2 \qquad (2)$$

where N is the quantity of calcite to be precipitated from solution to reach equilibrium; k is the crystal-growth-rate constant; and s is the concentration of seed crystal that is proportional to the surface area available for growth.

Mullin (1972) has described a crystallization parameter, "theoretical crystal yield" that is equivalent to N as defined above. The experimental value of N is determined by calculating the difference between total calcium concentration in the solution and the value for that term at equilibrium calculated from the calcite solubility product, the solution pH, and the total carbonate concentration. An integrated form of equation 2 is convenient for analysis of the experimental results:

$$N^{-1} - N_o^{-1} = k\, s\, t \qquad (3)$$

where N_o is the quantity of calcite to be precipitated from the supersaturated solution at the onset of the crystallization reaction.

The rate function (equation 3), which is a linear function of time, can be plotted so that the slopes of the lines are proportional to the rate constant k (Figure 5). For calcite growth in presence of magnesium ions, plots of the rate function are linear with time, which is in agreement with the proposed rate law. In the absence of magnesium ions, the rate-function plot has the largest slope and, correspondingly, the largest rate constant. As the magnesium ion concentration increases, the best-fit slope values and the rate constant for crystal growth decrease.

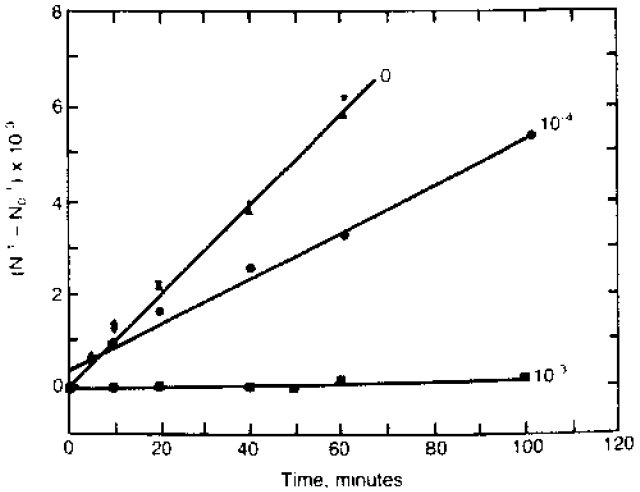

Figure 5. Plots of the integrated rate function as a function of time for growth of calcite seed crystals in the presence and absence of magnesium ions. Molar concentrations of added magnesium ions are indicated at the end of the curve (Reddy and Wang 1980).

The rate of calcite crystallization in the presence and absence of magnesium ions is consistent with equations 2 and 3, and with an interfacial rate controlling process. This indicates that the rate determining step in calcite-crystal growth involves the incorporation and dehydration of an adsorbed, partially hydrated calcium carbonate species into the crystal at a growth site on a crystal surface.

Rate constants for calcite-crystal growth for a range of magnesium ion concentrations indicate the crystal growth inhibition effect (Figure 6). There is a substantial decrease in the calcite-crystal growth-rate constant as the magnesium ion concentration increases.

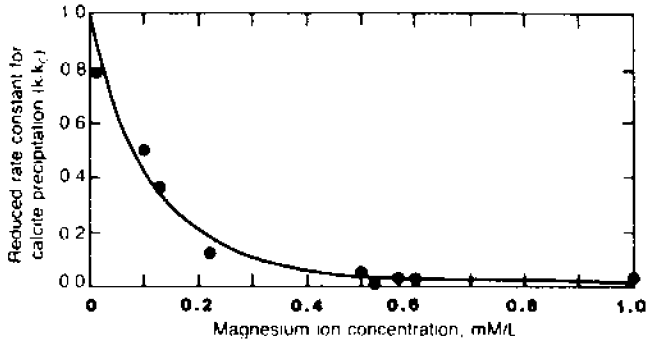

Figure 6. Calcite crystallization reduced-rate constant (k/k_o) as a function of the concentration of magnesium ions in solution (Reddy 1986).

Adsorption mechanisms commonly have been used to describe growth-rate decrease by added substances. A Langmuir adsorption isotherm model, for example, (Reddy 1977; Reddy and Wang 1980) yields equation 4, which relates the change in the crystal growth-rate constant to the additive ion concentration.

$$k_o (k_o - k)^{-1} = 1 + (A/C) \qquad (4)$$

In equation 4, the first rate constant, k_o, is that for a pure supersaturated solution. The second rate constant, k, is the rate constant in the presence of added ions. The first term, A, is a constant related to the rates of adsorption and desorption of the added ions. The second term, C, is the concentration of the added ions in solution. A plot of the Langmuir rate-function term as a function of the reciprocal of the magnesium ion concentration has a linear relation with an intercept of almost unity that supports the use of the Langmuir model to describe the inhibition effect of magnesium ions (Figure 7). This inhibition effect indicates that magnesium ions decrease the growth rate of calcite crystals through an absorption process at growth sites on the crystal surface.

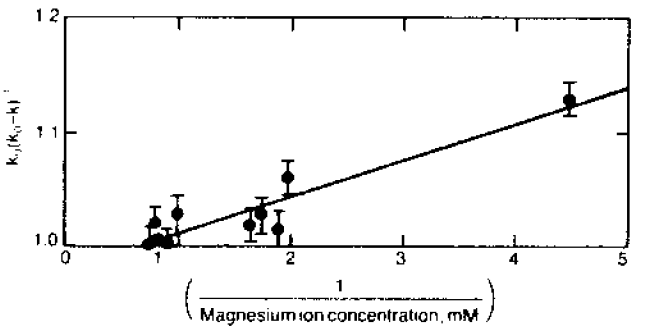

Figure 7. Langmuir isotherm plot of $k_o/(k_o-k)$ as a function of the reciprocal of the added magnesium ion concentration in solution for calcite seeded crystallization (Reddy 1986).

The surface mechanism for calcite crystallization involves incorporation of hydrated calcium species absorbed on the crystal surface at a growth site. For calcite-crystal growth in the presence of magnesium ions, a magnesium ion becomes adsorbed at the growth site. Because ionic dehydration after adsorption of the incorporating unit at a growth site is considered to be the rate determining step in calcite-crystal growth, the greater hydration energy of the magnesium ion in comparison to that for the calcium ion causes slower ion dehydration at the growth site, which decreases the overall calcite-crystal growth rate.

The effect of other ions on the calcite-crystal-growth mechanism has been studied using the seeded-growth technique. For example, glycerophosphate, a phosphorus containing ion in the terrestrial environment, and orthophosphate have been examined in detail (Reddy 1975, 1977). Glycerophosphate and phosphate ions have calcite-crystal-growth-inhibition characteristics that are consistent with the Langmuir absorption isotherm model, which indicates that calcite-crystal-growth inhibition by these ions is caused by absorption at growth sites on that crystal surface.

One of the requirements of the Langmuir absorption model is that the adsorbed ion does not incorporate into the crystal. This requirement can be tested, for example, by measuring the phosphate concentration in a supersaturated solution during a calcite-crystallization experiment. When these measurements were made in the experiments described above, the phosphorus concentration remained unchanged. Phosphorus ions were not incorporated into the growing calcite crystals in substantial quantities, rather these ions function as a surface inhibitor by blocking the calcite- crystal growth sites (Reddy 1980).

SUMMARY

Mechanisms that regulate crystallization processes, for growth onto seed crystals in a metastable supersaturated solution, have been much more clearly defined than those for spontaneous precipitation. In the instance of calcite crystallization from a seeded supersaturated solution, the rate limiting step is a surface-controlled reaction. A Langmuir absorption mechanism describes the measured calcite-crystallization-rate decrease for several additive ions discussed in this paper (magnesium, phosphate, and glycerophosphate ions). There is an absence of mineral phases other than calcite during the calcite seeded crystal growth in the presence of phosphate and magnesium ions when supersaturation values are small.

Crystallization mechanisms can vary substantially for several minerals that are involved in biomineralization. Supersaturation values, when large, cause the formation of complex mineral polymorph and hydrate mixtures that may transform or dissolve or both as the solution composition approaches equilibrium with the thermodynamically stable phase. At the present time, there is a general outline available for describing the precipitation of several biominerals (i.e., calcium carbonates and calcium phosphates). However, much additional research is needed to identify the effect of organic substances on mineral transformations in biomineralization processes.

REFERENCES

Amjad, Z. 1987. The influence of polyphosphates, phosphonates, and poly(carboxylic acids) on the crystal growth of hydroxyapatite. Langmuir 1987:1063-1069.

Bills, P.M. 1985. The precipitation of calcium carbonate polymorphs *in vitro* at 37°C. Calcif. Tissue Int. 37:174-177.

Compton, R.G. and P.J. Daly. 1987. The dissolution/precipitation kinetics of calcium carbonate: An assessment of various kinetic equations using a rotating disk method. J. Colloid and Interface Science 115:493-498.

Harned, H.S. and R. Davis, Jr. 1943. The ionization constant of carbonic acid in water and the solubility of carbon dioxide in water and aqueous salt solutions from 0 to 50°C. J. Amer. Chem. Soc. 65:2030-2037.

Harned, H.S. and S.R. Scholes, Jr. 1941. The ionization constant of HCO_3^- from 0 to 50°C. J. Amer. Chem. Soc. 63:1706-1709.

Helgeson, H.C. 1969. Thermodynamics of hydrothermal systems at elevated temperatures and pressures. Am. J. Sci. 267:729-804.

House, William A. 1987. Inhibition of calcite crystal growth by inorganic phosphate. J. Colloid and Interface Science 119:505-511.

House, W.A. and L. Donaldson. 1986. Adsorption and coprecipitation of phosphate on calcite. J. Colloid and Interface Science 112:309-323.

Inskeep, W.P. and P.R. Bloom. 1985. An evaluation of rate equations for calcite precipitation kinetics at pCO_2 less than 0.01 atm and pH greater than 8. Geochim. et Cosmochim. Acta 49:2165-2180.

Jacobson, R.L. and D. Langmuir. 1974. Dissociation constants of calcite and $CaHCO_3^+$ from 0 to 50° C. Geochim. et Cosmochim. Acta 35:1023-1045.

Lowenstam, H.A. and S. Weiner. 1985. Transformation of amorphous calcium phosphate to crystalline dahllite in the radial teeth of chitons. Science 227:51-53.

Mullin, J.W. 1972. In: Crystallization, CRC Press, Inc. Cleveland, Ohio. p. 480.

Nancollas, G.H. 1982. Phase transformation during precipitation of calcium salts. In: G.H. Nancollas (ed.) Biological Mineralization and Demineralization. Springer-Verlag, New York. p. 79-99.

Nancollas, G.H. and Michael M. Reddy. 1971. The crystallization of calcium carbonate. II. Calcite growth mechanism. J. Colloid and Interface Science 37:824-830.

Nancollas, G.H. and Michael M. Reddy. 1974. Crystal growth kinetics of minerals encountered in water treatment processes. In: A.J. Rubin, (ed.) Aqueous-environmental chemistry of metals. Ann Arbor Science Publishers. p. 219-252.

Nielsen, Arne E. 1981. Theory of electrolyte crystal growth. The parabolic rate law. Pure and Applied Chemistry 53:2025-2039.

Nielsen, Arne E. 1987. Rate laws and rate constants in crystal growth. Croatica Chemica Acta 60(3):531-539.

Nielsen, Arne E. and J. Christofferson. 1982. The mechanism of crystal growth and dissolution. In: G.H. Nancollas, (ed.) Biological Mineralization and Demineralization. Springer-Verlag, New York. p. 37-77.

Ogino, Takeshi, Toshio Suzuki and Kiyoshi Sawada. 1987. The formation and transformation mechanism of calcium carbonate in water. Geochim. et Cosmochim. Acta 51:2757-2767.

Reardon, E.J. and D. Langmuir. 1974. Thermodynamic properties of the ion pairs $MgCO_3$ and $CaCO_3$ from 10 to 50° C. Am. J. Sci. 274:599-612.

Reddy, M.M. 1975. Kinetics of calcium carbonate formation. Proceedings of the International Association of Theoretical and Applied Limnology 19:429-438.

Reddy, M.M. 1977. Crystallization of calcium carbonate in the presence of trace concentrations of phosphorus containing anions. I. Inhibition by phosphate and glycerophosphate ions at pH 8.8 at 25° C. Journal of Crystal Growth 41:287-295.

Reddy, M.M. 1978. Kinetic inhibition of calcium carbonate formation by waste water constituents, In: A.J. Rubin (ed.) Chemistry of Wastewater Technology. Ann Arbor Science Publishers, Ann Arbor, Mich., p. 31-57.

Reddy, M.M. 1980. Sediment phosphorus characterization in the Genesee River watershed, N.Y. In: R. Baker (ed.) Contaminants and Sediments. Ann Arbor Science Publishers, Inc., Ann Arbor, MI, V. 2, p. 119-136.

Reddy, M.M. 1983. Characterization of calcite dissolution and precipitation using an improved experimental technique. Sciences Geologiques, 71:109- 117.

Reddy, M.M. 1986. Effect of magnesium ions on calcium carbonate nucleation and crystal growth in dilute aqueous solution at 25°. In: F.A. Mumpton (ed.) Studies in Diagenesis. U.S. Geological Survey Bulletin 1578: 169-182.

Reddy, M.M. and W.D. Gaillard. 1981. Kinetics of calcium carbonate (calcite)-seeded crystallization: Influence of solid/solution ratio on the reaction rate constant. J. Colloid and Interface Science 80:171-178.

Reddy, M.M. and G.H. Nancollas. 1976. The crystallization of calcium carbonate. IV. The effect of magnesium, strontium and sulfate ions. J. Crystal Growth 35:33-38.

Reddy, M.M., L.N. Plummer and E. Busenburg. 1981. Crystal growth of calcite from calcium bicarbonate solutions at constant pCO_2 and 25° C: A test of a calcite dissolution model. Geochim. et Cosmochim. Acta 45:1281-1289.

Reddy, M.M. and K.K. Wang. 1980. Crystallization of calcium carbonate in the presence of metal ions. I. Inhibition by magnesium ion at pH 8.8 and 25°. J. Crystal Growth 50:470-480.

Smallwood, P.V. 1977. Some aspects of the surface chemistry of calcite and aragonite. Colloid and Polymer Sci. 255:994-1000.

Spencer, R.J., H.P. Eugster, B.F. Jones and S.L. Rettig. 1985. Geochemistry of Great Salt Lake, Utah. I. Hydrochemistry since 1850. Geochim. et Cosmochim. Acta 49:727-737.

Wheeler, A.P. and C.S. Sikes. 1984. Regulation of carbonate calcification by organic matrix. Amer. Zool. 24:933-944.

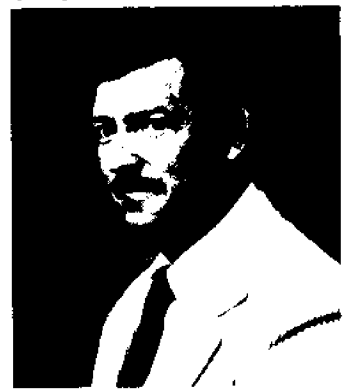

Michael Reddy is an Hydrologist with the U.S. Geological Survey in Denver. He received the B.S. in 1966 and the Ph.D. in 1970, both in chemistry from the State University of New York at Buffalo. He worked as an Instructor at SUNY at Buffalo for several years, then took a position as Research Scientist at the New York Department of Health before beginning work with the U.S.G.S. in 1980. Michael has been studying the physical chemistry of calcification throughout his career, producing a number of insightful papers on inhibition of crystallization, including effects of soluble organic compounds.

Chemical Aspects of Regulation of Mineralization. C.S. Sikes and A.P. Wheeler, editors, University of South Alabama Publication Services, Mobile, Alabama, 1988.

Organic Matrix from Carbonate Biomineral as a Regulator of Mineralization.

A.P. Wheeler[1], Kirt W. Rusenko[1] and C. Steven Sikes[2]

[1]Department of Biological Sciences,
Clemson University,
Clemson, SC 29634-1903 USA

[2]Department of Biological Sciences,
University of South Alabama,
Mobile, AL 36688 USA

ABSTRACT

Recent studies of the proteins of the organic matrix from the $CaCO_3$ shell of bivalve molluscs suggest the following as working hypotheses as to the correlation between matrix structure and function: (1) the primary structures of matrix molecules are critical to understanding their function in regulating shell mineral growth; (2) the degree of phosphorylation of matrix proteins may be in part responsible for control of mineral structure; (3) much of shell matrix is made up of similar structures or subunits and it is the deployment or higher order organization of these subunits which dictates their function in shell formation; and (4) the primary mechanism by which matrix initiates, regulates and limits mineral growth is through adsorption to growing crystals or crystal nuclei.

Introduction

One of the most abundant and conspicuous biominerals is the $CaCO_3$ molluscan shell. Because of the ease in obtaining large quantities of material and the theoretical accessibility of the mineralizing compartment, these systems are in many ways ideal for studying extracellular organic matrix-mediated mineralization. However, because of the natural tendency for research to develop around vertebrate systems, relatively less is known about matrix in any such carbonate system when compared to their mechanistic counterparts from calcium phosphate structures such as teeth and bone. Our long term goal is to understand the relationship between the structure of molluscan matrix molecules and their function in regulating biomineralization. In this contribution we will present a brief summary of the isolation and some functional analyses of matrix proteins and then emphasize preliminary structural analyses we have performed on the proteins.

Isolation of Matrix

We have focused largely on the matrix extracted from one organism, the common oyster *Crassostrea virginica*. The shell of this bivalve is composed of two principal microstructurally distinct mineral layers, an outer prismatic and an inner foliated (calcitostracum; pseudonacre). Both layers are calcitic, with the inner layer constituting the majority of the shell structure. In addition to these microstructures, the shell contains varying quantities of structurally less well defined chalky calcite and a relatively small quantity of aragonitic myostracum which forms under the adductor muscle. The organic outer covering of molluscan shells, the periostracum, appears to be absent from the majority of the surface of the shells we use (Galstoff 1964), especially following cleaning of the shells. Although generally we do not separate shell layers before isolation of the matrix from the oyster shell, it is very likely that the principal protein classes would be present in and largely derived from the foliated layer.

EDTA is used to dissolve powdered shell and the resulting extract is fractionated into soluble and insoluble matrix upon centrifugation. Specifically, shell from freshly-shucked animals is scrubbed free of adhering organisms and debris, crushed in a press and the centimeter pieces powdered in a hammer mill. Approximately 100 g of mineral is dissolved by rotating the powder contained in a 10-12 kDa dialysis bag at 6-8 rpm in 8 l. of 10% EDTA, pH 8.0. The mineral dissolves relatively rapidly (2-3 days), albeit slower than if the powder were in the bulk solution. However, the resulting volume of the extract using the dialysis method is only 100-200 ml, which facilitates processing in the remaining steps.

The contents of the dialysis bag are fractionated according to the scheme in Fig. 1. The centrifugation step (27,000 xg, 30 min.) separates a biphasic insoluble matrix (IM) pellet from the soluble matrix (SM) in the supernatant. The upper, viscous, translucent layer of the pellet (light IM) can be separated by repeated centrifugation steps from the dark, nearly particulate lower pellet (dark IM).

The supernatant is dialyzed by a tangential flow system (Millipore, Minitan) using 10 kDa nominal pore size membranes. This method seems to be more effective for eliminating EDTA

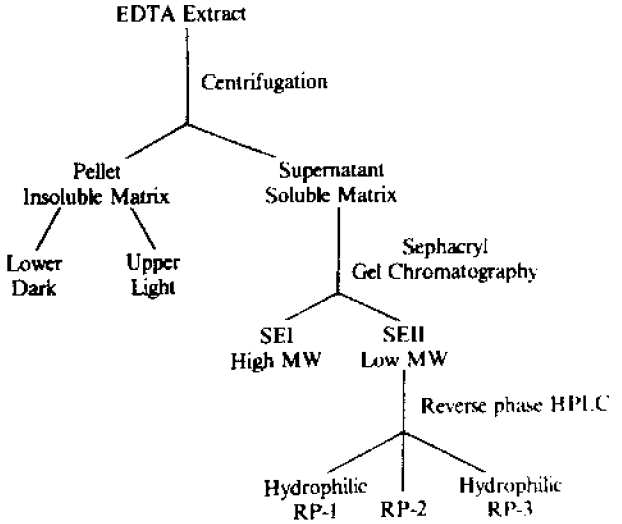

Fig. 1. Abbreviated flow diagram for fractionation of oyster matrix. Whole demineralized extract is centrifuged at 27,000xg for 30 min resulting in a biphasic insoluble matrix pellet and the soluble matrix in the supernatant. The soluble matrix is chromatographed on Sephacryl S-300 which eliminates any residual EDTA and fractionates the SM into high (SEI) and low (SEII) molecular weight classes. Upon further chromatography with gradient reverse phase HPLC, SEII is subfractionated into three classes of protein. These fractions are named according to the order in which they elute from the column as: RP-1 (most hydrophilic), RP-2, and RP-3 (most hydrophobic). Most of RP-2 will resolve into RP-1 and 3 upon rechromatography, indicating that this intermediate class results from an interaction between the other two classes.

than conventional dialysis. In fact, the evidence suggests (Wheeler *et al*. 1987) that associations between EDTA and matrix proteins can occur, making complete removal of the chelator difficult. All EDTA can be removed by this system; however, chromatography can be used to effect removal of any final residue as well.

The SM has been fractionated by numerous chromatographic methods including gel permeation, ion exchange and reverse phase (Wheeler and Sikes 1989), giving repeatable fractions of increasing homogeneity and increasing activity in crystal growth assays. Upon gel permeation, two main classes of protein appear, a high molecular weight (> 500 kDa) identified as SEI and a lower molecular weight class identified as SEII (M_r range of entire peak 15-500 kDa). SEII is considerably more active than SEI in mineralization assays (Wheeler *et al*. 1988) and this fraction has been studied in some detail and subjected to further fractionation by ion exchange and reverse phase. Reverse phase HPLC subfractionates SEII into two definitive classes of proteins, one highly hydrophilic (RP-1) and one relatively hydrophobic (RP-3), and a third class which appears to result from an interaction between the other two (Fig. 1). The highly hydrophilic (RP-1) class is also the most active in mineralization assays and has been studied in some more detail than the more hydrophobic material.

Function of Matrix

A partial list of generally recognized matrix function in biomineralization would include nucleation (initiation) of crystal growth, limitation (inhibition) of crystal growth and control of crystal microstructure and mineralogy. Relevant to those functions, we have examined SM isolated from oyster in a number of ways. For example, the efficacy of test molecules as inhibitors of crystal growth are evaluated in a variety of *in vitro* assays (see also Sikes and Wheeler, this volume). One such *in vitro* assay is a simple pH-stat method (Fig. 2) in which the rate of base titration is auto-adjusted to keep pH constant as crystals grow according to the overall equation:

$$Ca^{2+} + HCO^{-}_{3} = CaCO^{-}_{3} + H^{+}.$$

After an initial control growth period, a test molecule is added to the solution of growing crystals. As can be seen in Fig. 2B, as the dose of SM is increased, the rate of growth declines. Replotting the results as the ratio of inhibited to control growth rate versus concentration of inhibitor (Fig. 2C), one can characterize any inhibitor by the extrapolated concentration required to give 50% inhibition (I_{50}).

A number of matrix fractions and synthetic analogs have been compared using this and related techniques with the assumption that the efficacy in this assay reflects the propensity of test molecules to interact with crystals or crystal nuclei in biomineralization. In fact, radio-labeled matrix molecules in these assays is adsorbed to (and possibly incorporated within) growing crystals (Sikes and Wheeler 1986; Wheeler and Sikes 1989). Further, the morphology of crystals grown in the presence of matrix is altered dramatically compared to the regular rhombohedral crystals which form in control assays (Wheeler and Sikes 1984).

Finally, the influence of the matrix molecules on crystal growth has been studied *in vivo* by examining the rate of mineralization of the spicules of sea urchins in the presence of exogenously supplied oyster (and other) matrix (Sikes and Wheeler 1986). The results of these studies show that matrix present in the embryo culture medium can reduce the rate of spicule mineralization

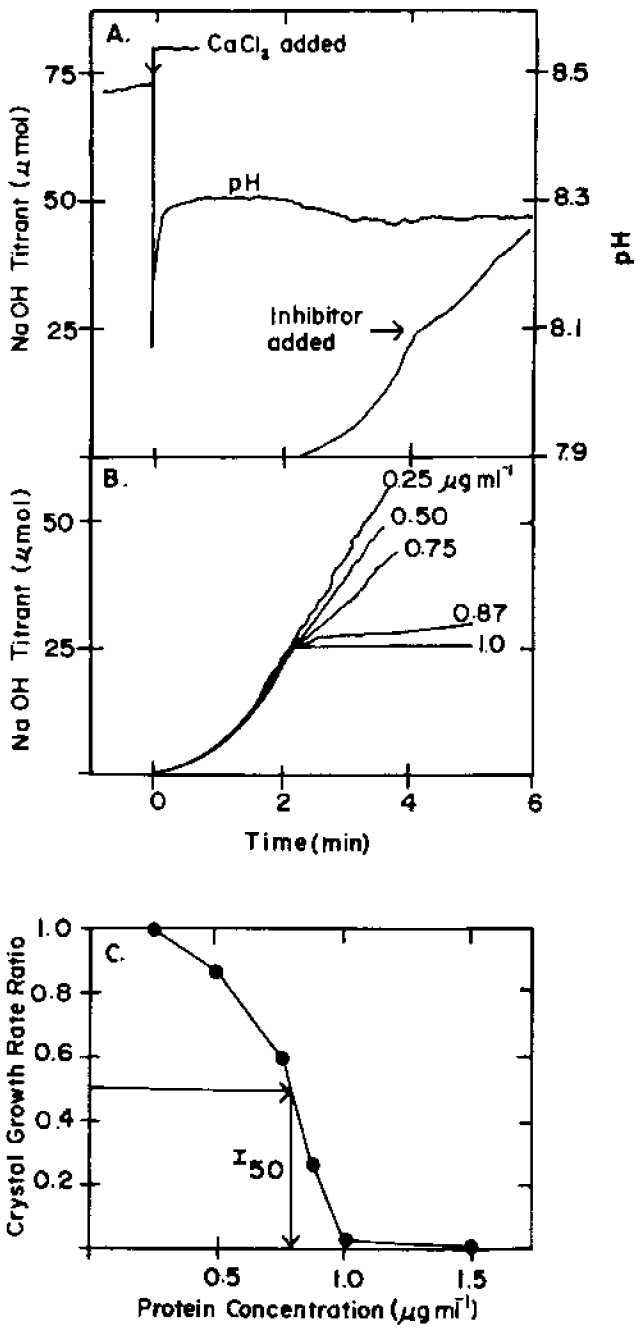

Fig. 2. Inhibition of $CaCO_3$ crystal growth *in vitro*. A. Representative pH-stat inhibition experiment. To initiate crystal growth, 125 μl of 2 M $CaCl_2$ was added to 25 ml of medium containing 10 mM inorganic carbon and 500 mM NaCl, pH 8.45 - 8.50. After the initial decrease, the pH was held constant at 8.30 ± 0.02 by auto-titration of 0.5N NaOH. In each case inhibitors were added at the level of crystal growth equivalent to 25 μmol of NaOH titrant. In this case the inhibitor was SEII at a final concentration of 0.75 μg ml^{-1} on the basis of Lowry protein weight. B. Series of pH-stat inhibition experiments for various concentrations of an SEII fraction. Note, no inhibition of growth occurred at 0.25 μg ml^{-1} but inhibition was complete at 1.0 μg ml^{-1}. C. Example of method for determining concentration of inhibitor required for 50% inhibition (I_{50}) of crystal growth in pH-stat experiments. For each concentration in (B), the rate of crystal growth immediately following addition of the inhibitor was divided by the rate immediately preceding addition of inhibitor. These ratios were plotted as a function of the inhibitor concentrations and the extrapolated concentration for a ratio of 0.5 is taken as the I_{50} (Wheeler *et al*. 1988).

through access to and adsorption on the biomineral. In fact, the matrix quantities per unit weight of biomineral which result in significant inhibition *in vivo* are remarkably similar to those quantities adsorbed per unit weight of calcite required for inhibition *in vitro*.

Soluble Matrix Primary Structure

We have attempted to determine structural features of the oyster matrix molecules that ultimately may give some clue as to their functional properties. In this approach, we have first attempted to partially determine the primary structure of the most active fractions of soluble matrix with respect to inhibition of crystallization.

As has been reported for many other molluscan soluble matrix molecules, the amino acid composition of RP-1 is made up largely of three amino acids: serine, aspartic acid and glycine. What has not been generally recognized for carbonate matrix is that the serine is mostly phosphoserine, much like the phosphoproteins extracted from bone and dentin, (*e.g.*, see Butler 1987).

One prominent current hypothesis suggests that these polyanionic proteins have the aspartic acids deployed in such a way as to provide some kind of template onto which crystals may initiate and grow (Weiner and Hood 1975; Weiner and Traub 1984; Mann 1988). The purported preferred spacing is -Asp-X-Asp- with X being largely serine or glycine. The data supporting this conclusion comes from single time point hydrolyses of matrix molecules in dilute acid (*e.g.*, Weiner and Hood 1975; Weiner 1983), a treatment which theoretically can be relatively specific for peptide bonds on both sides of aspartic acid residues.

Using this approach, we have hydrolysed RP-1 using formic acid at pH 2.0 (Inglis 1983). The results showed that the rate of release of aspartic acid far exceeds the release of serine and glycine together (Fig. 3; Rusenko *et al.* in prep.). Therefore, it would appear that -Asp-X-Asp- is not a prominent arrangement otherwise the release of X (serine and glycine) would more nearly match the release of aspartate. Rather, it can be hypothesized that much of the aspartic acid is deployed in runs of polyaspartic acid.

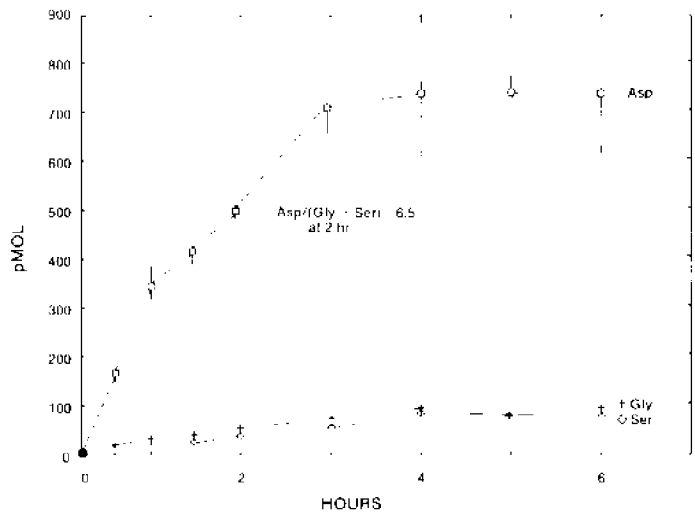

Fig. 3. Release of amino acids from an oyster soluble matrix fraction (RP-1) by treatment with formic acid. This fraction was incubated for various time intervals in formic acid (pH 2.0, approx. 2%) at 108°C. This treatment is relatively specific for peptide bonds on either side of aspartic acid residues. The liberated amino acids were dabsylated and identified by reverse phase chromatography. Values are plotted as means of hydrolysates from different matrix preparations with standard deviations shown for aspartic acid values only (n = 3 to 9).

The idea that most of the aspartate exists as polyAsp in the natural material is supported by studies in which matrix analogs, such as those containing repeating sequences of-Asp-Gly-Ser-, were hydrolyzed (Rusenko *et al.*, in prep.). In this case, in addition to release of the Gly-Ser dipeptide, significant Gly and Ser were also released. This finding indicates that the Gly and Ser released from natural matrix may be due in large measure to hydrolysis of peptide bonds other than those involving aspartate. Further, the absence of Gly-Ser (or Ser-Gly) dipeptides in matrix hydrolysates reduces the possibility that sequences such as -Asp-X-Y-, with X or Y being either serine or glycine, dominate matrix molecules such as RP-1.

Finally, in both inhibitor studies (see also Sikes and Wheeler, this volume) and studies involving direct measurement of adsorption of peptides to crystals (Wheeler *et al.* in progress), polyaspartate interacts better with calcite crystals than peptides with other sequences. For example, a typical I_{50} value in the pH-stat assay for polyaspartate or RP-1 would be less than 1 $\mu g\ ml^{-1}$ whereas for peptides containing -Asp-X- it would be approximately 1 $\mu g\ ml^{-1}$ or greater and for those containing -Asp-X-Y-, in many cases, it would be several times higher.

Interestingly enough, the residues resulting from the dilute acid hydrolyses contain both hydrophilic and hydrophobic fragments as determined by reverse phase HPLC (Rusenko *et al.* in prep.). These fragments persist even after the maximum release of aspartate has occurred. In addition, the fragments remain highly phosphorylated. These findings taken collectively suggest that phosphoserine may be deployed in separate domains from aspartic acid.

The persistence of hydrophobic fragments in the hydrolysates suggests that domains including mostly hydrophobic amino acids are present in RP-1, an interesting observation given the low percentage of these amino acids in the overall composition of the protein. Using a variety of carboxypeptidases to hydrolyze RP-1, we have determined that one of these domains may well be at the carboxy terminus of the protein (Rusenko *et al.* in prep.). The significance of such a domain for the activity of a matrix protein is discussed in the following paper.

To summarize, the following hypotheses regarding the primary structure of RP-1 from oyster matrix can be proposed:

1) Aspartic acid is deployed more as polyAsp than as -Asp-X- or -Asp-X-Y-.
2) Phosphoserine may exist in discrete domains.
3) Hydrophobic domains exist, with one possibly located at the carboxy terminus.

Phosphorylated and Non-phosphorylated Matrix

Our identification of phosphoprotein soluble matrix from a calcium carbonate structure such as oyster shell bears further examination. Although as mentioned above, matrix phosphoproteins are common in phosphate mineral and have been identified in at least one other carbonate system (Veis *et al.* 1986), they do not appear to be ubiquitous in calcified biomineral. Specifically, a survey of shells and shell layers having different mineral microstructure reveals that only the SM (SEII) from foliated calcite was highly phosphorylated (Borbas *et al.* in prep.). The matrix from the more primitive aragonitic layers and calcitic prismatic layers contained little or no phosphate.

The general correlation between shell structure and degree of matrix phosphorylation suggests that the matrix-phosphate may be significant for regulating the morphology of carbonate by an as yet undetermined mechanism. This general conjecture is

supported by the fact that low phosphate matrices and dephosphorylated oyster matrix are much less effective quantitative regulators of calcite growth *in vitro* (higher I_{50}'s in the pH stat assay) than phosphorylated matrix from oyster or scallop.

Perhaps even more interesting than the quantitative results are some more qualitative observations on *in vitro* crystal growth behavior in the presence of phosphorylated and non-phosphorylated matrix. For example, pH stat assays were compared in which the initial level of inhibition of crystal growth for various matrices was nearly identical (Fig. 4). If the crystal growth was allowed to continue, it was clear that dephosphorylated oyster SEII loses inhibitory activity very quickly; however, phosphorylated matrix retains inhibitory activity even as carbonate continues to accumulate. The mechanism underlying this phenomenon is unknown.

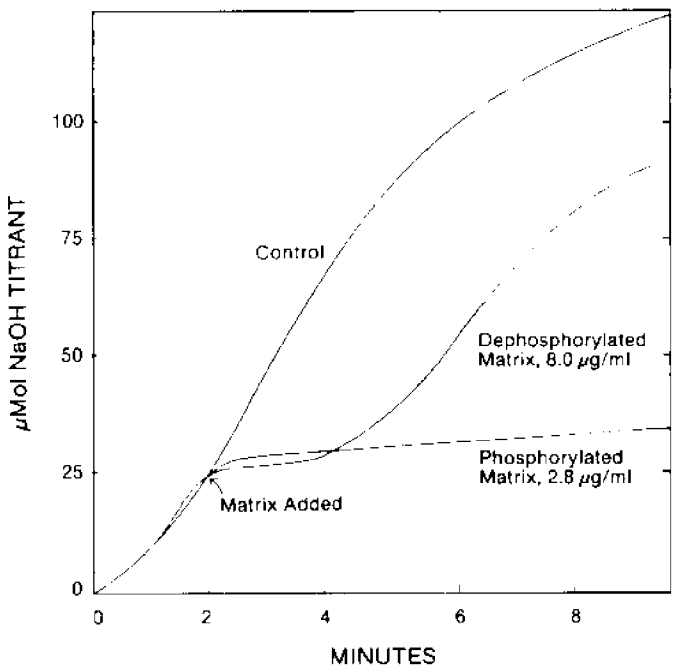

Fig. 4. Comparison of the effect of phosphorylated and dephosphorylated matrix on crystal growth in the pH-stat assay. Conditions for the assay are as described in Fig. 2. In this figure, the time scale indicates minutes after crystal growth initiation. Again, matrix was added at 25 µmol of base titrated ($CaCO_3$ precipitated). The matrices represented are the low molecular weight fractions from Sephacryl chromatography (SEII; Fig. 1). Appropriate doses of untreated and alkaline phosphatase dephosphorylated oyster matrix were chosen to provide an equivalent level of initial inhibition. It is clear that the untreated oyster matrix retains inhibitory activity at a quantity of calcium carbonate accumulation for which the oyster matrix without phosphate starts to lose activity (Borbas *et al.*, in prep.).

In general, our observations to date regarding bivalve matrix phosphate can be summarized as: 1) High matrix phosphate is correlated with specific calcitic microstructures. 2) A correlation exists between matrix phosphate content and enhanced inhibition of calcite crystal growth *in vitro*.

Insoluble Matrix

The general notion about the function of IM is that it is a structural framework to which the soluble matrix attaches (*e.g.*, Degens 1976; Weiner *et al.* 1983). We have made a number of observations on IM that bear on this general hypothesis.

Upon amino acid analysis of crude matrix fractions (see Fig. 1), we find that much of matrix, including low molecular weight SM (SEII), high molecular weight SM (SEI) and light IM are similar both in composition and in the ratio of charged to non-polar amino acids (Table 1). However, dark IM is dramatically different in composition from the rest of matrix and overall is a much more hydrophobic protein. In addition, the dark IM contains DOPA residues which are absent from the rest of matrix. Possibly these latter residues are involved in cross-links (Wheeler *et al.* 1988) which, working together with the general hydrophobicity of this form of matrix, would make dark IM an excellent candidate for the structural framework.

Table 1. Selected Amino Acid Composition of Oyster Matrix Fractions[1]

Amino Acid	Soluble Matrix		Insoluble Matrix	
	SEI (HMW)	SEII (LMW)	Light	Dark
ASP	288	302	258	88
SER	216	221	201	102
GLY	285	292	334	228
ALA	18	16	14	246
DOPA	0	0	0	8
TOTAL CHARGED[2]	366	371	343	167
TOTAL NON-POLAR[3]	89	75	82	404
Ratio of Charged to Non-polar Residues				
	4.1	4.9	4.2	0.41

[1]Residues per thousand

[2]Sum of aspartate, glutamate, histidine, lysine and arginine residues.

[3]Sum of proline, alanine, valine, methionine, isoleucine, leucine and phenylalanine residues.

The similarity among the other fractions of matrix extends beyond the amino acid composition. For example, if light IM or SEI are treated with dilute base, concomitant with reduction in the molecular weight of these fractions, the I_{50} of the various treated fractions in the pH stat assays approaches that of SEII (Wheeler *et al.* 1988). This finding suggests that there are functional components of similar primary structure in all these matrix materials. The possibility of such a structural homogeneity is further supported by the fact that dilute acid hydrolysis of SEI or light IM results in a pattern of amino acid release nearly identical to that described above for RP-1 (Rusenko *et al.* in press).

If the majority of the components of matrix are similar in primary structure, differing largely on the basis of molecular size, then it may be that subunits of matrix are incorporated into larger entities, and as they do so, their function in regulation of mineral growth may change. The idea that similar matrix molecules can express different functions in a cycle of mineralization has been offered repeatedly (*e.g.*, see Crenshaw and Ristedt 1976; Wheeler and Sikes 1984). An hypothesis as to how our findings would fit with such an idea is outlined in Fig. 5.

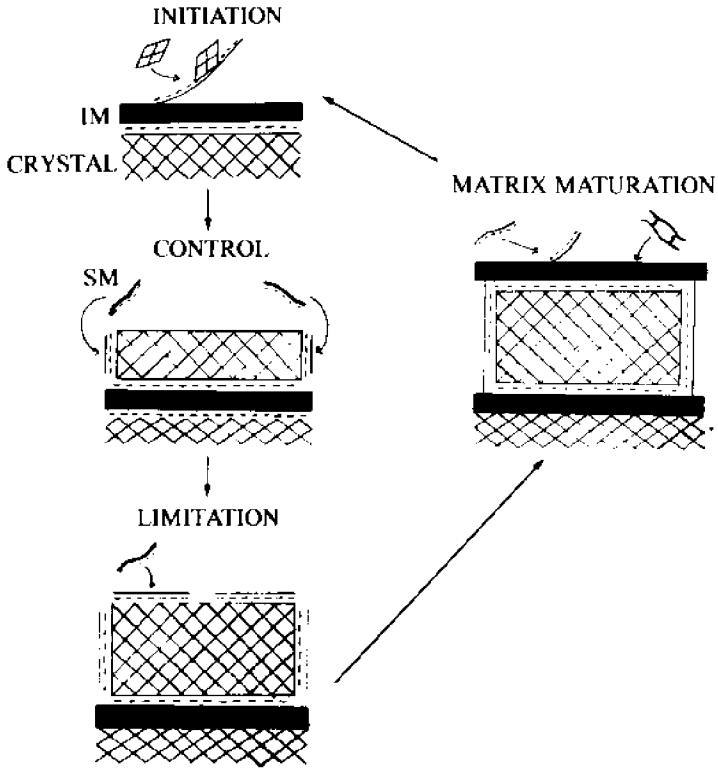

Fig. 5. An hypothetical scheme for the cycle of mineralization in matrix-mediated molluscan shell layer formation. In this diagram, the dashed lines represent the negative changes on matrix proteins such as found in SM and light IM. Initiation of a new crystal layer: Nucleation sites exist as part of the IM structure. Here nucleation is shown as the result of matrix stabilizing crystal nuclei rather than through calcium binding (Wheeler *et al*. 1987). Control of crystal growth: Crystals grow under the influence of anionic matrix, here depicted as regulating lateral growth. Limitation of crystal growth: Because anionic matrix molecules are excellent inhibitors of crystal growth, it is not difficult to appreciate that their adsorption to crystal surfaces could terminate the growth of the mineral. Matrix maturation: Here incorporation of subunits of dark IM (structural) precursors and additional anionic SM-like components into higher molecular weight entities (SEI, light IM) results in the final form of interlamellar matrix including sites for initiation of the next cycle of crystal growth.

Conclusion

In summary, our studies support the general working hypothesis that matrix function in the regulation of mineralization *in situ* depends on the primary structure of the protein subunits, the deployment of the subunits, and their organization into higher order structures. In any case, it appears that the fundamental process by which matrix controls crystal growth is through adsorption to growing crystal surfaces.

Acknowledgements

Many of the studies discussed herein were supported by grants from the South Carolina and Mississippi/Alabama Sea Grant Consortia, NSF and the Alabama Research Institute.

Literature Cited

Butler, W.T. 1987. Mineralized tissues: an overview. Meth. Enzymol. 145:255-261.

Crenshaw, M.A. and H.A. Ristedt. 1976. The histochemical localization of reactive groups in septal nacre from *Nautilus pompiliu*. In: Watabe, N., and K.M. Wilbur (eds.) The mechanisms of mineralization in the invertebrates and plants. Univ. of South Carolina Press, Columbia, South Carolina, p. 355- 367.

Degens, E.T. 1976. Molecular mechanisms of carbonate, phosphate and silica deposition in the living cell. Top. Curr. Chem. 64:1-112.

Galstoff, P.S. 1964. The American oyster *Crassostrea virginica* (Gmelin). Fish. Bull. US 64:U.S. Fish and Wildlife Service.

Inglis, A.S. 1983. Cleavage at aspartic acid. Meth. Enzymol. 91:324-332.

Mann, S. 1988. Molecular recognition in biomineralization. Nature 332:119-124.

Sikes, C.S. and A.P. Wheeler. 1986. The organic matrix from oyster shell as a regulator of calcification *in vivo*. Biol. Bull. 170:494-505.

Veis, D.J., T.M. Albinger, J. Clohisky, M. Rahima, B. Sabsay and A. Veis. 1986. Matrix proteins of the teeth of the sea urchin *Lytechinus variegatus*. J. Exp. Zool. 240:35-46.

Weiner, S. 1983. Mollusk shell formation: isolation of two matrix proteins associated with calcite deposition in the bivalve, *Mytilus californianus*. Biochemistry 22:4139-4145.

Weiner, S. and L.H. Hood. 1975. Soluble protein of the organic matrix of mollusc shells: a potential template for shell formation. Science 190:987- 989.

Weiner, S. and W. Traub. 1984. Macromolecules in mollusc shells and their function in biomineralization. Phil. Trans. R. Soc. London 304B:425-434.

Weiner, S., W. Traub, and H.A. Lowenstam. 1983. Organic matrix in calcified exoskeletons. In: Westbroek, P., and E.W. de Jong (eds.) Biomineralization and biological metal accumulation. D. Reidel Publ. Co., Dordrecht, Holland. p. 205-224.

Wheeler, A.P. and C.S. Sikes. 1984. Regulation of carbonate calcification by organic matrix. Amer. Zool. 24:933-944.

Wheeler, A.P. and C.S. Sikes. 1989. Matrix-crystal interactions in $CaCO_3$ biomineralization. In: Mann, S., J. Webb, and R.J.P. Williams (eds.) Chemical perspectives on biomineralization. VCH Publishers, Weinheim, W. Germany, in press.

Wheeler, A.P., K.W. Rusenko, J.W. George and C.S. Sikes. 1987. Evaluation of calcium binding by oyster shell soluble matrix and its role in biomineralization. Comp. Biochem. Physiol. 87B:953-960.

Wheeler, A.P., K.W. Rusenko, D.M. Swift and C.S. Sikes. 1988. Regulation of *in vitro* and *in vivo* $CaCO_3$ crystallization by fractions of oyster shell organic matrix. Mar. Biol. 98:71-80.

Hap Wheeler is a Professor of Biological Sciences at Clemson University. He received the B.S. in chemistry and zoology from Butler University in Indiana in 1969 and the Ph.D. in zoology from Duke University in 1975. In 1987-89, he has been Visiting Professor in the Coastal Research and Development Institute of the University of South Alabama. Hap's primary research interests have dealt with biochemical regulation of biomineralization, with particular emphasis on the structure and function of organic matrix proteins.

Chemical Aspects of Regulation of Mineralization. C.S. Sikes and A.P. Wheeler, editors, University of South Alabama Publication Services, Mobile, Alabama, 1988.

Control of $CaCO_3$ Crystallization by Polyanionic-hydrophobic Polypeptides

C.S. Sikes[1] and A.P. Wheeler[2]

[1]University of South Alabama
Department of Biological Sciences
Mobile, AL 36688 USA

[2]Clemson University
Department of Biological Sciences
Clemson, SC 29634-1903 USA

ABSTRACT

Oyster shell matrix and other protein inhibitors of crystal formation have polyanionic and hydrophobic domains, often at separate ends of the molecules. The polyanion-hydrophobe (PAH) hypothesis states that the polyanionic region adsorbs to the mineral surface, stopping mineral formation there, and the hydrophobic region extends from the surface, disrupting diffusion of lattice ions to the surface. Evaluation of the PAH hypothesis using synthetic peptides composed of polyaspartate and polyalanine regions demonstrated that an hydrophobic terminus did in fact enhance inhibition of $CaCO_3$ crystallization by the peptides. The primary effect was on crystal nucleation rather than crystal growth. A polyaspartate molecule of 40 residues appeared to be the optimal size for inhibition of crystal nucleation. Ordered copolymers of Gly-Asp, Ser-Asp, and Gly-Ser-Asp were not very effective inhibitors of crystallization.

Introduction

Our recent studies have focused in part on understanding the chemical and structural requirements for inhibition of crystallization by polypeptides and other polymers. A number of natural proteinaceous inhibitors of calcium carbonate and phosphate formation have been studied, including the oyster shell matrix (Wheeler and Sikes 1984, 1989; Sikes and Wheeler 1983, 1986; Wheeler *et al.* 1981, 1987, 1988), salivary proteins (Schlesinger and Hay 1979, 1986; Wong *et al.* 1979; Wong and Bennick 1980), acidic bone and dentin proteins (Poser *et al.* 1980; Butler *et al.* 1983; Wasi *et al.* 1985; Oldberg *et al.* 1986; Prince *et al.* 1987), some fossil proteins from foraminiferans (Robbins 1987; Sikes and Robbins, unpubl.), and a spicule protein from sea urchins (Benson *et al.* 1987; Sikes and Benson, unpubl.). Each of these proteins has distinct polyanionic and hydrophobic domains. For example, both the salivary protein statherin (Hay *et al.* 1979) and the most active inhibitory component of the oyster shell matrix (Wheeler *et al.* 1988; Rusenko 1988) have polyanionic N-termini, including both aspartate and phosphoserine residues, and hydrophobic C-terminal regions.

In the case of statherin, there are 43 residues, with the first five at the N-terminus anionic (H-Asp-$(PSer)_2$-$(Glu)_2$-) and the last two-thirds of the molecule hydrophobic (Schlesinger and Hay 1979). Interestingly, while the anionic region alone gave maximal inhibition of calcium phosphate crystal growth, both the anionic and the hydrophobic regions were necessary for complete inhibition of crystal nucleation (Hay *et al.* 1979). This led to the hypothesis that statherin disrupts crystallization in two ways: 1) the negatively-charged part of the molecule adsorbs onto crystal surfaces, blocking further growth and 2) the non-polar, hydrophobic portion creates a region around crystal nuclei through which lattice ions can not readily diffuse. The purpose of this paper is to report a partial evaluation of this hypothesis about the action of polyanionic-hydrophobic proteins.

Methods

Synthesis of peptides. An automated, solid-phase peptide synthesizer (Applied Biosystems, Model 430A) was used to prepare peptides. A family of polyaspartate molecules ranging in size from Asp_5 to Asp_{60} was synthesized by repetitive couplings of t-Boc-L-aspartic acid residues with β-carboxyl protection by O-benzyl linkage. A C-terminal residue of 0.5 mmole was preloaded on a resin of a polymer of styrene cross-linked with 1% of divinylbenzene. The C-terminal amino acid was linked to the resin via a phenylacetamidomethyl (PAM) group. Peptide bond formation was promoted by use of dicyclohexyl carbodiimide and formation of symmetric anhydrides of the incoming amino acid. At the appropriate times during a synthesis, a subsample of the peptide-resin was taken to provide the desired size of the polyaspartate, then the synthesis was allowed to continue to produce the next larger size, and so forth until all desired sizes had been synthesized and collected.

The same procedure was followed in synthesizing a family of aspartate$_{15}$ alanine$_x$ molecules ranging from $Asp_{15}Ala_2$ to $Asp_{15}Ala_{10}$. In this case, t-Boc-L-alanine residues were used. For peptides containing serine or glycine residues, t-Boc-L-serine-O-benzyl and t-Boc-L-glycine were used.

In all cases, coupling efficiency of each residue was checked by automated sampling of peptide resin for measurement of unreacted free amine by the ninhydrin method (Sarin *et al.* 1981). Coupling efficiencies routinely were greater than 99% per cycle of synthesis.

Following synthesis, peptide-resin was repeatedly washed with methanol then dried and weighed. Then peptides were cleaved from the resin using a modification of the trifluoromethyl sulfonic acid (TFMSA) procedure, with precautions taken to prevent aspartimide formation. (Bergot *et al.* 1986). For 100 mg samples, peptide-resins in a scintillation vial were treated for 10 minutes with 150 μl of anisole to swell the resin, making it more accessible for reaction. Then 1.0 ml of neat trifluoroacetic acid (TFA) was added with magnetic stirring and allowed to react for 10 minutes. Next, 100 μl of concentrated TFMSA (Aldrich Chemical Co.) were added with cooling using an ice bath, followed by cleavage of the peptide from the resin at room temperature for 30 minutes. For cleavage of other amounts of peptide-resin, the amounts of reagents used were changed proportionally.

Following cleavage, 20 ml of methyl butyl ether (MBE) (Aldrich) were added to the vial to insure precipitation of the peptide, which already was relatively insoluble in the acidic reaction medium due to the acidic nature of the peptides. After stirring for 1-2 minutes, the entire slurry was passed through a 4.25 cm glass fiber filter (Fisher G4) using a filter funnel and vacuum pump at 15 psi. This removed the TFA, TFMSA, anisole, and any soluble reaction products, leaving the cleaved peptide and resin on the filter. After washing on the filter with 100 ml of

MBE, the peptide was extracted into a clean, dry flask with 10 ml of Na_2CO_3 (0.02 M, pH 10.2), using 5 successive rinses of 2 ml, with at least 1 minute extraction on the filter prior to applying the vacuum each time. Using this procedure, the filtrate containing the solubilized peptides had pH values >5. The filtrate was then dialyzed twice with stirring against 2 liters of distilled water for 2 hours using dialysis tubing (Spectrapor, nominal MW cutoff of 1000 daltons). The dialysate was frozen and lyophilized, yielding white flakes or powders. The average yield of the peptides was 40%.

Following isolation, purity of the peptides was checked by high performance liquid chromatography (Varian 5500 LC) using gel permeation columns designed for separations of peptides (Toya Soda 2000 SW and 3000 PWXL). Single, sharp peaks at the appropriate MW were obtained. Because the peptides were isolated partially as sodium salts, the sodium content was determined by atomic absorption (Perkin Elmer model 360). Sodium levels typically were less than 5% by weight. Amounts of peptides reported were corrected for sodium content. Concentrations of peptides in aqueous stock solution were based on lyophilized dry weight but were also checked by comparison of UV spectra.

$CaCO_3$ Crystallization Assays. Three types of assays were used: 1) a screening assay for comparison of the general activity of a set of peptides using 15 simultaneously running experiments, 2) a nucleation assay for determining effects on crystal nucleation, and 3) a seeded-crystal assay for determining effects on crystal growth. Each of the assays relies on the production of H^+ ions according to: $Ca^{2+} + HCO_3^- = CaCO_3 + H^+$. The crystallization was monitored by the drift in pH or by the amount of titrant added to maintain pH (pH-stat).

Screening Assay. Solutions supersaturated with respect to $CaCO_3$ were prepared by separately pipetting 0.3 ml of 1.0 M $CaCl_2$ dihydrate and 0.6 ml of 0.4 M $NaHCO_3$ into 29.1 ml of artificial seawater (0.5 M NaCl, 0.011 M KCl). This resulted in initial concentrations of 10 mM Ca and 8.0 mM dissolved inorganic carbon (DIC). Actual concentrations of Ca were confirmed by atomic absorption and of DIC by Gran titration (Stumm and Morgan 1981). The reaction vessels were 50 ml bottles with screwtops. These were partially immersed in a 1-gallon, plastic aquarium fitted for flow-through to a thermostated recirculating water bath (VWR model 1115) at 20°C containing a submersible magnetic stirplate with 15 stirring locations (Cole Parmer). Crystallization was initiated by adjusting pH upward to 8.3 by titration of μl amounts of 1 N NaOH. Final pH was read after 24 hours. Following addition of Ca but before addition of DIC, peptides were added to reaction vessels by manual digital pipetting from stock solutions of 1.0 or 0.1 mg peptide/ml. After experiments, reaction glassware was washed with 0.1 N HCl for at least 10 minutes followed by a treatment of at least 10 minutes with a solution of sodium hypochlorite (5.25 μg NaOCl/ml, a 1/1000 dilution of commercial bleach). These treatments were necessary to dissolve crystals that formed on the surface of the glassware and to destroy and remove peptides that may adhere to the glass. Failure to perform either treatment led to abnormal results in control experiments. Following HCl and NaOCl treatments, reaction glassware was rinsed with several volumes of distilled water and dried for use in subsequent experiments. Results in control experiments demonstrated the importance of using the same reaction vessels for a set of measurements.

Nucleation Assay. The reaction conditions were the same as described for the screening assay. However, the reaction vessel was a 50 ml, round-bottom flask fitted with a pH electrode and closed to the atmosphere to minimize exchange of CO_2 after experiments began. The reaction was monitored continuously by strip chart. The vessels were partially submersed in a water bath at 20°C. After an induction period characterized by a stable pH for about 6 minutes during which crystal nuclei form, the pH began to drift downward until the reaction ceased due to depletion of reactants and the lowering of pH. Inhibition of nucleation was indicated by increased induction periods.

Seeded crystal growth assay. The reaction conditions consisted in 50 ml of artificial seawater as above at 2 mM each of $CaCl_2$ and DIC at pH 8.5. The reaction vessel was a 100 ml, water-jacketed, glass cylinder with a stoppered top fitted with a pH electrode and 2 burette delivery tips. The reaction was thermostated at 20°C. The solution was stable until initiation of the reaction by addition of 2.5 mg of $CaCO_3$ seeds (Baker Analytical) which began to grow immediately. Seeds were aged prior to use by stirring as a slurry of 100g $CaCO_3$ in 1 liter of distilled water for 3 weeks in a closed vessel. This aging of seeds was necessary to provide reproducible control curves. In some cases, 1 ml batches of aged seeds were sealed in ampules until opening for use. It also was acceptable to pipette seeds directly from the 1 liter slurry. However, frequent opening of the slurry to the atmosphere may lead to changes in the solution with resultant changes in the seeds, probably due to exchange of atmospheric CO_2. Peptides were added to the reaction vessel prior to the addition of the seeds. Reaction conditions during growth of seeds were held constant by autotitration of stocks of 0.1 M each of $CaCl_2$ and Na_2CO_3 (pH 11.1) from separate burettes controlled by a computer-assisted titrimeter (Fisher CAT). This replenished the lattice ions to the solution as they were removed due to crystallization and kept the pH at 8.50 ± 0.02.

Results

Example chromatograms of polyaspartate molecules of different molecular sizes are shown in Figure 1. The homogeneity of the peptides was evident from the fact that they each elute as single well-defined peaks, and the relative molecular weight of the peptides is confirmed by the order of elution of the peaks. The effect of molecular size of polyaspartate molecules on inhibition of crystal nucleation is shown in Figure 2.

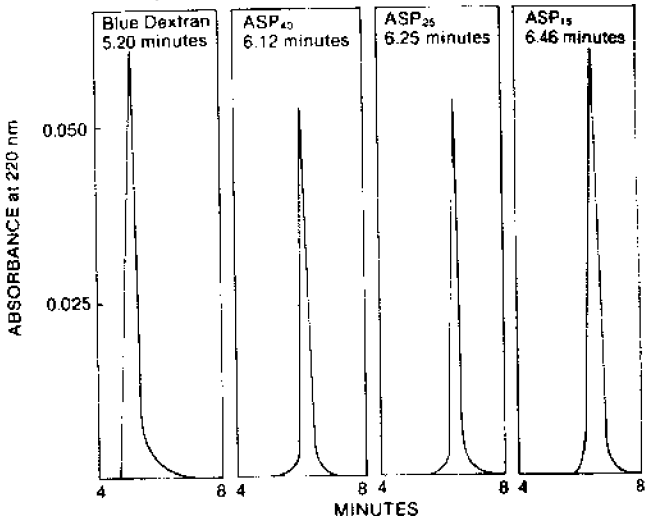

Figure 1. Gel permeation liquid chromatography of polyaspartate molecules. The molecules were injected as 100 μl of 0.1 mg/ml stock solutions. The mobile phase was 0.05 M tris, pH 8.0, at 1.0 ml/min, 25°C, 2 atm. The column was a TSK 3000 PWXL (Toyo Soda), 30 cm, 7.8 mm I.D. Blue dextran, M.W. 2,000,000 daltons, was used to mark the void volume.

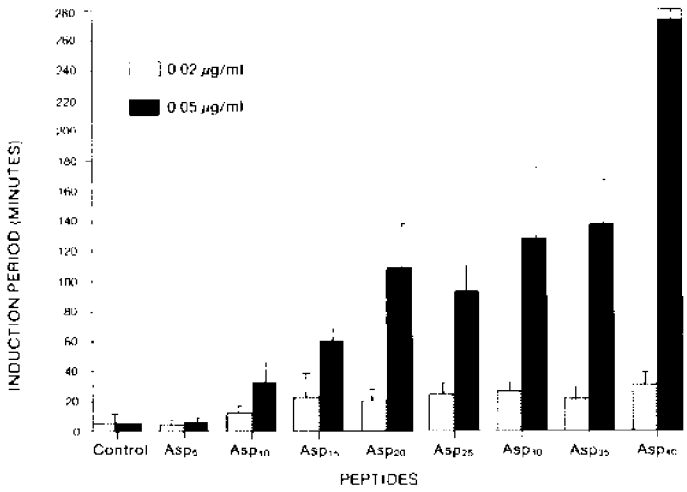

Figure 2. The effect of molecular size of polyaspartate molecules on $CaCO_3$ nucleation, as measured using a pH-drift nucleation assay. Values for induction period are plotted as means ± standard deviation, n = 3 to 9.

These results indicated that the Asp_{15} molecules had significant activity and would serve as acceptable model polyanions for use in attaching hydrophobic polyalanine domains.

Results from the screening assay comparing the general inhibitory activity of some polyaspartate molecules and a polyaspartate-alanine molecule is seen in Figure 3. These results indicated a general enhancement of activity of the alanine-containing polyaspartate. However, whether the enhancement was due to effects on crystal nucleation, crystal growth, or both was not determined in this approach. Accordingly, the effects of polyaspartate and polyaspartate-alanine molecules on both crystal nucleation using the nucleation assay (Figure 4) and crystal growth using the seeded-crystal assay (Figure 5) were measured. Analysis of variance (Zar 1974) of differences in mean values of induction periods indicated a significant enhancement of inhibition of nucleation by $Asp_{15}Ala_8$ relative to the 3 smallest alanine-containing peptides and to Asp_{15} and Asp_{25} ($p < 0.01$). A similar analysis for rates of crystallization (Figure 5) did not reveal significant differences between the alanine-containing polyaspartate and Asp_{15} at $p < 0.05$, although the data were suggestive of some level of enhancement of inhibition of crystal growth by the alanine-containing peptides. Overall, the results indicated an increased inhibition of crystal nucleation by the polyaspartate-

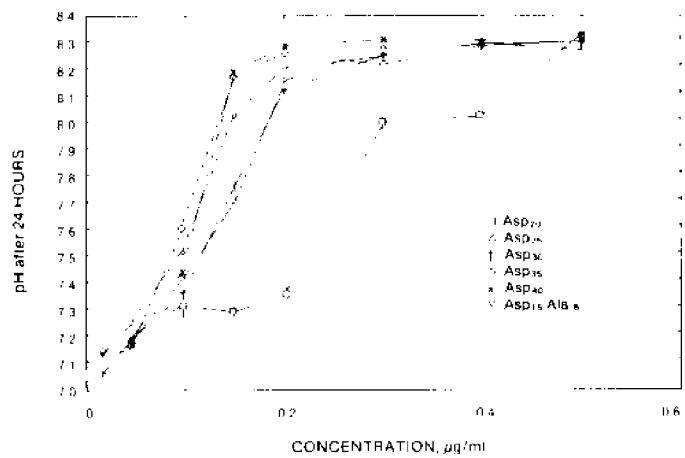

Figure 3. General inhibitory action of polyaspartate molecules and a polyaspartate-alanine measured using the screening assay for $CaCO_3$ crystallization. Values are plotted as means with standard deviations shown for selected points (n = 3 to 6).

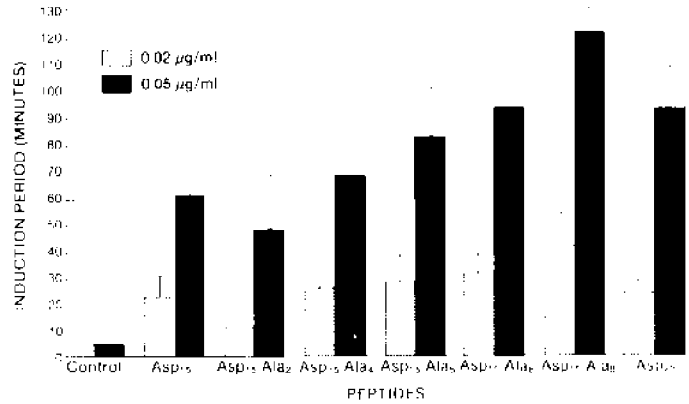

Figure 4. The effect of polyaspartate and polyaspartate-alanine molecules on $CaCO_3$ nucleation, as measured using a pH-drift nucleation assay. Values are plotted as means ± standard deviation, n = 3 to 9.

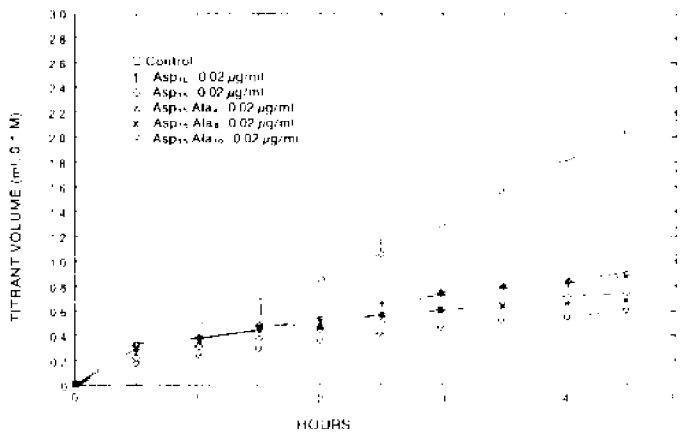

Figure 5. The effect of polyaspartate and polyaspartate-alanine molecules on $CaCO_3$ crystal growth as measured using a seeded-crystal, constant composition assay. Values are plotted as means with standard deviations shown for selected points (n = 3).

alanine molecules, but little effect on inhibition of crystal growth itself due to the presence of the alanine domains.

The effects on $CaCO_3$ crystallization of a variety of model peptides that are potential analogs to components of natural organic matrix proteins are summarized in Table I. The aspartate-glycine copolymers and aspartate-serine-glycine terpolymers were not particularly effective inhibitors of $CaCO_3$ formation. Only the polyaspartate molecules exhibited levels of activity that are similar to those of the natural protein inhibitors from oyster shell.

Discussion

The general purpose of this study was to evaluate the idea that an hydrophobic domain added to a polyanionic protein might enhance the inhibitory activity of the protein with respect to mineral formation. Before this could be addressed, however, some questions about the nature of the effects of simple polyanionic peptides on mineral formation needed to be answered.

Polyaspartate, for example, had been studied as a simple model of protein matrix from both calcium carbonate and calcium phosphate biominerals, including observations of its general activity as an inhibitor of crystallization (e.g., Hay *et al.* 1979; Sikes and Wheeler 1983). Sikes and Wheeler (1985) reported that the activity of polyaspartate on a weight basis as an inhibitor of $CaCO_3$ formation increased as molecular weight decreased

Table 1. Inhibition of $CaCO_3$ crystallization by synthetic peptides as measured using a pH-drift nucleation assay. Relative rates of crystal growth are given as the slope of the curve during crystallization. The oyster matrix protein is the highly hydrophilic fraction obtained from reverse phase chromatography (see Wheeler *et al.*, this volume) with a molecular weight based on globular protein standards of approx. 50 kDa. Values are reported as means ± standard deviations, n = 3 to 9.

Peptide	Concentration μg/ml	Induction Period, Min.	Crystal Growth Rate, pH/Min
CONTROL	—	7.1 +/- 1.96	0.048 +/- 0.0041
H-$(ASP)_{20}$-OH	0.05	93.0 +/- 16.4	0.0205 +/- 0.0009
H-$(ALA)_6$-$(ASP)_{15}$-OH	0.05	123 +/- 20.1	0.0047 +/- 0.0013
H-$(ALA)_{10}$-$(ASP)_{15}$-OH	0.10	32.0 +/- 10.4	0.042 +/- 0.0039
H-$(GLY\text{-}ASP)_{10}$-OH	0.10	36.0 +/- 5.20	0.047 +/- 0.0097
H-$(ALA)_6$-$(GLY\text{-}ASP)_7$-OH	0.20	7.2 +/- 0.83	0.048 +/- 0.0042
H-$(SER\text{-}ASP)_{10}$-OH	0.10	29.8 +/- 4.99	0.048 +/- 0.0040
H-$(GLY\text{-}SER\text{-}ASP)_7$-OH	0.10	18.0 +/- 4.24	0.041 +/- 0.0034
H-$(GLY\text{-}SER\text{-}ASP)_{10}$-OH	0.10	9.1 +/- 1.16	0.048 +/- 0.006
Oyster Shell Matrix (RP-I)	0.05	56.0 +/- 26.0	0.035 +/- 0.0088
Polyaspartate (MW 20,000)	0.05	32.1 +/- 9.20	0.038 +/- 0.0027

over the range 20,000 to 8,500 daltons. Similar results were obtained for polyacrylate, used as an inhibitor of mineral scale formation industrially, with highest inhibitory activity on a weight basis at around 2000 daltons (Rohm and Haas 1985).

In view of these observations, we undertook a study of the inhibitory activity of a set of low molecular weight polyaspartate molecules to determine the optimum molecular size for inhibition of $CaCO_3$ formation, expressed on a weight basis of polyaspartate. The idea was that knowing the relationship between molecular size and activity of polyaspartate would allow selection of an appropriate polyaspartate molecule for attaching hydrophobic domains. The effect of this modification on inhibitory activity, could then be evaluated with consideration given to possible effects of modifying molecular size itself, independent of the hydrophobic or polyanionic nature of the added domain.

Results were presented on a weight basis, as is often the case in studies in polymer science, rather than a molar basis not only because commercial uses are on a weight basis but also because several smaller molecules of a homogeneous polymer may be functionally equivalent to one larger molecule of the same polymer. Therefore, the total mass of polymer rather than the total number of molecules can be the functionally important parameter.

As seen in Figure 2, the inhibitory activity of polyaspartate increased with molecular size over the range of 5 to 40 residues at doses of 0.02 and 0.05 μg of peptide/ml. The effect was clearer at the higher dose, possibly due to removal of proportionally less of peptides by adsorption onto surfaces of the reaction vessel and electrode when compared to lower doses. There was significant activity in polyaspartate molecules of 15 residues, and this size was selected for attachment of hydrophobic domains of 2 to 10 alanine residues at the N-terminus. The reason why polyaspartate molecules of 5 residues or less are not effective inhibitors of crystallization is not known, although it seems likely that, at some level lower numbers of negatively-charged residues per molecule would result in lower affinity for crystals.

It is equally unclear as to why a polyaspartate of 40 residues would be such an effective molecular size for inhibition of crystal nucleation. It is possible that this molecular size matches in some fashion the size of $CaCO_3$ crystal nuclei that form during the nucleation assay. Crystal nuclei are theoretical entities and therefore to date have not been directly observable. Although thermodynamic considerations suggest a possible size of a stable crystal nucleus as small as 8 ion pairs (Stumm and Morgan 1981), the fact that polyaspartate-40 molecules seem to interact with the crystal nuclei most effectively suggests that the nuclei may be much larger than this.

The addition of an hydrophobic domain onto Asp_{15} molecules clearly enhanced inhibitory activity as compared to comparable polyaspartate molecules. This was seen in screening assays (Fig. 3) and confirmed in both nucleation assays (Fig. 4) and to a lesser extent, in seeded-crystal growth assays (Fig. 5). The primary effect seemed to be on crystal nucleation.

There is some theoretical basis for this differential effect of polyanionic-hydrophobic peptides on crystal nucleation relative to crystal growth. That is, the growth of seed crystals in the absence of inhibitory molecules generally is thought to be limited not by diffusion but rather by the rate of surface reactions in which adsorbed lattice ions become incorporated into crystal growth sites (Nancollas and Reddy 1971; Nancollas 1979). This conclusion is based on calculated energies of activation of crystallization of about 11.0 kcal/mole (e.g., Howard *et al.* 1960), which is too high for a diffusion-controlled mechanism, and on the reported lack of effect of the rate of stirring on rates of seeded crystal growth.

On the other hand, diffusion often may be the rate-limiting factor for crystal nucleation. For example, the rate of stirring is critical to the reproducibility of the nucleation assays, with decreased stirring leading to greatly increased induction periods. In addition, the surface reactions that are thought to be rate-limiting during crystal growth are not especially relevant to crystal nucleation (Reddy 1988). Therefore, the hypothesized action of the polyanionic-hydrophobic peptides and proteins as diffusion barriers would result in more pronounced effects on crystal nucleation than crystal growth, as was observed.

The enhancement of activity of polyanionic industrial polymers as crystallization inhibitors and dispersants by inclusion of hydrophobic and nonpolar monomers also has been reported. For example, when acrylamide was polymerized with acrylate, a copolymer containing 30% acrylamide showed improved performance relative to that of polyacrylate (Pierce and Hoots 1988). Although sequence data for the copolymer was not available and the distribution of the acrylamide and acrylate monomers was thought to be random, it is possible that predominantly polyanionic and nonpolar domains occurred in the copolymer. For example, in thermally polymerized peptides, anionic and hydrophobic residues spontaneously clustered together during synthesis, probably due to the mutual affinity of like residues (Melius 1979). Thus, it seems possible that the industrial polyanionic-hydrophobic polymers have structures and a mechanism of action analogous to that of the PAH peptides.

The role of the hydrophobic zone as a diffusion barrier seems straightforward, provided it is present in sufficient coverage and effects a sufficient separation of surface from bulk phase. The necessary dimensions of an hydrophobic barrier can be calculated from the dimensions of the residues, given the estimated distance of hydrophobic interactions of 0.5 nm compared to the roughly 3 nm over which electrostatic interactions occur (Norde 1983).

Thus an hydrophobic zone of about 3 nm would be required to prevent attraction between ions in the bulk phase and surface charges of nuclei. Accepting that the bond length in peptides measured along the backbone is about 0.35 nm per residue (Corey and Pauling 1953), it is evident that only about 10 or so hydrophobic residues would be needed to interrupt the electrostatic interaction of lattice ions in solution and forming crystal nuclei.

This is particularly interesting in view of the finding (Figure 4, Table 1) that an hydrophobic domain larger than 8 alanine residues did not seem to further enhance inhibitory activity. In fact, as seen in Table 1, activity of polyaspartate-15-alanine-10 as a nucleation inhibitor was less than that of the other polyaspartate-alanine molecules, suggesting that increasing the size of the hydrophobic domain beyond a certain level is not useful in inhibition of crystallization. It is also possible that the molecules may begin to form hydrophobic interactions among themselves at a certain size of hydrophobic domain. This might modify their function as well.

In this regard, the hydrophobic domains of polyanionic matrix proteins from biominerals are quite extensive, suggesting that they fulfill roles beyond inhibition of crystallization. Some possibilities for these roles have been reviewed elsewhere (Wheeler and Sikes 1989) and include promotion of interactions with more hydrophobic matrix proteins, provision of cell recognition sites, and enhancement of mobility of the matrix proteins within cells and tissues en route to the mineralization front.

The primary function of the polyanionic regions of matrix proteins, on the other hand, may well be limited to regulation of mineralization through direct matrix-crystal interactions. Although possible inhibition of crystallization by typical globular proteins like serum albumin (Hay and Moreno 1979) and polycationic peptides like polylysine (Hay *et al.* 1979; Sikes and Wheeler 1983, 1985) has been studied, only the polyanionic matrix molecules and polyamino acids like polyaspartate inhibited crystallization. Interestingly, this was true even though each of the molecules bind to the crystals (Wheeler and Sikes 1989), indicating that only certain binding sites on crystal surfaces are involved in crystal formation.

For effective inhibition of $CaCO_3$ crystallization, evidently the anionic residues must be clustered together. As shown in Table 1, only the polyaspartate-containing peptides had inhibitory activity on the level of that observed for the most potent matrix protein from oyster shell. Interruption of polyaspartate regions of molecules by the neutral residues glycine and serine significantly diminished the inhibitory activity of the peptides. This supports the observations of Wheeler *et al.* (1988) and Rusenko (1988) that the matrix from oyster shell contains domains of polyaspartate separate from other regions that may be enriched in phosphoserine, glycine, and some hydrophobic residues. If this matrix had significant portions of ordered copolymers of aspartate-glycine, aspartate-serine, as suggested in earlier studies (e.g., Weiner and Hood 1975; Weiner 1983), or aspartate-serine-glycine then it would not have the levels of inhibitory activity that have been observed. This is not to say that ordered copolymers do not exist in the matrix from oyster shell, but that they may be present in relatively small amounts, perhaps at highly localized initiation sites (Weiner and Traub 1984).

In view of the fact that most of the serine residues of the matrix protein from oyster shell are phosphorylated (Wheeler and Sikes 1989; Borbas *et al.* unpubl.), it will be interesting to evaluate the influence of phosphoserine residues on inhibitory activity of peptides and matrix proteins. The importance of phosphorylation or phosphonation of crystallization inhibitors has been the subject of some excellent studies involving both small organic compounds (e.g., Reddy and Nancollas 1973; Williams and Sallis 1982) and proteins (Lee and Veis 1980; Veis 1985; Aoba *et al.* 1984; Schlesinger *et al.* 1988). In fact, the effect on regulation of crystallization by anionic derivatives of proteins in general, including sulfated residues, would be of interest as well and promises to be a fruitful area of research (Sikes *et. al.* 1989).

Acknowledgements

This work was supported in part by grants from the Mississippi-Alabama and the South Carolina Sea Grant Consortia, the Alabama Research Institute, the Office of Naval Research, and the National Science Foundation.

References

Aoba, T., E.C. Moreno and D.I. Hay. 1984. Inhibition of apatite crystal growth by the amino-terminal segment of human salivary acidic proline-rich proteins. Calcif. Tissue Int. 36:651-658.

Benson, S., H. Sucov, L. Stephens, E. Davidson and F. Wilt. 1987. A lineage- specific gene encoding a major matrix protein of the sea urchin embryo spicule. Dev. Biol. 120:499-506.

Bergot, J.B., R. Noble, and T. Geiser. 1986. TFMSA/TFA cleavage and deprotection in SPPS. Applied Biosystems Bulletin.

Butler, W.T., M. Bhown, M.T. Dimuzio, W.C. Cathran and A. Linde. 1983. Multiple forms of rat dentin phosphoproteins. Arch. Bioch. Biophys. 225:178-186.

Corey, R.B. and L. Pauling. 1953. Fundamental dimensions of polypeptide chains. Proc. Roy. Soc. Lond. Ser B 141:10-20.

Hay, D.I. and E.C. Moreno. 1979. Differential adsorption and chemical affinities of proteins for apatitic surfaces. J. Dent. Res., Special Issue B 58(B):930-940.

Hay, D.I., E.C. Moreno, and D.H. Schlesinger. 1979. Phosphoprotein- inhibitors of calcium phosphate precipitation from salivary secretions. Inorg. Persp. Biol. Med. 2:271-285.

Howard, J.R., G.H. Nancollas and N. Purdie. 1960. The precipitation of silver chloride from aqueous solutions. Trans. Faraday Soc. 56:278-283.

Lee, S.L. and A. Veis. 1980. Cooperativity in calcium ion binding to repetitive, carboxylate-serylphosphate polypeptides and the relationship of this property to dentin mineralization. Int. J. Peptide & Protein Res. 16:231-240.

Melius, P. 1979. Non-random non-ribosomal assembly of amino acids in proteins and proteinoids. Biosystems 11:125-132.

Nancollas, G.H. 1979. The growth of crystals in solution. Adv. Coll. Int. Sci. 10:215-252.

Nancollas, G.H. and M.M. Reddy. 1971. The crystallization of calcium carbonate: calcite growth mechanisms. J. Coll. Int. Sci. 37:824-830.

Norde, W. 1983. The role of charged groups in the adsorption of proteins at solid surfaces. Croat. Chem. Acta 56:705-720.

Oldberg, A., A. Granzen and D. Deinegard. 1986. Cloning and sequence analysis of rat bone sialoprotein (osteopontin) cDNA reveals an Arg-Gly-Asp cell-binding sequence. Proc. Nat. Acad. Sci. USA 83:8819-8823.

Pierce, C.C. and J.E. Hoots. 1988. Use of polymers to control scale in industrial cooling water and boiler water systems. In: C.S. Sikes and A.P. Wheeler (eds.) Chemical Aspects of Regulation of Mineralization. University of South Alabama Publication Services, Mobile, AL.

Poser, J.W., F.S. Esch, N.C. Ling and P.A. Price. 1980. Isolation and sequence of the vitamin K-dependent protein from human bone. J. Biol. Chem. 255:8685-8691.

Prince, C.W., T. Ossawa, W.T. Butler, M. Tomana, A.S. Bhown, M. Bhown and R.E. Schrohenloher. 1987. Isolation characterization and biosynthesis of a phosphorylated glycoprotein from rat bone. J. Biol. Chem. 262:2900-2907.

Reddy, M.M. 1988. Physical-chemical mechanisms that affect regulation of crystallization. In: C.S. Sikes and A.P. Wheeler (eds.) Chemical Aspects of Regulation of Mineralization. University of South Alabama Publication Services, Mobile, AL.

Reddy M.M. and G.H. Nancollas. 1973. Calcite crystal growth inhibition by phosphonates. Desalination 12:61-73.

Robbins, Lisa L. 1987. Morphologic variability and protein isolation and characterization of recent planktonic foraminifera. Ph.D. Dissertation. University of Miami, Coral Gables, FL. 302 p.

Rohm and Haas Company. 1985. Acrysol QR-1086, Calcium phosphate stabilizer; polymer additives. Cs-321.

Rusenko, K.W. 1988. Studies on the structure and function of the organic matrix proteins extracted from the shell of the oysters, *Crassostrea virginica*. Ph.D. Dissertation. Clemson University, Clemson, SC. 276 p.

Sarin, V.K., S.B.H. Kent, J.P. Tam, and R.B. Merrifield. 1981. Quantitative monitoring of solid-phase peptide synthesis by the ninhydrin reaction. Anal. Bioch. 117:147-157.

Schlesinger, D.H., A. Buku, H.R. Wyssbrod and D.I. Hay. 1988. Solution synthesis of phosphoseryl-pohosphoserine, a partial analogue of human salivary statherin, essential for primary and secondary precipitation of calcium phosphate in human saliva. In: C.S. Sikes and A.P. Wheeler (eds.) Chemical Aspects of Regulation of Mineralization. University of South Alabama Publication Services, Mobile, AL.

Schlesinger, D.H. and D.I. Hay. 1979. Complete amino acid sequence of human anionic proline-rich protein (PRP-IV). In: E. Gross and J. Meienhofer (eds.) Peptides: Proceedings of the 6th American Peptide Symposium. p. 133-136.

Schlesinger, D.H. and D.I. Hay. 1986. The complete covalent structure of a proline-rich phosphoprotein, PRP-2, an inhibitor of calcium phosphate crystal growth from human parotid saliva. Int. J. of Peptide & Protein Res. 27:373.

Sikes, C.S. and A.P. Wheeler. 1983. A systematic approach to some fundamental questions of carbonate calcification. In: P. Westbrock and E.W. deJong (eds.) Biomineralization and Biological Metal Accumulation. Reidel Publishing Co., Dordrecht. pp. 285-289.

Sikes, C.S. and A.P. Wheeler. 1985. Inhibition of inorganic or biological $CaCO_3$ deposition by polyamino acid derivatives. U.S. Patent #4,534,881. 16 p.

Sikes, C.S. and A.P. Wheeler. 1986. The organic matrix from oyster shell as a regulator of calcification *in vivo*. Biol. Bull. 170:494-505.

Sikes, C.S., A.P. Wheeler, and K.W. Rusenko. 1989. Regulation of calcium carbonate and phosphate formation by matrix proteins and their synthetic analogs. Third International Conference on the Chemistry and Biology of Mineralized Tissues. Abstract.

Stumm, W. and J.J. Morgan. 1981. Aquatic Chemistry. Wiley-Interscience, New York.

Veis, A. 1985. Phosphoproteins of dentin and bone. Do they have a role in matrix mineralization? In: W.T. Butler (ed.) The Chemistry and Biology of Mineralized Tissues. Ebsco Media, Birmingham, AL. p. 170.

Wasi, S., T. Hofmann, J. Sodek, L. Fisher, H.C. Tenebaum and J.D. Termine. 1985. Studies on the primary structure of osteonectin. In: W.T. Butler (ed.) The Chemistry and Biology of Mineralized Tissues. Ebsco Media, Birmingham, AL. p. 434.

Weiner, S. 1983. Mollusk shell formation: Isolation of two organic matrix proteins associated with calcite deposition in the bivalve *Mytilus californianus*. Biochemistry 22:4138-4145.

Weiner, S. and L. Hood. 1975. Soluble protein of the organic matrix of mollusc shells: a potential template for shell formation. Science 190:987-989.

Weiner, S. and W. Traub. 1984. Macromolecules in mollusc shells and their functions in biomineralization. Phil. Trans. Roy. Soc. Lond. B304:425-434.

Wheeler, A.P., J.W. George and C.A. Evans. 1981. Control of calcium carbonate nucleation and crystal growth by soluble matrix of oyster shell. Science 212:1397-1398.

Wheeler, A.P., J.W. George, K.W. Rusenko and C.S. Sikes. 1987. Evaluation of calcium binding by molluscan shell organic matrix and its relevance to biomineralization. Comp. Biochem. Physiol. 87B:453-460.

Wheeler, A.P., K.W. Rusenko, D.M. Swift and C.S. Sikes. 1988. Regulation of *in vitro* and *in vivo* $CaCO_3$ crystallization by fractions of oyster shell organic matrix. Mar. Biol. 98:71-80.

Wheeler, A.P. and C.S. Sikes. 1984. Regulation of carbonate calcification by organic matrix. American Zool. 24:933-934.

Wheeler, A.P. and C.S. Sikes. 1989. Matrix-crystal interactions in $CaCO_3$ biomineralization. In: S. Mann, J. Webb and R.J.P. Williams (eds.) Chemical Perspectives on Biomineralization. VCH Publishers, Weinheim, W. Germany, in press.

Williams, G. and J.D. Sallis. 1982. Structural factors influencing the ability of compounds to inhibit hydroxyapatite formation. Calcif. Tissue Int. 34:169-177.

Wong, R. and A. Bennick. 1980. Tryptic digests of PRP-1. J. Biol. Chem. 255:5943-5948.

Wong, R., T. Hofmann, and A. Bennick. 1979. The complete primary structure of a proline-rich phosphoprotein from human saliva. J. Biol. Chem. 254:4800-4808.

Zar, J.H. 1974. Biostatistical Analysis. Prentice-Hall Inc., Englewood Cliffs, N.J.

Steve Sikes is an Associate Professor of Biological Sciences at the University of South Alabama. He received the B.S. (1971) and M.S. (1973) in biological sciences at John Carroll University in Cleveland and the Ph.D. (1976) in the limnology and oceanography program of the University of Wisconsin-Madison. Steve did post-doctoral work at Duke University and spent a year as a participant in a Fulbright exchange at the University of the West Indies in Jamaica before taking his current position in 1981. His work on mechanisms of biomineralization has included studies of pH control, ion transport, enzymatic involvement, and the role of organic matrix. His current research is focused on chemical interactions of dissolved polyelectrolytic peptides and industrial polymers with solid surfaces.

Chemical Aspects of Regulation of Mineralization. C.S. Sikes and A.P. Wheeler, editors, University of South Alabama Publication Services, Mobile, Alabama, 1988.

Control of Calcium Carbonate Nucleation in Pre- and Postecdysial Crab Cuticle

Robert D. Roer, Sybil K. Burgess, Charles G. Miller and Mary Beth Dail

Institute for Marine Biomedical Research
and Department of Chemistry,
University of North Carolina at Wilmington
Wilmington, North Carolina 28403

ABSTRACT

Prior to molting (ecdysis), crabs deposit the two outermost layers of the new cuticle beneath the old exoskeleton, while at the same time they resorb the mineral and organic components of the old cuticle. These new (pre-exuvial) layers of the cuticle remain uncalcified until immediately after ecdysis, whereupon calcite deposition is evident within a few hours. At least partial control of calcite nucleation resides in the structure of the cuticle itself, since pre-exuvial cuticle removed from the animal and stripped of underlying hypodermal tissue is incapable of calcifying *in vitro*, while cuticle removed from crabs just after ecdysis does calcify under the same circumstances. Electrophoretic analysis of EDTA digests of pre- and postecdysial cuticle reveal differences in protein composition which may account for the onset of nucleation.

Introduction

The integument of crustaceans is composed of an exoskeleton or cuticle underlain by a cellular hypodermis. The exoskeleton is heterogeneous, having four discrete layers (Richards 1951; Travis 1963). The outermost layer of the cuticle is the thin epicuticle, which consists of tanned lipoprotein impregnated with calcite. The exocuticle and the endocuticle are proximal to the epicuticle. Both layers contain fibrils of chitin and protein arranged in parallel lamellae stacked with a continuously changing orientation. The exocuticle is hardened, in part, by quinone tanning, and both layers are impregnated with calcite crystals situated between the fibers of the organic matrix. The innermost layer is the membranous layer, which is in contact with the cellular hypodermis and is composed of chitin and protein, but which lacks mineral (see Roer and Dillaman 1984 for review).

It is now clear that the chemical nature of the organic matrix of the crustacean cuticle plays a significant role in the determination of the crystal habit of the mineral. As shown by Roer and Dillaman (1984), the decalcified cuticles of all crabs studied display a regular array of chitin-protein fibrils. In the family of xanthid crabs, however, the calcite crystals do not simply fill in the spaces between the organic fibrils as they do in the family Cancridae. Instead, there are domains of calcitic spherulites arranged in a lamellar pattern in certain areas, and nonlamellar domains comprised of randomly arranged, larger spherules in other areas. There is no corresponding morphological difference in the organic matrix between these two domains.

The rigid nature of the crustacean integument necessitates that animals undergo a molt (ecdysis, exuviation) in order to grow. The cyclic shedding of the exoskeleton and its replacement with a new and larger cuticle is referred to as the molt cycle. In preparation for the molt (a stage referred to as premolt or stage D; Drach 1939; Drach and Tchernigovtzeff 1967), the hypodermis separates from the old cuticle, organic and inorganic elements of the old cuticle are resorbed through the hypodermis, and the outermost two layers of the new cuticle (the pre-exuvial epi- and exocuticles) are deposited. As the molt approaches these two pre-exuvial layers are structurally complete, but do not become sclerotized or calcified until just after the animal molts (Paul and Sharpe 1916; Drach 1939; Travis 1963, 1965; Travis and Friberg 1963). The fact that the pre-exuvial layers do not mineralize, despite the fact that Ca^{2+} and $CO_3^{=}$ are being resorbed through these layers and are present in metastable concentrations (Travis and Friberg 1963) provides a valuable model system for the control of the onset of nucleation. We have a system which displays a discrete chronology in which the ability to mineralize is turned on at the time of the molt, and from which tissue may be acquired for analysis both before and after this critical event.

We have been studying the changes which occur in the pre-exuvial cuticle at the time of the molt to try to ascertain what is responsible for the prevention of mineral nucleation in the cuticle before ecdysis, and the onset of nucleation immediately following the molt.

Methods

Two species of brachyuran crabs were employed in the present studies: the blue crab, *Callinectes sapidus*, and the sand fiddler crab, *Uca pugilator*. Premolt blue crabs were obtained from a local shedding operation, and fiddler crabs were collected from tidal flats in Wrightsville Beach, NC by hand. All animals were held in aquaria in local sea water, and were fed Purina trout chow.

For both the *in vitro* recalcification and biochemical studies detailed below, pieces of dorsobranchial carapace were removed from both sides of crabs, and stripped of underlying hypodermal tissue by placing the cuticles in Petri dishes of crustacean ringer solution (Roer 1980) or isotonic NaCl solution (270 mM), and rubbing them free of soft tissue with a cotton swab.

In Vitro Mineralization

Pieces of pre-exuvial cuticle were moved from premolt (stage D_2-D_4) and newly molted cuticle from postmolt (stage A) *Uca*, and stripped of hypodermis. All cuticular pieces were then fixed for at least 24 hr in 4% paraformaldehyde (pH 8.0-8.3). Both pre- and postmolt cuticles were immersed in 0.1M EDTA in 4% paraformaldehyde (pH 8.0-8.3) for at least 24 hr, and until no calcite induced birefringence was observed when the cuticular pieces viewed through crossed polarizers in a Zeiss microscope.

Following the decalcification procedure, cuticles were washed in 4% paraformaldehyde for 4 days, with daily changes of fixative, to remove the EDTA, as contamination might cause heterogeneous nucleation (Weiner 1979, 1983). The mineralization procedure consisted of alternately placing cuticular pieces in 200 ml of 0.5M $CaCl_2$ and 200 ml of 0.5M $NaHCO_3$, with a 30 sec. rinse in distilled water interspersed. All solutions were adjusted to a pH of 8.0-8.3, and were agitated on a magnetic stir plate. The

mineralization cycle was repeated either 2 or 4 times. Pieces of cuticle were mounted in glycerin on glass slides, and observed through crossed polarizers to assess the degree of calcite accretion.

Gel Electrophoresis

Pieces of cuticle were removed and stripped of hypodermis as described above, and were minced into test tubes containing ten volumes of ice cold 0.1M EDTA (pH 8.0). The tissues were then homogenized with a Tekmar Tissumizer for 5 min. with the sample kept in an ice bath. The homogenate was transferred to a 125 ml Ehrlenmeyer flask and agitated on a Vibrax rotary shaker in the refrigerator for 40 hrs. The tissue slurry was re-homogenized and centrifuged at 20,000g in a Sorvall RC-2B refrigerated centrifuge. Supernatants were frozen in aliquots until immediately before being used for electrophoresis.

Tissue extracts were assayed for protein concentration using a Bio-Rad protein assay. From 50 to 200 μl of sample (yielding 50-80 μg of protein) was applied to a 3mm thick polyacrylamide slab gel (Elcam, CAMAG) consisting of a 2.5% stacking gel (25% crosslinking) on top of a 7% resolving gel (2.6% crosslinking). A TRIS-glycine buffer (1.2g/l TRIS, 5.8g/l glycine, pH 8.3) was used, and the apparatus was run at 500V at 25°C (175-116 mA). Gels were stained overnight in Coomassie blue, and destained in 10% trichloroacetic acid.

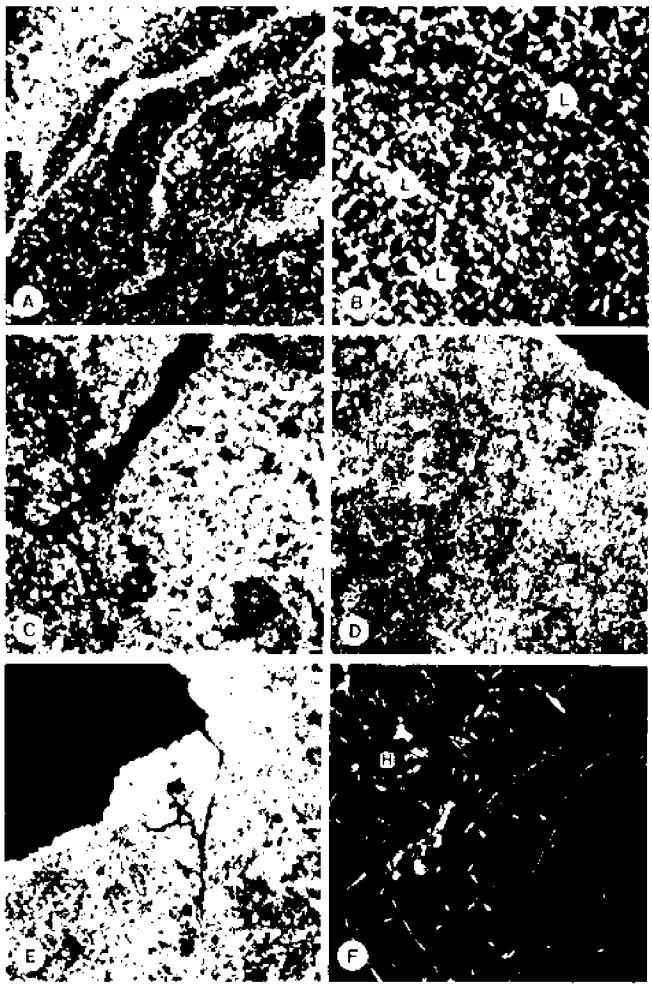

PLATE 1: Untreated pieces of dorsobranchial carapace of *Uca pugilator* viewed through crossed polarizers. X31.
A. Cuticle removed from animal within 24 hrs. of the molt.
B. Cuticle from animal 1 day postmolt, showing lines (L) of denser mineralization.
C,D, & E. Cuticles removed from animals 2, 3, and 4 days postmolt, respectively.
F. Pre-exuvial cuticle removed from beneath the old carapace of a premolt (stage D_2) crab.

Results

Observation of undecalcified pre-exuvial premolt cuticles removed from *Uca* just prior to the molt revealed no evidence of calcite crystal formation, and only displayed form birefringence due to folds in the cuticle, setae and tegumental ducts (Plate 1,F). Within only a few hours after the molt, mineral nucleation was present, and was evident as birefringent crystals (Plate 1,A). As the animals progressed through days 1 to 4 postmolt, the degree of mineralization of the cuticle increased markedly, and the individual crystals fused into large birefringent areas (Plate 1,B-E). Following fixation and treatment with EDTA, only form birefringence was apparent in the pre- and postmolt cuticles and all were indistinguishable from the untreated pre-exuvial cuticle.

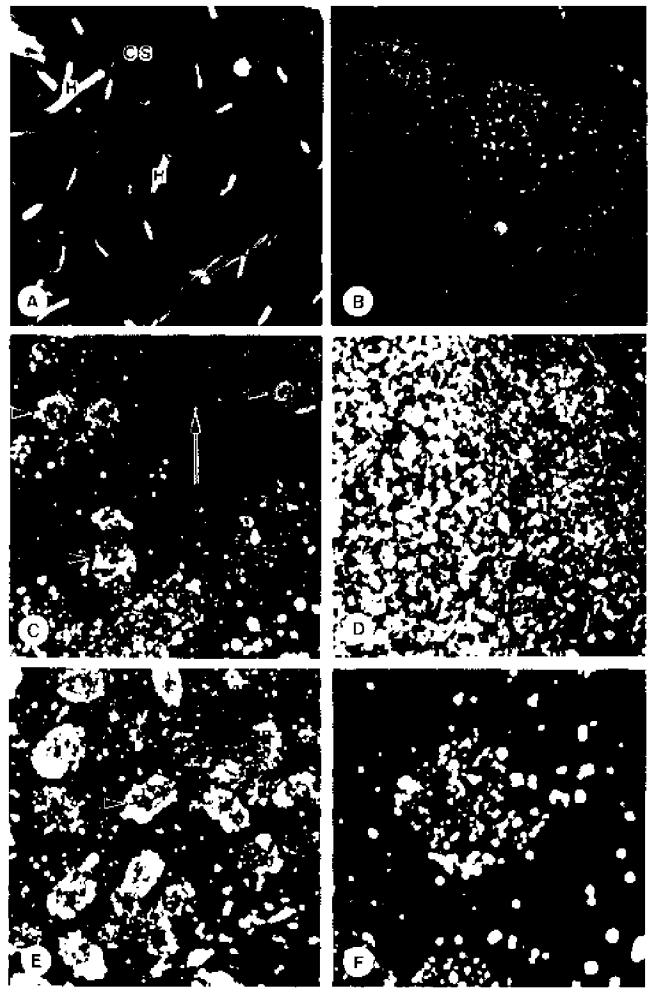

PLATE 2: Pieces of *Uca* dorsobranchial carapace following *in vitro* mineralization procedure and viewed through crossed polarizers.
A. Pre-exuvial cuticle (stage D) after 2 cycles (4 hr.) in mineralization media. Note the form birefringence associated with cuticular hairs (H) and cuticular sutures (CS). X31.
B. As in A, but following 8 hr. mineralization procedure. Note occasional ectopic crystals. X31.
C. Cuticle removed from crab within 24 hrs. of molting and subjected to 4 hr. mineralization procedure. Note individual crystals and crystals in rosette-like clusters (arrows). X125.
D. As in C, but following 8 hr. mineralization procedure. Note increased densities of rosettes (arrow). X31.
E. As in D. X125.
F. As in D. X313.

Following 4 or 8 hrs. of *in vitro* mineralization, the pre-exuvial cuticles generally showed only form birefringence, although occasionally a few scattered crystals were present on the cuticular surface (Plate 2,A-B). Cuticular pieces removed from animals within 24 hrs. of its molt, however, displayed a substantial accretion of birefringent crystals which were acid labile and which possessed the typical 90° birefringence extinction and rhombohedral shape of calcite. The crystals appeared individually and in rosette shaped clusters (Plate 2, C-F). The extent of crystal accretion induced by the mineralization procedure increased in cuticles removed from animals 1 to 4 days postmolt (Plate 3, A-F). The crystal growth observed in the postmolt cuticles was not simply ectopic since crystals were observed at various focal planes within the sections.

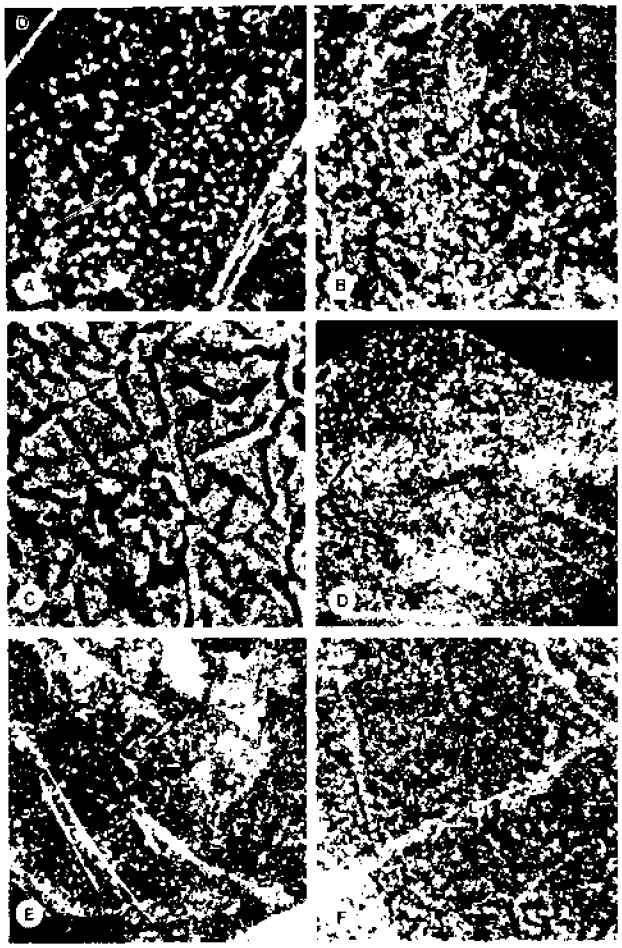

PLATE 3. Pieces of *Uca* dorsobranchial carapace following *in vitro* mineralization procedure and viewed through crossed polarizers. X31.

A. Cuticle removed from animal 1 day postmolt and subjected 4 hr. mineralization procedure. Dark area (D) in upper right represents the edge of the section. Both rosettes and individual crystals are apparent (arrows).
B. As in A, but following 8 hr. mineralization procedure.
C. Cuticle removed from animal 2 days postmolt and subjected to 4 hr. mineralization procedure.
D. As in C, but following 8 hr. mineralization procedure.
E. Cuticle removed from animal 3 days postmolt and subjected to 4 hr. mineralization procedure.
F. As in E, but following 8 hr. mineralization procedure. Note heavier deposition along lines (L).

The electrophoretic patterns of the cuticular proteins revealed marked differences in tissues removed from *Callinectes* at different molt stages. The pre-exuvial cuticles possessed three prominent bands which were less evident in cuticles removed from crabs in the process of molting (stage E), and virtually absent in newly molted cuticle (Plate 4).

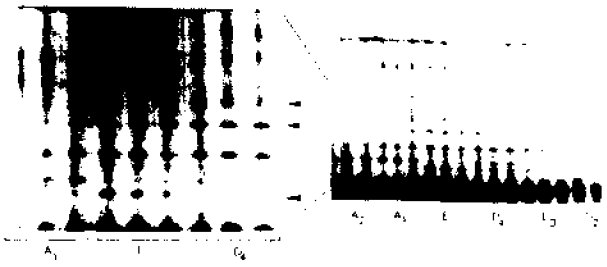

PLATE 4. Polyacrylamide slab gel of protein extracts derived from stage D, E, and A carapace of *Callinectes*, stained with Coomassie blue. Note several protein bands disappear at the time of the molt (arrows).

Discussion

Travis (1963, 1965) and Travis and Friberg (1963) have suggested that the prevention of mineral deposition in the pre-exuvial layers of crab cuticle was due to action of the underlying hypodermal layer via control of ion concentrations and pH in the mineralizing microenvironment. An alternative hypothesis, that mineral nucleation is under the control of the cuticular organic matrix, was suggested by Yano (1972) and Roer (1979). Yano (1972) suggested that an acid mucopolysaccharide complexed to the protein of the pre-exuvial matrix inhibits precocious calcification.

The present study supports the contention that mineral nucleation is at least in part under the control of the organic matrix of the crab cuticle. Removal of the hypodermis and fixation of the tissue precludes any active hypodermal involvement in the prevention of *in vitro* mineral nucleation in the pre-exuvial cuticle and accretion of crystals in the postmolt cuticle.

That changes in fact take place in the organic matrix is apparent in the abrupt and pronounced differences in the protein electrophoretic pattern evident at the time of the molt and ensuing 2 to 8 hours. At least three protein bands begin to disappear just as the crab enters the molt, and disappear completely concomitant with the onset of calcite deposition. The role of these proteins in the prevention of precocious calcification of the pre-exuvial cuticle of crabs is circumstantial at present, but they present themselves as likely candidates for further study.

The crustacean cuticle is particularly well suited for the study of the control of nucleation, due to the discrete nature of the onset of mineralization. The change in the ability of the tissue to mineralize is total; the cuticle shows no evidence of crystal deposition prior to the molt, nor can it be induced to mineralize *in vitro*. The temporal change is also discrete and very predictable; the ability of the cuticle to mineralize changes completely within a period of approximately 2 hrs. at the time of the molt. Using this system it should, therefore, be possible to learn a great deal both about the nature of nucleation inhibitory proteins and about their control.

Acknowledgements

This work was supported by a grant from the North Carolina Biotechnology Center to R.D.R. and S.K.B., and by a N.C. Sea Grant graduate fellowship to M.B.D.

References

Drach, P. 1939. Mue et cycle d'intermue chez les crustacés décapodes. Annals de l'Institut Océánographique, Monaco 19: 103-391.

Drach, P. and C. Tchernigovtzeff. 1967. Sur la méthode de détermination des stades d'intermue et son application générale aux crustacés. Vie et Milieu, Series A: Biologie Marin 18: 595-610.

Paul, J.H. and J.S. Sharpe. 1916. Studies in calcium metabolism. I. The deposition of lime salts in the integument of decapod Crustacea. Journal of Physiology 50: 183-192.

Richards, A.G. 1951. The integument of arthropods. University of Minnesota Press, Minneapolis.

Roer, R.D. 1979. Mechanisms of deposition and resorption of calcium in the carapace of the green crab, *Carcinus maenas*. Ph.D. Dissertation, Duke University, Durham, N.C. 154 p.

Roer, R.D. 1980. Mechanisms of resorption and deposition of calcium in the carapace of the crab, *Carcinus maenas*. Journal of Experimental Biology 88: 205-218.

Roer, R.D. and R.M. Dillaman. 1984. The structure and calcification of the crustacean cuticle. American Zoologist 24: 893-909.

Travis, D.F. 1963. Structural features of mineralization from tissue to macromolecular levels of organization in decapod Crustacea. Annals of the New York Academy of Sciences 109: 177-245.

Travis, D.F. 1965. The deposition of skeletal structures in the Crustacea. V. The histomorphological and histochemical changes associated with the development and calcification of the branchial exoskeleton in the crayfish, *Orconectes virilis* Hagen. Acta Histochemica 20: 193-222.

Travis, D.F. and U. Friberg. 1963. The deposition of skeletal structures in the Crustacea. VI. Microradiographic studies of the exoskeleton of the crayfish *Orconectes virilis* Hagen. Journal of Ultrastructural Research 9: 285-301.

Weiner, S. 1979. Aspartic acid-rich proteins: Major components of the soluble organic matrix of mollusk shells. Calcified Tissue International 29: 163-167.

Weiner, S. 1983. Mollusk shell formation: Isolation of two organic matrix proteins associated with calcite deposition in the bivalve *Mytilus californianus*. Biochemistry 22: 4139-4145.

Yano, I. 1972. A histochemical study on the exocuticle with respect to its calcification and associated epidermal cells in a shore crab. Bulletin of the Japanese Society of Scientific Fisheries 38: 733-739.

Bob Roer is an Associate Professor and Research Physiologist in the Department of Biological Sciences and Institute for Marine Biomedical Research at the University of North Carolina at Wilmington. He received the B.S. in aquatic biology at Brown University in 1974 and the Ph.D. in zoology at Duke University in 1979. Bob's research principally has involved mechanisms of ion transport and calcification in the crustacean cuticle, although he maintains an interest in fluid dynamics as related to bone formation as well.

Sybil Burgess is an Assistant Professor in the Department of Chemistry at UNC-W. She received the B.S./B.A. degrees in biology and chemistry from Meredith College in Raleigh, North Carolina in 1975 and the Ph.D. in biochemistry at North Carolina State in 1980. Sybil has worked on structure and activation of carboxylesterases and more recently on isolation and characterization of the proteins from the crustacean cuticle.

Chemical Aspects of Regulation of Mineralization. C.S. Sikes and A.P. Wheeler, editors, University of South Alabama Publication Services, Mobile, Alabama, 1988.

A Lineage Specific Gene Encoding a Major Matrix Protein of the Sea Urchin Embryo Spicule

Steve Benson[1], Henry Sucov[2], Eric Davidson[2] and Fred Wilt[3]

[1]Department of Biological Sciences
California State University - Hayward
Hayward, CA 94542

[2]Department of Biology
California Institute of Technology
Pasadena, CA 91125

[3]Department of Zoology
University of California - Berkeley
Berkeley, CA 94720

ABSTRACT

The micromere-mesenchyme lineage in sea urchin embryos produces an elaborate calcareous spicule or skeleton. Antibodies against the protein organic matrix of the spicule were used to screen a λgt11 cDNA expression library. A cDNA was isolated which encodes a prominent 50-kDa spicule matrix protein (SM-50). RNA blot analysis indicates a 2.3 kb transcript is detected hours before overt spicule formation and increases over 100 fold during development. *In situ* hydridization demonstrates that this gene is transcribed only in cells of the primary mesenchyme lineage. The gene is over 9 kb in length, occurs once per haploid genome and contains a single intron. The putative protein contains a proline rich domain, a very basic C-term region and a tandemly repetitive domain composed of 13 amino acids which comprises 45% of the length of the protein. The consensus sequence of the repetitive domain is: Trp-Val-Gly-Asp-Asn-Gln-Ala-$^{Leu}_{Trp}$-Val-$^{Ile}_{Asp}$-Asn-$^{Gln}_{Pro}$-$^{Val}_{Glu}$

Introduction

During early development the sea urchin embryo forms a tier of four cells at the fourth cell division. These micromeres, which are located at the vegetal pole, are the founder cells that give rise to the primary mesenchyme, which in turn construct the calcite-containing endoskeletal spicules of the pluteus larva. Our approach is to apply the tools of embryology, biochemistry, cellular and molecular biology to learn how these cells progress through the complex series of epigenetic steps that result in skeleton formation, and to understand better how differential gene expression is regulated as the cells of the lineage progress toward their final fate.

The sea urchin embryo forms a distinctive quartet of small cells, the micromeres, at the fourth cell division. The cells undergo a limited number of divisions, and their progeny leave the epithelial wall of the blastula just prior to gastrulation to form primary mesenchyme. As gastrulation progresses, the primary mesenchyme cells congregate in groups in the blastocoel near the prospective oral side of the pluteus larvae, and the cells fuse into an elaborate syncytial array. Within the cytoplasmic cables that form the syncytial connections between cells, vacuoles appear, and within these vacuoles calcite is deposited to form the spicules that constitute the endoskeleton of the pluteus (Reviewed in Decker and Lennarz 1988; Wilt and Benson 1988).

The Spicule Matrix:

The endoskeletal spicules of the embryo are calcite composed primarily of $CaCO_3$. Since most biomineralized tissues also contain an organic matrix, we thought it was likely that spicules possessed one, and that components of this matrix would provide a convenient marker for following the overt terminal differentiation of the micromere lineage which culminates in a biomineralized skeleton.

Spicules have been purified from larvae by a novel technique that involves extensive washing with detergent mixtures followed by sodium hypochlorite. The purified spicules may be demineralized, and the remaining matrix visualized by electron microscopy as concentric lamellae of reticular material forming a putative armature for the biomineralization process (Benson *et al.* 1983). The organic matrix is soluble, and is comprised of at least 9 acidic proteins, 7 of which are glycoproteins. This collection of proteins is very rich in glycine, alanine, serine, aspartic acid and glutamic acid. The predominant proteins have apparent molecular weights of 47, 50, 57, and 64 kDa. Treatment of the proteins with Endo F, an endoglycosidase, which is capable of hydrolyzing N-linked complex carbohydrate side chains, decreases the apparent molecular weight of each of the different electrophoretically resolved bands by about 4000 daltons (Benson *et al.* 1986). These matrix glycoproteins have many of the properties expected from studies on the biochemistry of proteins found in other tissues active in biomineralization (Mann 1983; Weiner 1984, 1986). Namely they are acidic, glycosylated and have calcium binding properties. Equilibrium dialysis experiments indicate that the total soluble matrix binds calcium with a Kd of about 10^{-4}M. We are not yet certain which of the several proteins in the matrix binds calcium. These properties are summarized in Table 1.

Table 1. Characteristics of Spicule Matrix Proteins

Amount	0.01% of total protein of pluteus 0.2% of weight of spicule
Components	Multiple components, at least 10, with molecular weight ranging from 20 to 117 kd. Principle components of 47, 50, 57, 64 and 117 kd
Carbohydrate	Reducing carbohydrate content of 4% Major components of 117, 57, 50 and 47 kd are endo F but not endo H sensitive; no 0-linked oligosaccharides
Ca binding	Mixture binds 2.4 mole Ca per 54 kd of protein with K_d of 1.5×10^{-4} M
Amino acids	All components very acidic. Mixture of proteins is 65% glx, asx, gly, ser, ala. No hydroxyproline

Polyclonal antibodies to total spicule matrix were raised in rabbits. The polyclonal IgG preparation shows high specificity for spicule matrix (Wilt *et al.* 1987). Immunoblots of the spicule matrix revealed the same protein constituents visualized by silver staining. In addition, immunoblots after Endo F treatment indicates that the antigenic entity is the protein rather than the carbohydrate moiety (Benson *et al.* 1986).

Use of this antisera in immunocytochemical analysis has shown that the proteins are localized in the forming spicule and are not present in other regions of the embryo. The matrix proteins accumulate primarily during the period between gastrulation and the pluteus larva stage, concomitant with calcite deposition.

The antibodies against the spicule matrix proteins have been used to isolate a cloned cDNA that encodes the most prominent spicule matrix protein, one that has an apparent molecular weight of 50 kDa, and which we term SM 50. Dr. Henry Sucov used the polyclonal antibody to screen a lambda expression vector library made from cDNA of pluteus stage larva in Dr. Eric Davidson's laboratory at the California Institute of Technology. The cognate gene that encodes the mRNA has also been isolated and partially sequenced by Sucov. The gene encodes a protein of 449 amino acids, and is interrupted by one intron near the amino terminus of the protein (Fig. 1). The amino terminal contains a proline rich domain, and the carboxy terminal half of the protein contains an imperfectly repeated motif of 13 amino acids:

Trp-Val-Gly-Asp-Asn-Gln-Ala-$^{Leu}_{Trp}$-Val-$^{Ile}_{Asp}$-Asn-$^{Gln\ Val}_{Pro\ Glu}$

which, to the best of our knowledge, has not been found in other types of proteins (Sucov *et al.* 1987).

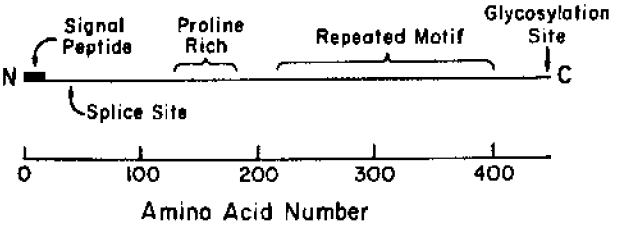

Figure 1. Diagram of the SM 50 protein. The amino acid sequence was deduced from the cDNA clone (Sucov *et al.* 1987) has a signal peptide, a 7 kb intron, a proline rich region, an unusual repeated 13 amino acid motif, and a glycosylation site near the carboxyl terminus.

The Accumulation of SM 50 Transcripts During Development

The cloned cDNA has been used to probe RNA blots to determine the time when transcripts from this gene begin to accumulate (Benson *et al.* 1987). RNA was isolated from embryos of various stages, separated by electrophoresis in agarose gels, and blotted to nitrocellulose. These blots were probed with single stranded anti-sense RNA probes synthesized from the SM 50 cDNA in the transcription vector, pGEM 1. A 2.2 kb transcript is first detected at a very low level in the late cleavage stage of development. The transcript concentration increases over twenty fold when the mesenchyme cells ingress into the blastocoel. An additional two to four-fold increase occurs by gastrula formation, and this level persists during subsequent development.

Single-stranded RNA probes obtained from cDNA subcloned into SP-6 transcription vectors were used to examine the cellular location of the gene products by *in situ* hybridation techniques (Benson *et al.* 1987). Embryos at stages before the primary mesenchyme has ingressed into the blastocoel show no hydridization above background. As soon as primary mesenchyme cells are present within the blastocoel cavity, localized silver grains, indicating the presence of mRNA, can be detected in the mesenchyme cells (Fig. 2). The hybridization signal becomes more prominent as gastrulation and spicule formation proceeds. The transcripts remain exclusively localized in primary mesenchyme cells and their descendants. Thus the expression of the SM 50 gene is regulated in a temporal and spatial manner.

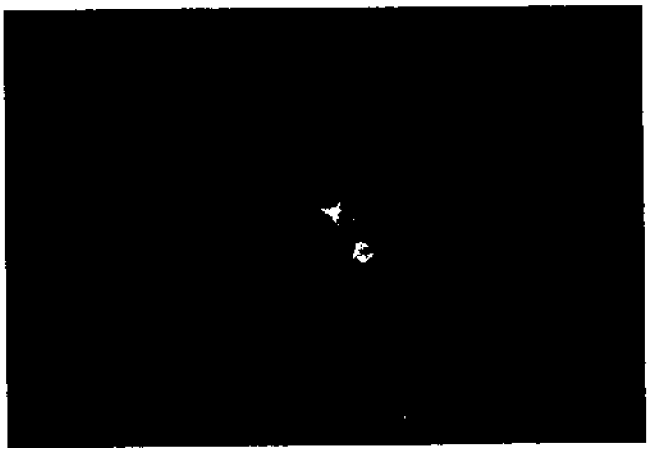

Figure 2. *In situ* hybridization of single stranded SM 50 RNA probe to sectioned mesenchyme blastula embryo. The dark field photo shows the silver grains as bright dots on the dark background. Localization is exclusively over the mesenchyme cells.

One presumes that the accumulating transcript is presiding over synthesis of spicule matrix protein, and an investigation of the intracellular distribution of the transcript confirms this (Killian and Wilt 1988). Embryos at the mesenchyme blastula stage, when rapid accumulation of SM 50 transcripts is under way, were used as a source of polysomes, which were resolved on sucrose gradients. RNA was isolated from the different size polysomes that had been fractionated on a sucrose gradient, and this RNA was subjected to electrophoresis, blotted and probed with the SM 50 cDNA. The transcript was almost exclusively located in large polysomes (>350 S). Hence, the SM 50 gene product is apparently utilized for protein synthesis at all times when it is present. Thus at least one of the proteins involved in biomineralization, SM 50, is synthesized at least 24 hours before overt skeleton formation.

This apparently precocious synthesis of SM 50 presumably reflects the time required for adequate processing, transport, deposition and accumulation of this spicule matrix protein. We are currently attempting to determine if other matrix proteins follow a similar ontogeny.

We have utilized RNA blotting analysis to examine adult tissues for the presence of the SM 50 gene transcript (Richardson *et al.*, in preparation). The 2.2 kb SM 50 transcript is easily detectable in extracts from spines of the adult, but not in RNA from the gut, ovary, or coelomocytes. Thus, it appears that the gene active in spicule formation in mesenchyme cells of the embryo is also active in mineralizing cells of the adult spine. We also examined the RNA extracted from tube feet of the adult, and were surprised to see that the 2.2 kb transcript is present in this tissue also. The tube feet do, however, contain calcite, in the form of rosette like structures at the distal end, as well as supporting structures embedded in the walls of the tube foot. The correlation of calcite deposition with SM 50 transcript accumulation is consistent with the idea that the SM 50 gene is involved in some aspect of biomineralization.

Finally, we are confident that studies of the spicule matrix proteins and the genes that encode them will help in understanding how the spicule, and other hard calcareous structures, are formed, and how their architecture arises. Since the individual matrix proteins are either present as part of a heterogeneous mixture or present in small quantities, nucleic acid cloning procedures should be very useful in learning more about the proteins themselves. We are attempting to produce additional monospecific and monoclonal antibodies that recognize individual spicule matrix proteins. These antibodies could be used to rescreen cDNA expression libraries and hopefully isolate cDNAs that encode other spicule matrix proteins. The structural features of these proteins may be deduced from the nucleic acid sequence of some of these cloned probes. These structural features may in turn suggest how the proteins function in biomineralization. Likewise one could use full length cDNA clones in expression vectors such as baculovirus system developed by Summers (Luckow and Summer 1988) to produce matrix proteins of various sorts to use in functional assays of biomineralization. Though the spicule matrix is complex, it is not overwhelming, and powerful methods of molecular biology may enable us to analyze the roles of matrix in biomineralization.

References

Benson, S., H. Sucov, L. Stephens, E. Davidson and F. Wilt. 1987. A lineage specific gene encoding a major matrix protein of the sea urchin embryo spicule I. Authentication of the cloned gene and its developmental expression. Dev. Biol. 120:499-506.

Benson, S., N. Benson, and F. Wilt. 1986. The organic matrix of skeletal spicule of sea urchin embryos. J. Cell Biol. 102:1878-1886.

Benson, S., E. Jones, N. Crise-Benson, and F. Wilt. 1983. Morphology of organic matrix of the spicule of the sea urchin larvae. Exp. Cell Res. 148:249-253.

Decker, G. and W. Lennarz. 1988. Skeletogenesis in the sea urchin embryo. Development 103:231-247.

Killian, C. and F. Wilt. 1988. Expression of a spicule matrix gene during sea urchin development. Submitted for publication.

Luckow, V. and M. Summer. 1988. Trends in the development of baculovirus expression vectors. Biotechnology 6:47-55.

Mann, S. 1983. Mineralization in biological systems. Struct. Bonding 54:125-142.

Sucov, H., S. Benson, J. Robinson, R. Britten, F. Wilt and E. Davidson. 1987. A lineage specific gene encoding a major matrix protein of the sea urchin spicule II. Structure of the gene and derived sequence of the protein. Dev. Biol. 120:507-519.

Weiner, S. 1986. Organization of extracellular mineralized tissues: A comparative study of biological crystal growth. CRC Critical Reviews in Biochemistry 20:365-408.

Weiner, S. 1984. Organization of organic matrix components in mineralized tissues. Amer. Zool. 24:945-952.

Wilt, F. and S. Benson. 1988. The development of the endoskeletal spicule of the sea urchin embryo. In: J. Varner (ed.) Self Assembly in Biological Systems. 46th Symposium Society for Developmental Biology. Alan Liss Pub. in press.

Wilt, F., S. Benson, and N. Benson. 1987. Spicule formation in sea urchin embryos. In: Molecular Approaches to Developmental Biology. Alan Liss, p. 223-230.

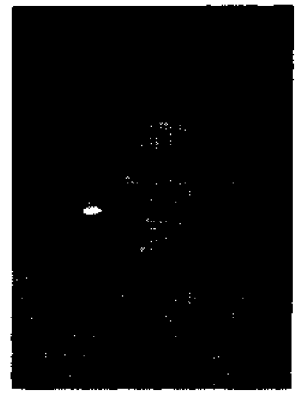

Steve Benson received the B.A. (1968), M.A. (1972), and Ph.D. (1973) at the University of California, Santa Barbara. He joined the faculty at California State University, Hayward, in 1974, assuming his current position there as a Professor in 1983. He has held research positions at the Bruce Lyon Memorial Research Laboratory of the Children's Hospital Medical Center in Oakland and in the Department of Zoology at the University of California, Berkeley, including a continuing appointment at Berkeley as a research associate since 1981. Steve has worked on biochemical aspects of atherosclerosis, hypertension, and pulmonary fibrosis. His current work emphasizes the regulation of protein synthesis and gene expression during development.

Chemical Aspects of Regulation of Mineralization. C.S. Sikes and A.P. Wheeler, editors, University of South Alabama Publication Services, Mobile, Alabama, 1988.

Osteopontin: A Bone Derived Cell Attachment Factor

William T. Butler[1], Charles W. Prince[2], Manuel P. Mark[3] and Martha J. Somerman[4]

[1]Dental Branch,
University of Texas Health Science Center at Houston,
Houston, Texas.

[2]University of Alabama at Birmingham,
Birmingham, Alabama.

[3]Universite Louis Pasteur,
Strasbourg, France.

[4]University of Maryland Dental School,
Baltimore, Maryland

ABSTRACT

Osteopontin (also called 44 kDa bone phosphoprotein, bone sialoprotein I, and 2ar) is a phosphorylated glycoprotein isolated from bone. With a molecular weight of about 41,500, this protein of 301 amino acid residues is rich in aspartic acid, serine and glutamic acid, and contains 12 phosphoserines and 1 phosphothreonine. It also contains about 33 carbohydrate residues present as 1 N-glycoside and 5-6 0-glycosides; ten of these residues are sialic acid.

Osteopontin is synthesized by osteoblasts, osteocytes and preosteoblasts, is secreted into osteoid and is incorporated into the calcified bone matrix. Immunolocalization and *in situ* hybridization experiments, as well as Northern blots, have shown that the protein is synthesized by several cell types other than bone cells, e.g. by certain neural and neurosensory cells of inner ear and brain. The biosynthesis by osteoblasts is stimulated at the transcriptional level by 1,25-dihydroxyvitamin D_3 and by transforming growth factor-β.

Numerous cell attachment experiments, along with the presence of an Arg-Gly-Asp cell binding sequence indicate that osteopontin promotes the attachment and spreading of certain cells (e.g. osteoblasts). These data taken together strongly suggest that this phosphorylated glycoprotein serves an important functional role in the early stages of osteogenesis.

Introduction

For a number of years it has been believed that phosphorylated proteins are primary components involved in, and responsible for, initiation and growth of crystals in mineralizing tissues (Veis 1985). Phosphoproteins of bone have been isolated and characterized by several groups of researchers (Cohen-Solal *et al.* 1978; Lee and Glimcher 1981; Franzén and Heinegård 1985a; Veis 1985; Uchiyama *et al.* 1986; Fisher *et al.* 1987; Prince *et al.* 1987). The data presented prior to 1986 indicated that bone phosphoproteins are rich in glutamic and aspartic acids, contain both phosphoserine and phosphothreonine and are glycoproteins.

Within the last few years information has emerged that shows that one of the bone phosphoproteins, osteopontin (Franzén and Heinegård 1985a; Prince et al. 1987), is a cell attachment and spreading factor (Oldberg *et al.* 1986; Somerman *et al.* 1987) and possesses an Arg-Gly-Asp cell binding sequence (Oldberg *et al.* 1986), common to many such attachment proteins that are in the same family as fibronectin. This protein has also been referred to as bone sialoprotein I (Franzén and Heinegård 1985a; Fisher *et al.* 1987), 44 kDa bone phosphoprotein (Prince *et al.* 1987; Somerman *et al.* 1987) and 2ar (Smith and Denhardt 1987; Nomura *et al.* 1988). Herein we review the known chemical and biological properties of osteopontin.

Methods

The methods for isolation and characterization of osteopontin and for determination of its biosynthesis by ROS 17/2.8 cells are published (Prince *et al.* 1987). The methods for studying the cell and matrix association of the protein by immunolocalization are published (Mark *et al.* 1987a, 1987b, 1988a, 1988b). The approaches for determining cell attachment and spreading are also documented elsewhere (Somerman *et al.* 1987).

Results and Discussion

The first clear experiments relating to osteopontin as a phosphorylated glycoprotein from bone were reported by Franzén and Heinegård (1985b). In our initial publication concerning osteopontin (Prince *et al.* 1987), we reported the isolation and characterization, along with some biosynthetic data. Our purification of the protein involved extraction from rat long bones, initial gel filtration on Sephacryl S-200, ion-exchange chromatography on DEAE- Sephacel and rechromatography on DEAE-Sephacel. The extraction and chromatography were in the continual presence of guanidine or urea (plus a cocktail of protease inhibitors) to prevent losses due to artifactual proteolysis. Using this procedure we obtained a product of high purity as shown by sedimentation equilibrium experiments, gel electrophoresis and Edman degradations (Prince *et al.* 1987).

The molecular weight was shown to be about 44,000 by sedimentation equilibrium; however, electrophoresis in 5% to 15% SDS gradient polyacrylamide gels gave an M_r of 75,000 while in 15% SDS polyacrylamide gels the M_r was 45,000. The anomalous behavior on gel electrophoresis can be used as a means of identification, for example when studying a biosynthetic product (Prince et al. 1987).

The first ten residues at the NH_2-terminus, Leu-Pro-Val-Lys-Val-Ala-Glu-Phe-Gly-Ser, are predominantly hydrophobic. Our compositional analyses predicted a protein with slightly over 300 amino acids and with 16.6% carbohydrate, representing about 33 residues. The carbohydrate includes about 10 residues of sialic acid. The mannose content suggested the presence of 1 N-linked oligosaccharide, while β-elimination experiments and the N-acetylgalactosamine levels indicated 5-6 O-linked oligosaccharides. In order to quantitate the phosphoserine and phosphothreonine, we utilized a β-elimination procedure with mild alkali and subsequent reduction of the resultant unsaturated amino acid sidechains with borohydride. Quantitation of the phosphate liberated, the serine and threonine losses and the alanine gained showed that the protein contained about 12 phosphoserines and 1 phosphothreonine.

The amino acid sequence predicted from a cDNA sequence (Oldberg *et al.* 1986) was entirely consistent with our compositional and structural data (Prince *et al.* 1987). The NH_2-terminal sequence we reported aligned with residues of 17-26 of the predicted sequence. Assigning the Leu-17 of the cDNA deduced sequence as residue 1 in the protein, one obtains a structure with 301 amino acid residues. The Asn-Glu-Ser sequence at positions 63-65 is the only site for N-linked oligosaccharide attachment. Several Ser-X-Glu sequences would be sites for 0-linked oligosaccharide attachment. Adding the amino acids, the phosphate and the carbohydrate, one can then compute a molecular weight of about 41,500, again consistent with our previous molecular weight determinations (Prince *et al.* 1987). The finding of Oldberg *et al.* (1986) of a Gly-Arg-Gly-Asp-Ser sequence identical to the cell attachment sequence in fibronectin, and their demonstration of cell adhesion activity by the protein, was independently established by us (Somerman *et al.* 1987) using a completely different approach (see later).

That osteopontin is synthesized and secreted by osteoblasts was established in biosynthetic experiments (Prince *et al.* 1987) with rat osteoblast-like osteosarcoma cells (ROS 17/2.8 cells), a clonal cell line established in Dr. Gideon Rodan's laboratory (Majeska *et al.* 1980). Pulsing with ^{14}C-serine yielded a variety of secreted, labeled proteins. One of these radiolabeled proteins eluted from DEAE-Sephacel in a position similar to that of osteopontin and after gel electrophoresis, it migrated to M_r 75,000 on 5% to 15% polyacrylamide gradient gels. When the cells were incubated with $^{32}PO_4$, a product was immunoabsorbed (using polyclonal antibodies to the protein) from the media; this product co-migrated with authentic osteopontin on 5% to 15% polyacrylamide gradient gels as well as on 15% polyacrylamide gels.

Extensive immunolocalization experiments (Mark *et al.* 1987a, 1987b, 1988a, 1988b) have also established that the phosphoprotein is synthesized and secreted by bone cells. Using tissues from fetal and neonatal rats, we have shown that osteoblasts, osteocytes and preosteoblasts are immunopositive. The appearance of osteopontin in preosteoblasts several hours before the formation of osteoid and bone (Mark *et al.* 1988b) indicates the importance of osteopontin at an early stage of osteogenesis. The protein was also found within the matrix of osteoid and bone (Mark *et al.* 1987a, 1988a, 1988b), indicating that it is secreted by the cells and retained in the extracellular matrix. This conclusion is also consistent with its detection in the Golgi apparatus (Mark *et al.* 1987a, 1988b). A surprising finding was the immunodetection in certain neural and neurosensory cells of the inner ear and brain (Mark *et al.* 1988a). Thus osteopontin is not totally "bone specific", although it must be considered to be an important component in osteogenesis. Our finding of the protein in tissues other than bone was confirmed by other investigators (Yoon *et al.* 1987; Nomura *et al.* 1988) using cDNA probes in Northern blotting and *in situ* hybridization experiments to detect osteopontin in mRNA.

The synthesis of osteopontin can be modulated by several factors added to cell cultures. For example, the levels of osteopontin and of osteopontin mRNA production by ROS 17/2.8 cells are significantly increased by incubating the cells with 1,25-dihydroxyvitamin D_3 (Prince and Butler 1987; Yoon *et al.* 1987; Noda *et al.* 1988) and by transforming growth factor-β (Noda *et al.* 1988). Several growth factors also appear to be effective in elevating the transcriptional level of osteopontin mRNA in other cell types (Nomura *et al.* 1988). The biological meaning of these results is currently unknown. TGF-β may act as an autocrine factor during the development of bone and differentiation of bone cells. Thus, it would be synthesized and secreted by osteoblasts which also have receptors and respond to the stimulus. Among the responses would be the synthesis of an increased level of osteopontin.

The finding that the phosphorylated protein has the property of promoting the attachment and spreading of fibroblasts (Somerman *et al.* 1987) and osteoblasts (Oldberg *et al.* 1986) to plastic substratum, in a manner that involves the Arg-Gly-Asp sequence has proven to be an extremely exciting clue. This activity is concentration dependent at low levels of protein and is longer lived than that of fibronectin (Somerman *et al.* 1987). In general, the attachment activity is effective with fibroblasts and osteoblasts but not with epithelial cells. One surprising finding is the inability of osteopontin to promote attachment of cells to type I collagen above that enhancement of collagen alone (Somerman *et al.* 1987). These data may suggest that the protein does not have a collagen attachment domain as does fibronectin. However, as stated above, the protein appears to be secreted by bone cells before bone is formed and to be localized within osteoid, a tissue consisting mostly of type I collagen. Therefore, an unresolved question is the mechanism whereby osteopontin is attached to osteoid. Is it associated with another macromolecule that provides the ligand for collagen binding? Or is the collagen binding domain of our preparation denatured during our preparation in guanidine and urea solutions? We are presently exploring these questions.

In summary, during the formation of bone, osteopontin is synthesized by preosteoblasts and osteoblasts, is secreted and found in osteoid and, after mineralization, is found within the mineralized matrix. Since osteopontin stimulates the attachment and spreading of cells to substratum *in vitro* via an Arg-Gly-Asp cell binding sequence, it is logical to assume that this property represents its biological function. Thus, preosteoblasts and osteoblasts would secrete this factor prior to, and/or during the time period that they are synthesizing other connective tissue macromolecules that give rise to osteoid. When this extracellular uncalcified matrix becomes organized, the cell attachment to nascent osteoid would be promoted by osteopontin. Mineralization ensues and the osteopontin along with type I collagen, proteoglycans and other components become a part of the mineralized matrix. This predicted function does not take into account the earlier speculations (Veis 1985) that bone phosphoproteins in general are in some way involved in mineralization of the tissue. However, the evidence for cell attachment activity is more convincing; no conclusive evidence has been presented that clearly establishes a role for osteopontin in the nucleation and/or growth of bone crystals.

References

Cohen-Solal, L., J.B. Lian, D. Kossiva and M.J. Glimcher. 1978. The identification of 0-phosphothreonine in soluble noncollagenous phosphoproteins of bone matrix. FEBS Lett. 89: 107-110.

Fisher, L., G.R. Hawkins, N. Tuross and J.D. Termine. 1987. Purification and partial characterization of small proteoglycans I and II, bone sialoproteins I and II and osteonectin from the mineral compartment of developing human bone. J. Biol. Chem. 262: 9702-9708.

Franzén, A. and D. Heinegård. 1985a. Isolation and characterization of two sialoproteins present only in calcified bone. Biochem. J. 232: 715-724.

Franzén, A. and D. Heinegård. 1985b. Proteoglycans and Proteins of Rat Bone. Purification and Biosynthesis of Major Noncollagenous Macromolecules, p 132-141. In: W.T. Butler (ed.), The Chemistry and Biology of Mineralization Tissues, EBSCO Media, Birmingham.

Lee, S.L. and M.J. Glimcher. 1981. Purification, composition and ^{31}P NMR spectroscopic properties for a noncollagenous phosphoprotein isolated from chicken bone matrix. Calcif. Tis. Int. 33: 385-394.

Majeska, R.J., S.B. Rodan and G.A. Rodan. 1980. Parathyroid hormone-responsive clonal cell lines from rat osteosarcoma. Endocrinol. 107: 1494-1503.

Mark, M.P., C.W. Prince, T. Oosawa, S. Gay, A.L.J.J. Bronckers and W.T. Butler. 1987a. Immunohistochemical demonstration of a 44-kD phosphoprotein in developing rat bones. J. Histochem. Cytochem. 35: 707-715.

Mark, M.P., C.W. Prince, S. Gay, R.L. Austin, M. Bhown, R.D. Finkelman and W.T. Butler. 1987b. A comparative immunocytochemical study on the subcellular distributions of 44 kDa bone phosphoprotein and γ-carboxyglutamic acid (Gla)-containing protein in osteoblasts. J. Bone Mineral Res. 2: 337-346.

Mark, M.P., C.W. Prince, S. Gay, R.L. Austin and W.T. Butler. 1988a. 44-kDal bone phosphoprotein (osteopontin) antigenicity at ectopic sites in newborn rats: kidney and nervous tissues. Cell Tissue Res. 251: 23-30.

Mark, M.P., W.T. Butler, C.W. Prince, R.D. Finkelman and J.V. Ruch. 1988b. Developmental expression of 44 kDa bone phosphoprotein (osteoponin) and bone γ-carboxyglutamic acid (Gla)-containing protein (osteocalcin) in rat calcifying tissues. Differentiation 37: 123-136.

Noda, M., K. Yoon, C.W. Prince, W.T. Butler and G.A. Rodan. 1988. Transcriptional regulation of osteopontin production by type β transforming growth factor. J. Biol. Chem. 236: 13916-13921.

Nomura, S., A.J. Wills, D.R. Edwards, J.K. Heath and B.L.M. Hogan. 1988. Developmental expression of 2ar (osteopontin) and SPARC (osteonectin) mRNA as revealed by *in situ* hybridization. J. Cell Biol. 106: 441-450.

Oldberg, A., A. Franzén, and D. Heinegård. 1986. Cloning and sequence analysis of rat bone sialoprotein (osteopontin) cDNA reveals an Arg-Gly-Asp cell-binding sequence. Proc. Natl. Acad. Sci. USA 83: 8819-8823.

Prince, C.W. and W.T. Butler. 1987. 1,25-Dihydroxyvitamin D_3 regulates the biosynthesis of osteopontin, a bone-derived cell attachment protein, in clonal osteoblast-like osteosarcoma cells. Collagen Rel Res 7, 305-313.

Prince, C.W., T. Oosawa, W.T. Butler, M. Tomana, A.S. Bhown, M. Bhown and R.E. Schronhenloher. 1987. J. Biol. Chem. 263: 2900-2907.

Smith, J.H. and D.T. Denhardt. 1987. Molecular cloning of a tumor promoter-inducible mRNA found in JB6 mouse epidermal cells: Induction is stable at high, but not low, cell densities. J. Cellular Biochemistry 34: 13-22.

Somerman, M.J., C.W. Prince, J.J. Sauk, R.A. Foster and W.T. Butler. 1987. Mechanism of fibroblast attachment to bone extracellular matrix: role of 44 kilodalton bone phosphoprotein. J. Bone Mineral Res. 2: 259-265.

Uchiyama, A., M. Suzuki, B. Lefteriou and M. Glimcher. 1986. Biochemistry 25: 7572-7583.

Veis, A. 1985. Phosphoproteins of dentin and bone. Do they have a role in matrix mineralization? p. 170-176. In: W.T. Butler (ed.) The Chemistry and Biology of Mineralized Tissues, EBSCO Media, Birmingham.

Yoon, K., R. Buenaga and G.A. Rodan. 1987. Tissue specificity and developmental expression of rat osteopontin. Biochem. Biophys. Res. Comm. 148: 1129-1136.

Bill Butler is Professor and Chairman of the Department of Biological Chemistry at the Dental Branch, the University of Texas, Health Science Center in Houston. He had been at the University of Alabama in Birmingham from 1967-1987. He received the B.S. in biology at Baylor in 1958, the Ph.D. in biochemistry at Vanderbilt in 1966, and did postdoctoral work at the National Institute of Dental Research in Bethesda in 1967. Bill has been a leader in research into mechanisms of formation of bones and teeth, including service as the organizer of the Second International Conference on the Chemistry and Biology of Mineralized Tissues and as a member of several editorial and advisory boards. His current research focuses on the role that matrix proteins may play in formation of bone and dentin.

Chemical Aspects of Regulation of Mineralization. C.S. Sikes and A.P. Wheeler, editors, University of South Alabama Publication Services, Mobile, Alabama, 1988.

Solution Synthesis of Phosphoseryl-phosphoserine, a Partial Analogue of Human Salivary Statherin, Essential for Primary and Secondary Precipitation of Calcium Phosphate in Human Saliva

David H. Schlesinger,[1] Angeliki Buku,[2]
Herman R. Wyssbrod [2] and Donald I. Hay[3].

[1]Departments of Medicine and Cell Biology. Member of the Kaplan Cancer Center. New York University Medical Center. New York, NY 10016.

[2]Department of Physiology and Biophysics and Center for Polypeptide and Membrane Research, Mount Sinai School of Medicine. New York, NY 10029.

[3]Department of Biochemistry, Forsyth Dental Center, 140 Fenway. Boston, MA 02115.

ABSTRACT

Human salivary secretions are supersaturated with respect to basic calcium phosphates but spontaneous precipitation of these salts from saliva, or surface-induced precipitation of calcium phosphates onto dental enamel, does not normally occur. This unexpected stability has been attributed to the inhibitory activities of two kinds of salivary phosphoproteins-statherin and the acidic, proline-rich phosphoproteins (PRP).

Investigation of the structure-function relationships of statherin, the most potent inhibitor of primary (spontaneous) and secondary (seeded) precipitation of calcium phosphate salts in human saliva has been limited to studies of peptide segments obtained from the native peptide by specific proteolysis. Solid phase peptide synthesis (SPPS) is a useful and potentially more flexible alternative. Phosphoserine residues (positions 2 & 3) play critically important roles in the precipitation-inhibition activities of statherin, but SPP synthesis of these phosphorylated peptides is precluded because of the instability of phosphoserine residues in the presence of HF. Thus, this peptide was synthesized by solution-phase methods starting with carbobenzoxy-serine and seryl-o-benzyl ester and the dipeptide formed with carbodiimide. The dipeptide was phosphorylated with diphenylphosphoryl chloride and the diphenyl protecting groups removed by hydrogenation with PtO_2 as catalyst. The deprotected phosphoserine dipeptide was purified on sephadex QAE-25 and on DEAE agarose and assayed for inhibition of primary and secondary precipitation of calcium phosphate salts. The dipeptide possessed substantial inhibitory activity in both systems, but was not as active as either N-terminal tryptic hexapeptide of statherin or intact statherin. Synthesis of other model phosphorylated peptides are underway to expand the structure-function relationships.

Introduction

Human salivary secretions are supersaturated with respect to basic calcium phosphates (Folsch 1959; Aoba *et al.* 1984) but spontaneous precipitation of these salts from saliva and crystal growth of calcium phosphates onto dental enamel do not normally occur. This unexpected stability has been attributed (Gron 1973a; 1973b; Hay 1973) to the inhibitory activities of two kinds of salivary phosphoproteins, statherin (Hay *et al.* 1979, 1982) and the acidic proline-rich phosphoproteins (PRP) (Lagerlof 1983; Hay *et al.* 1984). Statherin inhibits primary (spontaneous) and secondary precipitation (crystal growth) of calcium phosphates under salivary conditions (Merrifield 1963; Hay 1973), a highly specific property not possessed by any of the other 40 macromolecules in saliva (Merrifield 1964; Moreno *et al.* 1979), while the PRP, although less effective as inhibitors of primary precipitation, are highly potent inhibitors of crystal growth of calcium phosphate salts under these conditions (Hay 1973; Moreno *et al.* 1982). These activities are of biological significance in that they act to provide a supersaturated, but stable and protective environment for the dental enamel, which is important for the integrity of the teeth (Hay 1973).

Investigation of the structure-function relationships of these proteins has been limited to studies of peptide segments obtained from the native proteins by specific proteolysis (Hay *et al.* 1982, 1984, Lagerlof 1983), but it is often difficult to obtain desired molecular segments by these methods. Synthesis of such segments is a useful alternative approach, and convenient synthetic methods are available (Merrifield 1963, 1964). Phosphorylated residues such as phosphoserine, however, play critically important roles in the inhibition of calcium phosphate precipitation (Moreno *et al.* 1979, 1982), but incorporation of these residues into a conventional synthetic protocol is not straightforward (personal observation). The amino-terminal region of statherin represents a particularly difficult problem, since it contains the dipeptide sequence phosphoseryl-phosphoserine, at residues two and three. The purpose of the present work was to synthesize this dipeptide as a first step towards synthesizing more complex model phosphopeptides of interest in these investigations.

Methods

Synthesis of Z-seryl-serine-O-benzyl ester (Folsch 1959).

Twenty mmol of seryl-0-benzyl ester-p-toluenesulfonate in 30 ml dimethyl formamide (DMF) which contained 20 mmol triethylamine was coupled at 0° with 20 mmol N-carbobenzoxyserine in 50 ml DMF after the addition of 20 mmol dicyclohexyl-carbodiimide. The reaction was allowed to continue overnight at room temperature. The formed urea was filtered off, and the solvents evaporated. The oily residue was dissolved in ethyl acetate (200ml) and washed consecutively with 10% (w/v) $KHSO_4$ (25ml), three times, H_20, 10% (w/v) $NaHCO_3$ (25ml), three times, and H_20, and dried over $MgSO_4$ *in vacuo*. The product was crystallized from ethyl acetate/petroleum ether. Yield 65.4%, M.P. 152-154°; previously reported (Folsch 1959) 138-139°. Analysis, $C_{21}H_{24}O_7N_2$, M.W. 416.2, calculated, C 60.60, H 5.81, N 6.73; found, 59.84, 5.85, 6.63. Previously reported (Folsch 1959), calculated, N 6.7; found, 6.5. Proton NMR in $CDCl_3/(CD_3)_2SO$ gave the following values; d (PPM) 7.32 (s,10H,ArH), 5.18(s,2H,bzlCH_2), 5.09(s,2H,bzlCH_2), 3.93-4.10(m,4H,Ser β-CH_2), 4.20- 4.55(m,2H,Ser α-CH).

Racemization test.

The Z-seryl-seryl benzyl ester was deprotected by catalytic hydrogenolysis (Pd/C). About 1mg of the free peptide so obtained was hydrolyzed with leucine aminopeptidase M in 0.1M tris-HCl buffer, pH=8. After 24 hr the hydrolyzate was analyzed using a Beckman 6300 high performance amino-acid analyzer. A single peak of serine was obtained (retention time 16.7 min) which was well resolved from seryl-serine (retention time 29.8 min) analyzed under the same conditions. This enzymatic hydrolysis demonstrates that racemization of the L-seryl residues had not taken place during synthesis.

Phosphorylation

Ten mmol of Z-seryl-serine-o-benzyl ester in 10 ml anhydrous pyridine and 20 mmol of diphenylphosphoryl chloride (Aldrich Chemical Co.) were kept at 0° for two hours and overnight at room temperature. Excess acid chloride was destroyed with water. The product was taken up in ethyl acetate and water, and the ethyl acetate phase washed with 5N H_2SO_4, 10% $NaHCO_3$ and H_20, and dried over $MgSO_4$ *in vacuo*. A pale yellow oil was obtained, yield 90%, optical rotation $[\alpha]_D^{35} = +12.4$ (c 2.2 methanol). Analysis $C_{45}H_{42}O_{13}N_2P_2$ M.W. 879.94, calculated: C 61.12, H 4.81, N 3.18, P 6.39. Found: 61.10, 5.28, 3.70, 6.73. Proton NMR in $CDCl_3$ gave the following values; d(ppm) 7.58-7.11 (m,30H,ArH), 5.19(s,2H,bzlCH_2), 5.16 (s,2H,bzlCH_2), 4.25-4.90(m,6H,Ser α-CH, β-CH_2).

Hydrogenolysis

The fully protected phosphorylated peptide ester was dissolved in isopropanol-H_20-HOAc (50:5:0.5, V/V) and hydrogenated with Pd/C (10%) in an atmosphere of hydrogen. After 4 hr the catalyst was removed by filtration through a Celite filter and the filtrate evaporated *in vacuo*. NMR data and paper electrophoresis still showed the presence of some unremoved O-monophenyl phosphorylated protecting groups. Consequently, a second hydrogenation was performed in acetic acid, using PtO_2 as a catalyst at a pressure of 20 psi overnight. The catalyst was removed and the solvent evaporated to dryness. The residue was dissolved in water and the solution extracted twice with ethyl acetate. The aqueous phase was evaporated to dryness, and the residue triturated with ether.

Purification of the phosphoseryl-phosphoserine dipeptide, NH_2-PSer- PSer-COOH (PSer = O-phosphoserine) (Strid 1959).

Following the second hydrogenation the presence of aromatic residues from the phenyl protecting groups was still detected by ^1H NMR analysis. Separation of the totally deprotected peptide from the mono-phosphorylated peptide(s) and traces of the hydrolyzed peptide (NH_2-Ser-Ser-COOH) was accomplished on Sephadex QAE 25, a strong basic anion exchange resin with a pyridine-formate buffer gradient from 0.25-1.0 M, pH 4.5.

This product was purified further by ion exchange chromatography and gel filtration, primarily to remove residual salts which could affect subsequent assays. Deprotected phosphoseryl-phosphoserine, 10mg, was dissolved in 5ml of 0.1M pH 8 ammonium bicarbonate and chromatographed on a column (1.6 x 64cm) of DEAE-agarose (BioRad Laboratories, Richmond, CA) using a gradient of 0.01M to 0.1M pH 8 ammonium bicarbonate over 24 hr, at a flow rate of 14ml/hr and collecting 7ml fractions. All solutions contained 0.5% chloroform to prevent microbial growth. The column eluant was monitored at 220nm and the results obtained are shown in Fig. 1A. Aliquots of the fractions were lyophilized to remove ammonium bicarbonate and assayed for their ability to inhibit secondary precipitation of calcium phosphate salts, as described below, to detect the presence of phosphoseryl-phosphoserine. Significant activity was found only in fractions 40-60, associated with the main peak. These fractions were pooled, lyophilized and the material purified further by gel filtration chromatography on a column (1.6 x 53cm) of Trisacryl GF05 (LKB, Inc., Rockville, MD). The eluant used was 0.1M pH 8 ammonium bicarbonate, at a flow rate of 14ml/hr and 4.8ml fractions were collected. The eluant was monitored at 220nm and the results are shown in Fig. 1B. Aliquots of the fractions were lyophilized and assayed for inhibitory activity. This was found only in fractions 11-14 which were pooled and lyophilized.

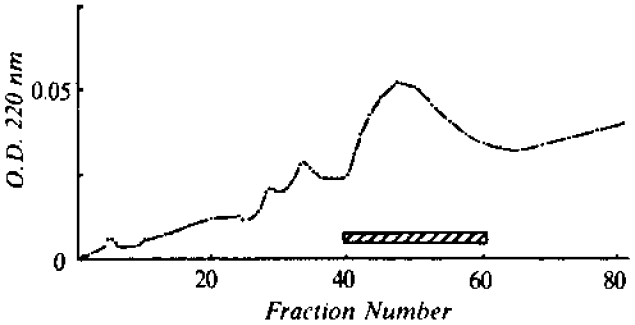

Figure 1a. Chromatography of phosphoseryl-phosphoserine on DEAE-agarose using an ammonium bicarbonate gradient (0.01-0.1M, pH 8). Inhibitory activity was found only in fractions 40-60 (cross-hatched bar) which were lyophilized for gel filtration.

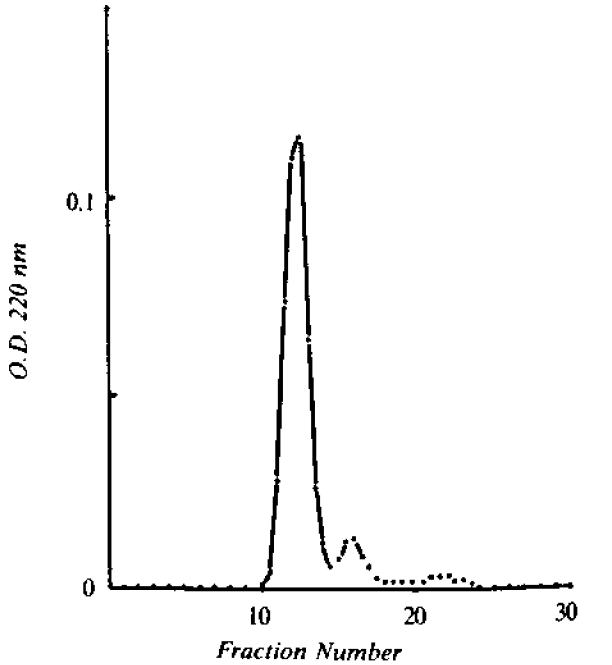

Figure 1b. Chromatography of the active material from 1a. on Trisacryl GF05 using 0.1M pH 8 ammonium bicarbonate as eluant. Inhibitory activity was found only in fractions 11-14 which were lyophilized to give the final purified product.

Assay for inhibition of secondary precipitation of calcium phosphate salts.

This assay is based on inhibition of precipitation during hydrolysis of dicalcium phosphate dihydrate (DCPD) to more basic calcium phosphate salts. The principle involved is that when DCPD partially dissolves into a suitable buffer (pH > 6.2), to saturate the solution with respect to itself, the resulting solution is supersaturated with respect to basic calcium phosphate salts. These salts precipitate by seeding onto the remaining solid DCPD. Under appropriate conditions, dissolution of DCPD and precipitation of basic salts continues until hydrolysis of the DCPD is complete. Inhibitors of calcium phosphate precipitation, at the concentrations used, do not affect the dissolution of DCPD, but adsorb to the solid phase and inhibit secondary precipitation of the basic salts. Consequently, hydrolysis of the DCPD is delayed to an extent which is related to the adsorption properties of a given inhibitor and proportional to its concentration. The experimental details for this assay have been reported previously (Gron 1973b; Hay *et al.* 1979). Briefly, samples of the serially diluted inhibitor are assayed using this method and inhibitory activity at 24hr is plotted versus concentration. The concentration of the inhibitor giving 50% inhibition at 24hr is obtained by interpolation. Standard solutions of polyaspartic acid, molecular weight 20,000 (Sigma Chemical Co., St. Louis, MO), were used to standardize the assay system.

The value of this method lies in its relative simplicity and high sensitivity; only microgram amounts of the inhibitor are required. These features are valuable for initial identification of inhibitory compounds, monitoring of inhibitory activity during purification procedures, and for preliminary studies of the type described here. Precise determinations of the inhibitory activity, in fundamental terms, involves determination of the relationship between the adsorption coverage of calcium phosphate seed crystals by an inhibitor, and the corresponding reduction in rate of crystal growth on the inhibitor-treated seed material when this is suspended in solutions with a defined degree of supersaturation with respect to itself. Such studies have been done (Moreno *et al.* 1979; Aoba *et al.* 1984) for selected salivary proteins which possess inhibitory activity, and will be done for the synthetic inhibitors obtained in these studies, but these determinations require considerably larger amounts of material.

Assay for inhibition of primary precipitation of calcium phosphate salts.

This assay was essentially identical to that used in previous studies (Hay *et al.* 1979, 1984). Briefly, stock solutions of calcium chloride and sodium phosphate are prepared. These are mixed to give a solution which resembles stimulated human saliva in its degree of supersaturation with respect to calcium phosphate salts (Hay *et al.* 1984). The sample for assay is sequentially diluted and included in the phosphate solution. Precipitation from this system occurs within 1 to 2 hr in the absence of inhibitors. In their presence, precipitation is delayed to an extent proportional to their concentration. A 24hr assay period is used at the end of which inhibitory activity is determined by analysis for calcium. The amount of calcium remaining in solution above the control value is used to calculate the degree of inhibition of precipitation. Results from the sequentially diluted inhibitor samples are plotted and the concentration of inhibitor giving 50% inhibition at 24hr is obtained by interpolation. The system is standardized using polyaspartate as a standard inhibitor, as described above.

Results and Discussion

Synthesis of the phosphoserine dipeptide, NH_2-PSer-PSer-COOH.

The yield of Z-seryl-serine-0-benzyl ester in crystalline form from the condensation of seryl-0-benzyl ester and carbobenzoxy-l-serine was 65%. The subsequent phosphorylation of this product with diphenylphosphoryl chloride was 86%. This product gave a single spot on thin-layer chromatography with no evidence of starting material.

Purification of the deprotected phosphoserine dipeptide

Following the two hydrogenation procedures described in the methods, some aromatic signals were detected by NMR. Following anion exchange chromatography on Sephadex QAE 25, however, the NH_2-PSer-PSer-COOH was isolated in homogeneous form with no aromatic signals on NMR in D_20. Residual salts from this purification precluded elemental analysis and mass spectrometry. Paper electrophoresis at pH 1.9 and 6.5 showed only one ninhydrin-positive spot migrating to the anode. ^{31}P NMR (D_20) gave two peaks (<) 4.10 and 3.10, reflecting the different environments of the two phosphate groups.

The deprotected phosphoseryl-phosphoserine was purified further by anion exchange chromatography on DEAE-agarose (Fig. 1a). Only fractions 40-60 were inhibitory in the secondary precipitation-inhibition assay, and these were pooled and lyophilized. The product was applied to a Trisacryl GF05 column. Only fractions 11-14 from this column (Fig. 1B) possessed inhibitory activity and these were pooled and lyophilized. The yield of the dipeptide was 76%, based on starting material used for these two purifications.

Inhibitory activity of purified phosphoseryl-phosphoserine.

The inhibitory activity of purified phosphoseryl-phosphoserine, comprising residues 2 and 3 in statherin, was compared with the inhibitory activities of intact statherin and its amino-terminal tryptic peptide, which has the structure NH_2-Asp-PSer-PSer-Glu-Glu-Lys-COOH (Schlesinger and Hay 1977). Inhibitory activities were determined using both the primary and secondary precipitation-inhibition assay systems described above, and are expressed as the concentration of inhibitor required to give 50% inhibition of precipitation in the assay at 24 hr. For the primary precipitation-inhibition assay, relative activities were as follows. Statherin, 1.8μM; the amino-terminal tryptic hexapeptide, 21μM; and phosphoseryl-phosphoserine, 60μM (Table 1).

Table 1 Inhibitory activities of phosphoseryl-phosphoserine, human salivary statherin and the amino-terminal hexapeptide of statherin

Inhibitor	Interpolated concentrations (μM) for 50% inhibition	
	Precipitation Inhibition Assay	
	Primary	Secondary
Statherin	1.8	0.3
Asp_1-Lys_6*	21	0.08
PSer-PSer	60	3.5

*NH_2-Asp-PSer-PSer-Glu-Glu-Lys-COOH

This is an interesting result considering that covalently bound phosphate groups are considered to play critically important roles in the activities of inhibitors of calcium phosphate precipitation of the type considered here (Williams and Sallis 1979, 1982). The threefold higher activity of the amino-terminal hexapeptide, compared with the synthetic dipeptide, can probably be explained in terms of the additional carboxyl groups present in the hexapeptide, a structural arrangement known to increase the effectiveness of this type of inhibitor (Williams and Sallis 1979, 1982). The rest of the statherin molecule (37 residues), however, consists of one negatively charged and three positively charged residues (Schlesinger and Hay 1977), with the remainder of the molecule being formed from neutral and hydrophobic residues which are not normally considered to contribute significantly to the kind of inhibitory activity considered here. Consequently, the far higher activity of statherin in inhibiting primary precipitation, compared with the synthetic dipeptide and the hexapeptide, is an unexpected level of activity, which would not have been readily predicted from existing knowledge. A possible explanation for this finding, however, is indicated by previous studies of inhibition of secondary precipitation (Moreno *et al.* 1982, 1984), discussed below.

The results from the secondary precipitation-inhibition assays are relatively more easily understood. Inhibition of secondary precipitation is usually explained in terms of adsorption of inhibitors onto crystal growth sites (Meyer and Nancollas 1973; Moreno *et al.* 1979), and adsorption is usually enhanced by increased numbers of negatively charged groups (Williams and Sallis 1979, 1982) (but see below). The higher activity of the hexapeptide compared with the synthetic dipeptide can be understood in these terms. Also, although the hexapeptide and intact statherin are identical in the first six residues, the lower activity of statherin in inhibiting secondary precipitation, compared with the hexapeptide, can probably be explained in terms of a decreased efficiency of adsorption of the larger statherin molecule compared with the hexapeptide, particularly as residues 7 to 43 of statherin contain only one further negatively charged group in addition to the C-terminal carboxyl group.

These differences in the behaviors of the peptides investigated in the primary and secondary precipitation-inhibition systems are not easy to reconcile. An important possible factor, however, is that recent studies (Moreno *et al.* 1982, 1984) of mechanisms underlying adsorption of acidic polypeptides onto hydroxyapatite showed that these adsorptions are endothermic, and are driven by an increase in entropy. Part of this entropy increase comes from displacement of ordered water from the surface of the adsorbent, but the major portion comes from loss of ordered water from, and disruption of secondary structure of the adsorbate. It seems possible that such structural changes may also underlie the relatively much higher activity of statherin, compared to its component segments, in inhibiting primary precipitation of calcium phosphate salts. It is curious, however, that this behavior is not also seen in inhibition of secondary precipitation, suggesting that significantly different mechanisms operate in the two precipitation-inhibition systems. These findings and considerations emphasize the need to determine the adsorption properties of the molecules of interest as a necessary step in understanding their mechanism of action and biological activities.

These studies represent the first steps towards obtaining specific molecular segments by a synthetic route for defining the molecular mechanisms underlying the inhibition of precipitation of calcium phosphate salts by statherin and the PRP from human saliva. The success with the synthetic strategy provides a basis for future studies for obtaining highly purified phosphoserine-containing analogs and variants of molecular segments of these unusual molecules, to begin to resolve the questions noted above.

Acknowledgements

This work was supported in part by grants DE-06159 to D.H.S. and DE-03915 to D.I.H. from the National Institute of Dental Research.

References

Aoba, T., E.C. Moreno, and D.I. Hay, 1984. Inhibition of apatite crystal growth by the amino-terminal segment of human salivary acidic proline-rich proteins. Calcif. Tissue Int. 36:651-658.

Folsch, G. 1959. Synthesis of phosphopeptides. II. O-phosphorylated dipeptides of L-serine. Acta Chem. Scand. 13:1407-1421.

Gron, P. 1973a. Saturation of human saliva with calcium phosphates. Archs. Oral Biol. 18:1385-1392.

Gron, P. 1973b. The demonstration of a dicalcium phosphate stabilizing factor in human saliva. Archs. Oral. Biol. 18:1379-1383.

Hay, D.I. 1973. The isolation from human parotid saliva of a tyrosine-rich acidic peptide which exhibits high affinity for hydroxyapatite surfaces. Archs. Oral Biol. 18:1531-1541.

Hay, D.I., D.H. Schlesinger, and E.C. Moreno. 1979. Phosphoprotein inhibitors of calcium phosphate precipitation from human salivary secretions. Inorg. Persp. Biol. Med. 2:271-285.

Hay, D.I., S.K. Schluckebier, and E.C. Moreno. 1982. Equilibrium dialysis and ultrafiltration studies of calcium and phosphate binding by human salivary proteins. Implications for salivary supersaturation with respect to calcium phosphate salts. Calcif. Tissue Int. 34:531-538.

Hay, D.I., D.J. Smith, S.K. Schluckebier, and E.C. Moreno. 1984. Relationship between concentrations of human salivary statherin and inhibition of calcium phosphate precipitation in stimulated human parotid saliva. J. Dent. Res. 63:857-863.

Lagerlof, F. 1983. Effect of flow rate and pH on calcium phosphate saturation in human parotid saliva. Caries Res. 17:403-411.

Merrifield, R.B. 1963. Solid-phase peptide synthesis. I. The synthesis of a tetrapeptide. J. Am. Chem. Soc. 85:2149-2154.

Merrifield, R.B. 1964. Solid-phase peptide synthesis. III. An improved synthesis of bradykinin. Biochemistry 3:1385-1390.

Meyer, J.L. and G.H. Nancollas. 1973. The influence of multidentate organic phosphonates on the crystal growth of hydroxyapatite. Calc. Tissue Res. 13:295-303.

Moreno, E.C., K. Varughese, and D.I. Hay. 1979. Effect of human salivary proteins on the precipitation kinetics of calcium phosphate. Calcif. Tissue Int. 28:7-16.

Moreno, E.C., M. Kresak, and D.I. Hay. 1982. Adsorption thermodynamics of acidic proline-rich human salivary proteins onto calcium apatites. J. Biol. Chem. 257:2981-2989.

Moreno, E.C., M. Kresak, and D.I. Hay. 1984. Adsorption of molecules of biological interest onto hydroxyapatite. Calcif. Tissue Int. 26:48-59.

Oppenheim, F.G., D.I. Hay and C. Franzblau. 1971. Proline-rich proteins from human parotid saliva. 1. Isolation and partial characterization. Biochemistry 10:4233-4238.

Schlesinger, D.H. and D.I. Hay. 1977. Complete covalent structure of statherin, a tyrosine-rich acidic peptide which inhibits calcium phosphate precipitation from human parotid saliva. J. Biol. Chem. 252:1689-1695.

Schlesinger, D.H. and D.I. Hay. 1981. Primary structure of the active tryptic fragments of human and monkey salivary anionic proline-rich proteins. Int. J. Peptide Protein Res. 17:34-41.

Strid, L. 1959. Separation of some O-phosphorylated amino acids and peptides on anion exchange resin. Acta Chem. Scand. 13:1787-1790.

Williams, G. and J.D. Sallis. 1979. Structure-activity relationship of inhibitors of hydroxyapatite formation. Biochem. J. 184:181-184.

Williams, G. and J.D. Sallis. 1982. Structural factors influencing the ability of compounds to inhibit hydroxyapatite formation. Calc. Tissue Int. 34:169-177.

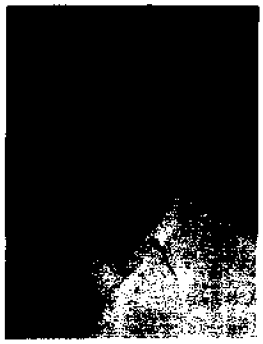

David Schlesinger is a Research Professor of Experimental Medicine and Cell Biology, Director of Macromolecular Sequencing and Synthesis, and Director of Neurosciences at the New York University Medical Center. He received the B.A. in chemistry and zoology at Columbia in 1962, the M.S. in physiology at Albany Medical College in 1965, and the Ph.D. at City University of New York in 1972. David has broad experience and accomplishments in the areas of protein sequencing and peptide synthesis, including pioneering studies into the structures of polypeptide hormones and salivary proteins. A current focus of his research is the synthesis of phosphorylated peptide analogs of statherin for use in structure/function studies.

Chemical Aspects of Regulation of Mineralization. C.S. Sikes and A.P. Wheeler, editors. University of South Alabama Publication Services, Mobile, Alabama, 1988.

A Chemist's Approach to Biomineralisation

Carole C. Perry[1] and Jennifer R. Wilcock[2]

[1]The Chemistry Department, Brunel, The University of West London, Uxbridge, Middx. UK

[2]Inorganic Chemistry Laboratory, South Parks Road. Oxford, UK.

ABSTRACT

Biominerals result from the regulation and organization of the inorganic solid state by biological systems. In this article we shall consider (1) crystal chemistry, (2) organic matrices, (3) the ionic environment and (4) external stresses as controlling factors in the regulation of the biomineralisation process.

Introduction

Biominerals result from the regulation and organization of the inorganic solid state by biological systems. Biominerals are complex materials, generally comprising both organic and inorganic phases with properties characteristic of the composite as a whole (Williams 1984). A wide range of biominerals are known in extant organisms (Lowenstam 1981). The major biominerals are calcium carbonates and phosphates which occur in many polymorphic forms, and are extensively used as skeletal supports. A wide range of iron oxides are known with diverse functions of magnetoreception and as a hardening agent in the cutting edge of teeth. Amorphous silica structures are widely known and functional roles include skeletal support and defence against physical and biochemical predators. Group IIA sulphates and transition metal sulphides are observed less extensively and appear to function as specific gravity devices or as deposits of waste material.

The formation of bioinorganic solids can occur within cellular space (intracellular), at the cell surface (epicellular) or within the extracellular matrix (Mann 1983). Many studies of biomineralisation in lower organisms have concentrated on defining the level of control organisms exercise over both the mineral species deposited and the growth of the mineral phase. At two ends of an integrated scale we have 'biologically induced' and 'matrix-mediated' biomineralisation (Lowenstam and Weiner 1983). In biologically induced mineralisation, membrane morphology and element pumps or diffusion limitations are proposed to ultimately determine the composition of the deposited solids (Mann 1983; Williams 1984). In matrix-mediated mineralisation, the rigid solid-state conformation of macromolecular assemblages decides the 'epitaxial' pattern of mineral growth *in vitro* and is thought to operate *in vivo* (Addadi and Weiner 1986). Researchers have concentrated on the control of nucleation and the promotion of growth but have proposed that 'lattice modifiers and crystal inhibitors' are an essential component of a mineralising system in order to obtain specific control of mineral morphology (Simkiss 1986). The control of mineralisation results in the adoption of well defined mineralogical properties such as particle size, structure, morphology, crystal growth direction and crystal orientation. It is thought that the utilization of amorphous inorganic polymers such as hydrated silica in the production of skeletal materials may involve different design and construction processes in the generation of functional structures (Mann 1987).

Characterisation of composite materials at the molecular level presents many problems and a combination of techniques must be utilised. The inorganic phase can be defined by a combined structural and analytical physico-chemical experimental approach. Structural techniques include electron microscopy (scanning, (SEM), transmission, (TEM) and ultra high transmission, (HRTEM)), solid state nmr, FT infrared and Raman spectroscopy. Analytical techniques include energy dispersive X-ray analysis (EDXA) and proton induced X-ray emission (PIXE) coupled to the scanning proton microprobe (SPM). In the following section of this article we will detail the information which may be obtained from these techniques.

The definition of the inorganic phase is the initial (easy) part of any study of biomineralisation. In order to understand, or at least start to understand, the biological mechanisms involved in the regulation and control of biomineral production we must consider the following factors: (1) crystallochemical control over morphogenic form, (2) the organic matrix and the extent of matrix/mineral interactions during both nucleation and subsequent mineral growth, (3) the local chemical/biochemical environment as biomineralisation takes place and the importance of the ionic environment as a morphology regulator, and (4) external physical stresses including the role of cell membrane and filament structures in the control of biomineral morphology.

In order to illustrate some of the above points we will consider two distinct mineralising systems: (A) Intracellular Group IIA sulphate depositions in unicellular organisms, and (B) Extracellular silica deposition in plants. In this article we shall present structural and analytical information obtained using electron microscopy, X-ray analysis and solid state nmr and show how studies of morphological structure and chemical analysis can aid us in our understanding of the biomineralisation process.

Materials and Methods

Sample Preparation: Full details of sample preparation for biogenic silica and group IIA sulphate samples may be found in papers by Perry *et al.* (1984a, 1984b, 1987) and Wilcock *et al.* (1988).

Electron Microscopy: HRTEM, TEM, and SEM and electron diffraction yield structural information at the molecular, microscopic and macroscopic structural levels. SEM and TEM provide information relating to the way in which a biological structure is built up from fundamental microscopic structural units. The techniques have shown that structural complexity is possible for amorphous materials and have, therefore, implied that significant chemical controls over mineral deposition must take place. HRTEM is an established method for investigating the local structure of crystalline and amorphous materials at the nanometre level. The structure and properties of materials are investigated by direct imaging of the crystal lattice under optimum defocus conditions in the electron microscope. For crystalline materials, defects in the crystal lattice may lead to information on mineral growth patterns. For amorphous minerals we may determine whether the structure is based upon a random network

of structural units connected via bonds of variable angle as opposed to a microcrystalline/cluster structure comprised of a random array of microcrystalline polyhedra. This will again give us information relating to the pattern of mineral growth as it is known that the presence of extraneous cations dispersed throughout a structure would tend to favor the latter type of structure (Mann and Perry 1987).

Solid State NMR: For suitable nuclei, solid state nmr spectroscopy is an excellent technique for studying the local environment of atoms in condensed phases. For ^{29}Si nmr the chemical shift position is highly sensitive to the coordination geometry of the Si atoms, such that, for example, the replacement of OH groups by -O- bridges can be readily detected. This technique is equally applicable to crystalline and amorphous materials and for the latter, peaks are expected to be broad in the absence of well-defined single sites for Si atoms (it is a reflection of the variations in bond length and bond angle which can be accommodated around the Si atoms). The proportions of the various resonances gives information on the chemical nature of the silica phase. Information on the nature of the silica surface can be obtained by pretreatment of surface silanol groups with a silylating agent (often trimethylchlorosilane) prior to spectroscopic accumulation (Mann *et al.* 1983). The spectra presented in this article were obtained from magic angle spinning experiments performed on a Bruker CXP 200 solid state spectrometer operating at 39.73 KHz for ^{29}Si.

Chemical X-ray Analysis: The techniques of energy dispersive X-ray analysis (EDXA) and scanning proton microprobe (SPM) analysis provide information on the inorganic elemental composition of a material but no information on the chemical identity, coordination chemistry and oxidation state of a particular element can be directly obtained. Both techniques rely upon the interaction of an incident beam of energetic particles (electrons for EDXA, >2MeV protons for SPM) with the sample to excite X-ray production. The X-rays are detected and analysed using a lithium drifted silicon detector. Elemental detection limits are 100ppm for EDXA and 1ppm for SPM analysis in bulk samples. An advantage of the proton microprobe analytical technique is that the problems of a high continuum background due to deceleration of electrons in the sample material is significantly reduced. Also, for thick samples, eg. whole cells etc., the high energy proton beam does not deviate significantly from its original trajectory on passing through the sample, so loss of resolution is not a problem. Both techniques can be utilised for point analyses and to provide spatial information via two dimensional mapping.

EDXA data in our studies were obtained using a JEOL 2000FX electron microscope operating at 200 KeV with a lithium drifted silicon detector and analysed using Tracor Northern software. SPM analyses were performed on the Oxford microprobe housed in the nuclear physics laboratory. Full details of the experimental setup can be obtained from the book by Watt and Grime (1987). Point analytical data give the most accurate quantitative elemental information but 2D mapping provides a means of studying the relationships between elemental distribution and biomineral composition or cellular organization.

Radiolabelling Experiments: Synthesis of cell wall components during silicification of grass hairs was investigated by *in vivo* radioactive labelling of plant inflorescences with [^{3}H]arabinose and [^{14}C]glucose at various stages of development. Polysaccharides synthesised were analysed by graded acid hydrolysis and by enzymatic digestion followed by chromatography. Full experimental details can be found in the paper by Perry *et al.* (1987). Labelling of macromolecules synthesised over specific time intervals provided information on the changing nature of the macromolecular assemblage in which deposition of the mineral phase occurs.

Results and Discussion

We will now show how physico-chemical studies of morphological structure and chemical analysis can aid in our understanding of the regulation and control of the biomineralisation process. We will consider each of the four factors detailed in the introduction in turn and illustrate our argument with examples from our studies on intracellular group IIA sulphate deposition and extracellular silica deposition.

(1) Crystallochemical control over Morphogenic Form

Studies of the crystallography and morphology of the celestite skeleton of the acantharian species *Phyllostaurus siculus H.* have provided much information relating to the competition between the desire of a biological organism to achieve structural functionality and crystallographic limitations imposed on growth patterns. Full experimental details and discussion can be found in the paper by Wilcock *et al.* (1988). We will also include a brief description of siliceous structures where although "crystallochemical" control cannot exist (the structures are always amorphous), structural variation exists at both the molecular and microscopic level.

Acantharia

Acantharia are marine protozoa with internal strontium sulphate skeletons which for the species *Phyllostaurus siculus H.* are composed of 20 spicules radiating from a central point, Figure 1. The spicules connect via lateral wing structures which are part of the base formations at the innermost end of each spicule, Figures 2a and 2b.

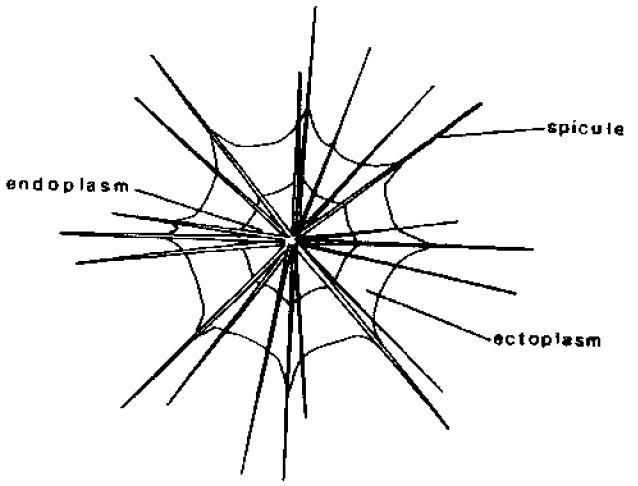

Figure 1. Schematic diagram of a typical acantharian species of the order Arcanthida, showing twenty spicules radiating from a central point. The crystals are single crystals of strontium sulphate enclosed by a vesicular membrane. The skeleton has a typical diameter of 0.2-1.00 mm.

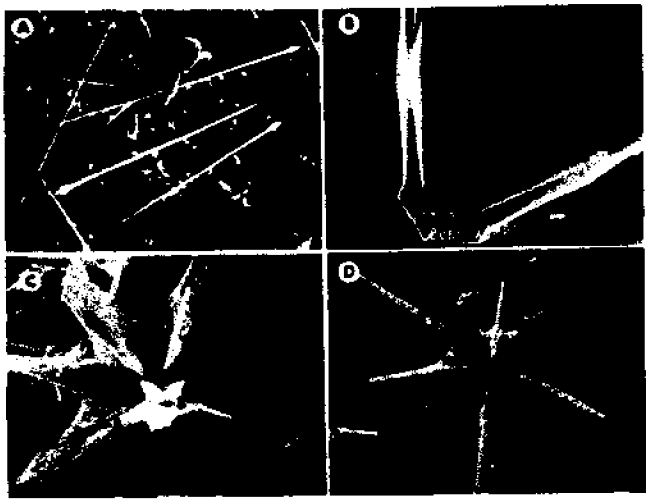

Figure 2. Morphological details of the skeleton of the acantharian species *Phyllostaurus siculus* H. [A] SEM of intact spicules, note arrow shaped bases. Bar represents 50 μm. [B] SEM of a pair of spicule bases connected by lateral wings lying in one plane. Bar represents 1 μm. [C] SEM of part of the skeleton showing the pattern of spicule connectivity. Three different types of spicule base connect to form the complete skeleton. The three types are labelled A, B and C. Bar represents 3 μm. [D] SEM of the virtually intact skeleton with the three spicule types labelled. The relative rotation of the type C spicule shafts is clearly shown. Bar represents 3 μm.

Morphological information has been obtained from SEM and TEM studies. The twenty spicules can be divided into 3 groups, type A, type B, and type C, according to the morphology of the bases and the number and orientation of the lateral wings, Figure 3. Electron diffraction and HRTEM imaging showed that the spicules were single crystals of strontium sulphate with long range perfect crystallinity, Figure 4a. All spicules were oriented along the crystallographic a axis. We must point out that spicule morphology is unlike that of geological or synthetic crystals which most commonly display a tabular form with growth parallel to the (001) plane. Electron diffraction was also used to determine the precise crystallographic orientation of the spicule lateral wings. The lateral wing attachments lie in low index preferred planes of strontium sulphate, Figure 3. The three dimensional spicule arrangement was characterised using SEM, electron diffraction and optical microscopy. Spicule bases were observed to join at the centre of the cell, by the connection of 2 lateral wings in one plane. The pattern of spicule connectivity is as follows: Four A type spicules lie in an equatorial plane and are attached to 8 type B spicules, 4 in a layer above and 4 in a layer below. The B type spicules are rotated around a central pole, perpendicular to the equatorial plane, by 45^0 relative to the A type spicules. In addition to the attachment to A type spicules, the B type spicules are also attached to C type spicules, 4 in each of two layers further out from the equator. These C type spicules lie directly over the A type spicules, Figures 2c and 2d.

We have seen that the acantharia adopts a spicule arrangement governed by lateral wing attachments lying in low index preferred planes of strontium sulphate, Figure 3. An examination of the efficiency of spicule packing indicates that the spicule arrangement observed is governed by a compromise between the drive for an efficient use of space at the cell centre and crystallographic limitations on lateral wing orientation. The most efficient use of space at the cell centre would require all spicules to be identical and to have three lateral wings inclined at 120° to one another.

Figure 3. Schematic representation of the three spicule types A, B and C, showing the relation between spicule morphology and crystallographic orientation. The planes of all the lateral wings are labelled; a, b and c refer to the orientation of the crystal axes of strontium sulphate.

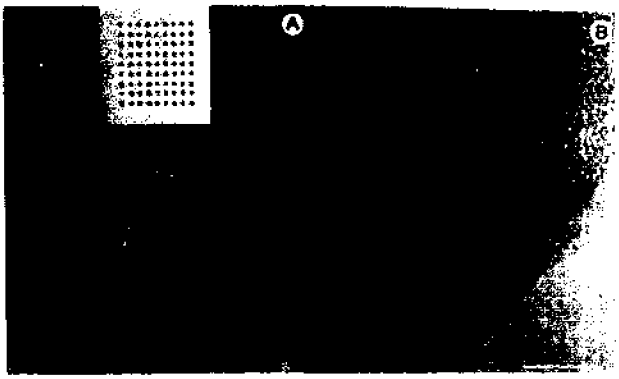

Figure 4. [A] HRTEM image of a spicule shaft edge with the major axis of the rounded rhombohedral spicule cross section and the long spicule axis lying in the [010] zone. The (100) and (001) planar separations are labelled. Note the long range perfect crystallinity. Bar represents 10 nm. Inset [010] electron diffraction recorded from this spicule, with corresponding theoretical diffraction pattern (right) showing the position of the double diffraction spots (⊗). [B] HRTEM image of amorphous plant silica. No order above 10Å is visible. Bar represents 5nm.

However, this is not compatible with the crystal chemistry of strontium sulphate and is not observed (Wilcock *et al.* 1988).

If we consider the symmetry of the organism, the spicule distribution obeys the general form of Müllers law, which describes a pattern of 20 spicules in simple D_{4h} symmetry. Now, although the pattern is closely related to this simple description, it actually has a different form from any simple pattern in several ways and the structural form of the skeleton would not appear to result merely from obedience to simple physical principles. The specific and unusual morphology and the well defined relative spicular orientation are indicative of the influence of cellular activity as well as crystallographic considerations in skeletal morphology.

Desmids

In direct contrast to the species specific strontium sulphate skeleton found in acantharia we turn now to barium sulphate deposition in unicellular organisms, desmids, Figure 5. Both barium and strontium sulphates are isostructural and it could, therefore, be expected that we might observe similar competitive effects between crystallographic requirements and biological control in the development of crystal morphology. This is not the case. There appears to be limited biological control over crystal development and the barium sulphate crystals found in these organisms lie in the same crystallographic plane as their synthetic

counterparts and both rhombic and hexagonal crystal forms are observed, Figure 6. The crystal chemistry of these organisms can be manipulated to produce either of the two major crystal morphologies as we shall see in section 3.

Figure 5. Optical micrograph of the desmid *Closterium moniliferum* showing vacuoles which contain barium sulphate crystals (arrowed) at either end. Bar represents 25 μm. Micrograph and desmids were provided by Prof. A.J. Brook, University of Buckingham.

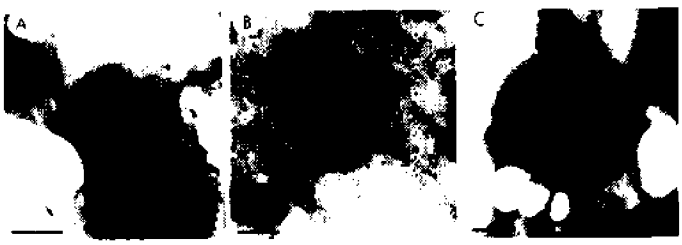

Figure 6. TEM of barium sulphate crystals obtained from the desmid *Closterium lunula*. The crystals all lie in the (001) plane. [A] rhombic crystals, bar represents 1 μm. $M^{2+}:SO_4^{2-} \leq$ 1:1. [B] an intermediate stage in the development of C, bar represents 500 nm. [C] hexagonal crystal $M^{2+}:SO_4^{2-}$ ~10:1. Bar represents 500 nm.

Plant Silica

If we now consider siliceous structures, "crystallochemical" control takes on a different meaning and we must consider both molecular and microscopic structures before we can realistically seek for controls over the mineralisation of such materials.

At the molecular level, in the electron microscope all biogenic silicas currently studied appear similar in that no lattice fringes are observed, Figure 4b, and no local order above 10Å (3 Si-O repeat units) is visible. The images indicate a structure based on a random network of SiO_4 units connected through Si-O-Si bonds of variable bond angle rather than a microcrystalline/cluster structure composed of a random array of microcrystalline polyhedra (Mann and Perry 1987). However, if we turn to solid state ^{29}Si NMR we observe that plant silica is markedly different from other silicas, e.g. limpet and sponge in the proportion of $Si(OSi\equiv)_3OH$ units found within the structure, Figure 7 (Mann and Perry 1987). A significant proportion of the hydroxylated units are in the interior of the structure (Mann *et al.* 1983).

Although biogenic silica exhibits no long-range crystallographic order we have recently shown that morphological order exists at the microscopic level. The study of specialised grass and stinging hairs has shown that biogenic silica can exhibit various structural motifs at the microscopic level, (Perry *et al.* 1984a; Mann and Perry 1987). Examples are shown in Figure 8. Each motif

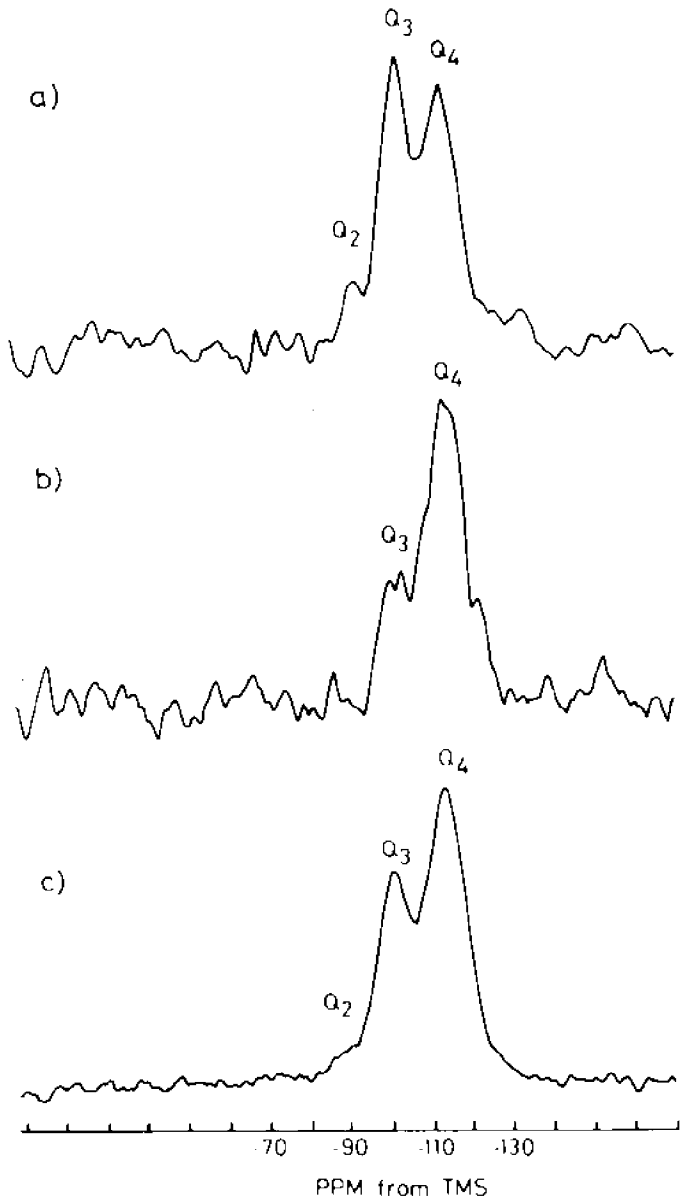

Figure 7. ^{29}Si solid state magic angle spinning (MAS) spectra for a) plant silica, b) limpet silica and c) sponge silica. Q_4 = $Si(OSi\equiv)_4$, Q_3 = $Si(OSi\equiv)_3OH$, Q_2 = $Si(OSi\equiv)_2(OH)_2$. TMS, tetramethylsilane.

comprises primary silica particles of characteristic size, stability in the electron beam (i.e. degree of hydration) and orientation. Detailed studies on grass hairs showed that substructures were formed at different stages of development. The sequence of events appears to be linked to changes in the ionic environment (Perry *et al.* 1987). These factors will be discussed in the following sections.

(2) Organic matrix control (over amorphous silica deposition)

Involvement of an organic matrix in mineralisation has been proposed to occur at different levels including, the simple provision of nucleation sites (Lowenstam 1981), the delimitation of a "reactive volume" (Mann 1983; Williams 1984), and action as a template for selection of defined inorganic microarchitectural features (Lowenstam 1981). Biogenic silica, because of its intrinsic amorphous nature requires chemical/biological/stress controls at

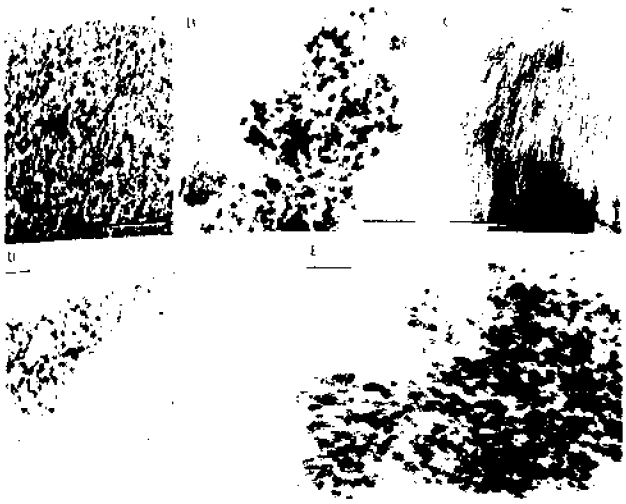

Figure 8. Examples of structural motifs exhibited by plant silicas. *Phalaris canariensis* L. hairs A)sheet-like, B)globular, C)fibrillar. In addition for nettle hairs D) and E) globular-fibrillar. For A), B), C), E) bar represents 0.4 μm. D) bar represents 0.2 μm.

all levels of structural organisation in order to produce a functional morphology. We will now consider information obtained from an *in vivo* radiolabelling study of silicifying plant hairs and indicate the possible extent of control over biomineral morphology. Full experimental details may be found in the article by Perry *et al.* (1987).

Biochemical studies performed on hairs from the lemma of the grass *Phalaris canariensis L.* have shown that silicification commences after cell growth is complete and primary cell wall synthesis has ceased. Radiochemical labelling studies of the organic matrix associated with the silica has provided chemical information on the changing compositional nature of the secondary cell wall material which may be correlated with different mineral deposits observed. Detailed results may be found in the article by Perry *et al.* (1987). Figure 9 shows graphically the changes occurring as the cell wall matures and as silicification takes place. Important points to note include (a) cell wall synthesis continues for at least 5 weeks after emergence of the inflorescence and that the process of silicification is not complete for at least six weeks after emergence of the inflorescence, and (b) cell wall biosynthesis appears to change from the synthesis of predominantly cellulose and arabinoxylans during the early stages of cell wall development to the synthesis of a β(1-3)(1-4)glucan during the latter stages of cell wall development.

Although there is no information at present concerning the precise stereochemistry of the organic polymers detailed above, we have shown that during silicification changes in mineral structural organization at the microscopic scale are associated with relative changes in the synthesis of organic matrix components. The sheet-like silicified material deposited at the early stages of macrohair development is laid down at the same time as cellulose and a heavily substituted arabinoxylan. The globular material is then laid down along with declining amounts of cellulose and arabinoxylan and rapidly increasing amounts of β(1-3)(1-4)glucan and mannan. The fibrillar silicified material is deposited into the mature organic phase, when further deposition of polysaccharide has virtually ceased.

Within the external boundaries of the mineralising volume organic material may play a role in determining spatial availability for silicification at the nanometre level. In the plant system

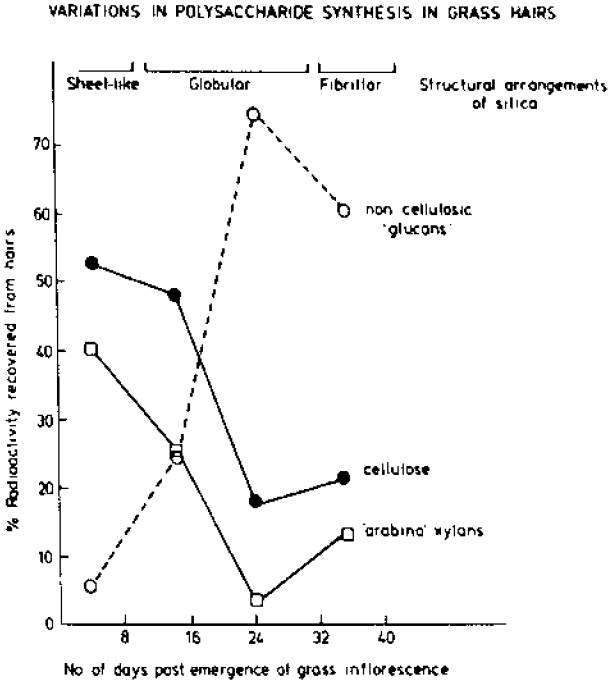

Figure 9. A graphical representation of the temporal variations in polysaccharide synthesis in grass hairs. Siliceous structural motifs are also indicated. Analysis of the polysaccharides was performed by *in vivo* radiochemical labelling followed by acid hydrolyses and paper and thin layer chromatography. The labelled monosaccharides were detected by scintillation counting.

discussed above, we have clear evidence that spatial availability for mineralisation will be dependent upon constraints imposed by secondary cell wall synthesis which proceeds in advance of silica deposition (Hodson *et al.* 1984). Generally, the three dimensional nature of carbohydrate polymers is affected by glycosidic linkage, monosaccharide sequence, whether periodic or interrupted, and on the presence, absence and chemical identify of any side chains present. As an example, the effect of glycosidic linkage on the shapes adopted by polymers of glucose is shown in Table 1. Side chain modifications have a significant effect on the three dimensional shapes adopted by polymers, on their mutual interactions and on the provision of ionic or hydrogen bonding centres for interaction with the developing mineral phase. The changing nature of the polysaccharides synthesised, for example, cellulose at the early stages, a mixed linkage glucan at the later stages, etc. will have clear consequences for both the 'shape' of the volume available for mineralisation and for the interactions possible between the organic and inorganic polymers. The siliceous

Table 1. glycosidic linkage polymer shape adopted β(1-4) cellulose ribbon α (1-4) amylose hollow helical tube β(1-3) callose 3 intertwined chains

glycosidic linkage	polymer	shape adopted
β (1-4)	cellulose	ribbon
α (1-4)	amylose	hollow helical tube
β (1-3)	callose	3 intertwined chains

structures observed for the plant systems (sheet-like, globular, fibrillar and variations) may result from a patterning of underlying organic polymers.

The question of nucleation and initial particle growth in the presence of organic molecules will be considered in conjunction with the effects of inorganic/ionic species on the development of morphology in the following section.

(3) The ionic environment as a morphology regulator

Amorphous Silica

The importance of the ionic environment as a morphology regulator for the deposition of silica is well documented (Iler 1979).

Electron microscopical studies of macrohairs from the grass *Phalaris canariensis L.* have shown that morphologically distinct silica structures are deposited at precise times and in well defined locations within these unicellular hairs (Perry *et al.* 1984a). In parallel with structural studies, EDXA and SPM analysis have been used to study changes in elemental distributions and concentrations in the developing hairs. These analytical investigations are of utmost importance in elucidating the chemical factors which modify the structural forms of biologically deposited silica. Although changes in the quantities of Si and K, Cl within the hairs could be observed using EDXA, SPM analysis of both immature and mature hairs provided greater detail concerning the changes in Si, P, S, Cl and K levels with time. In particular, the mapping of P and S provided an effective means of following cellular activity within the macrohairs during biomineralisation.

Both EDXA and SPM analysis on immature hairs have shown that silicification commences at the tip of the hair, Figure 10. SPM data showed that K and Cl (not shown) are concentrated behind the initial deposit of silica and are also present at lower levels throughout the entire macrohair, Figures 10 and 11. Low levels of P and S remained virtually constant along the entire length of the hair. At maturity, X-ray analysis showed that there was no specific localisation of inorganic elements. Levels of Si were high along the entire length of the hair, Figure 11. Levels of K and Cl were much lower than those found in the immature hairs and low levels of P were only detected at the base of the hairs. Levels of S were only slightly reduced (2X) and were present throughout the entire length of the hair.

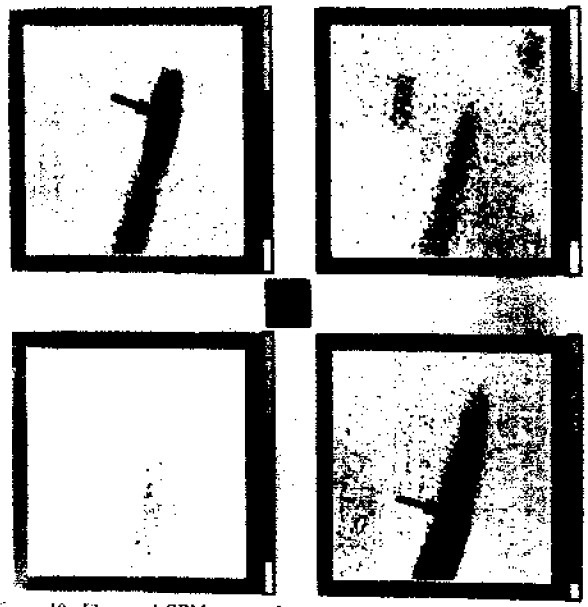

Figure 10. Elemental SPM maps of a grass hair tip 4 days after emergence of the inflorescence. Total area analysed was 60μm x 60μm. Silicification commences in the tip of the hair (arrowed). Localised maximae (arrowed) in the K and Cl (not shown) maps occur immediately behind the initial Si maximum. P and S are uniformly distributed at low levels throughout the hair. An exact correlation between colour and concentration can be found in the paper by Perry *et al.* (1984b).

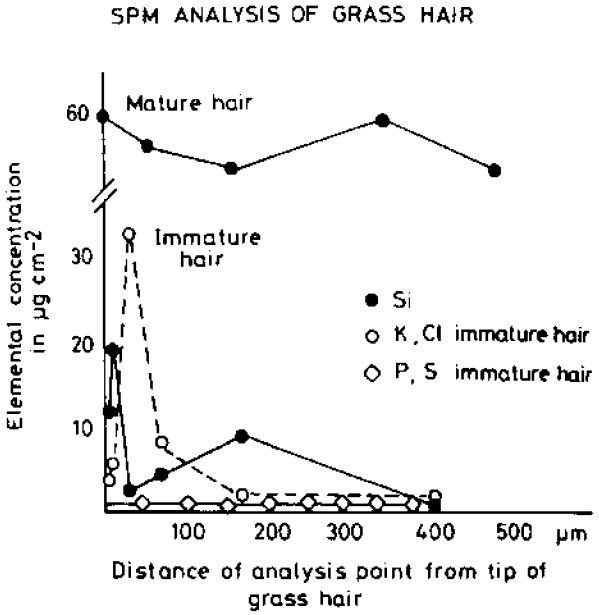

Figure 11. SPM elemental analysis of immature and mature grass hairs. Levels of silicon, potassium, phosphorous and sulphur are compared with distance of analysis point from the tip of the macrohair. At maturity levels of potassium, chlorine and phosphorous are barely above background and are not shown.

The presence of considerable quantities of K, Cl, P and S within the immature hairs indicated that cellular contents were present during the early stages of silicification. SPM studies on mature hairs and studies of sectioned material (Hodson *et al.* 1984) indicated that withdrawal of cellular contents occurs during silicification. The continued presence of S in the hairs at maturity suggests involvement with membranous structures within the organic component of the silicified cell wall. Similar analytical results have been found in a study of biomineral formation in stinging hairs from the common stinging nettle *Urtica dioica L.* (Hughes *et al.* 1988).

The temporal and spatial localisation of specific inorganic (ionic) elements during mineral deposition suggests that silicification is closely connected with underlying cellular processes which may ultimately control the aggregation of microscopic silica particles from supersaturated silicic acid solution. The presence of trace levels of ions throughout the mature hairs suggests possible involvement with neutralisation of surface charges on initially formed silica particles, thus aiding aggregation.

It is known that the growth of silica phases is governed by interfacial properties. Organic and inorganic (ionic) components may moderate the mineralisation process (Iler 1979). High levels of ionic activity 0.2-0.3M Na^+, K^+) may promote particle aggregation due to surface charge reduction between primary silica nuclei but do not (on their own) regulate the development of morphological features. Hydrogen bonding 'flocculants' such as alcohols, proteins, lipids and polysaccharides may act in a similar manner but only when ionic concentrations are low. It

can be suggested, therefore, that the changes in the relative importance of both the ionic and organic (see section previous) local environment may ultimately determine the distinctive morphological form of amorphous silica (Perry and Mann 1988).

Crystalline Barium Sulphate

The importance of the ionic environment as a morphology regulator in the deposition of group IIA sulphates has been probed by chemical and structural studies on desmids. We must note again that although strontium and barium sulphates are isostructural, we do not observe similar competitive effects between crystallographic requirements and biological control in the development of barium sulphate crystal morphology. There appears to be limited biological control over crystal form. The barium sulphate crystals found in these organisms lie in the same crystallographic plane as those produced by synthetic methods and may exhibit variations on rhombic or hexagonal crystal morphology. Desmids may be grown easily in culture and we have been able to investigate the extent of biological control on ion selective uptake and mineral formation. Full experimental details and results will be published elsewhere (Wilcock *et al.* in preparation). Here, we note some of the findings which are pertinent to our line of argument.

Changes in the cation:anion ratios, $Ba^{2+}:SO_4^{2-}$ in the external culture medium result in a change in morphology of crystals found in the desmid, Figure 6. If cation:anion, $M^{2+}:SO_4^{2-}$ ratios are $\leq$1:1, rhombic crystals are deposited. If $M^{2+}:SO_4^{2-}$ ratios are ~ 10:1, hexagonal crystals are formed. If strontium is added to the culture medium the crystals are found to incorporate strontium. The morphology of the crystals, whether rhombic or hexagonal is independent of cation identity whether strontium or barium but is dependent upon the cation:anion, $M^{2+}:SO_4^{2-}$ ratio in the external medium. This is well illustrated in Figure 12 where EDXA maps show the spatial location of the elements involved. In this experiment crystals were allowed to develop under conventional growth conditions, $M^{2+}:SO_4^{2-} \simeq$ 1:1, and then Sr^{2+} added such that $M^{2+}:SO_4^{2-} \simeq$ 10:1. Barium sulphate of rhombic morphology is found at the centre of the crystal from which is developing an hexagonal crystal containing significant levels of Sr in the outermost regions.

Quantitative experiments using EDXA have shown that the ratios of Sr:Ba incorporated into both biologically produced desmid crystals and synthetic crystals grown from similar media under identical conditions are virtually identical (Wilcock *et al.* in preparation). The desmid cells appear largely incapable of selecting for barium in the presence of significant levels of strontium and also of discriminating against changes in the cation:anion $M^{2+}:SO_4^{2-}$ concentrations in the external growth medium. The morphology of the resultant crystals is dependent, to a large extent upon the external environment and can be understood from inorganic chemical principles. The extent of biological control over crystal form appears minimal.

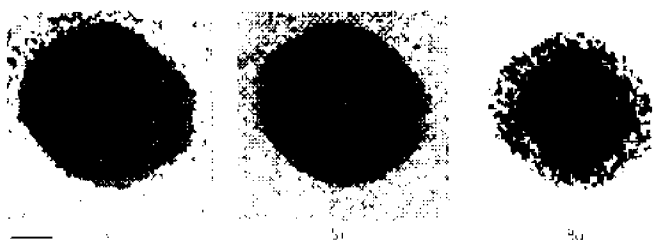

Figure 12. EDXA maps of desmid crystals initially grown in a culture containing $M^{2+}:SO_4^{2-} \leq$ 1:1 to which Sr^{2+} was added giving a $M^{2+}:SO_4^{2-}$ ratio of ~10:1. The initial crystal was rhombic in appearance but on addition of Sr^{2+} to the culture medium is now developing an hexagonal form. Black represents high concentrations. The centre of the crystal contains largely Ba^{2+} and SO_4^{2-}, the outermost regions contain significant levels of Sr^{2+}. Scale bar represents 0.25 μm.

This we believe to be in direct contrast to mineralisation in many other species where the regulation of the ionic environment is of fundamental importance in determining the precise morphology of the crystals formed. It is interesting to note that in acantharia, low levels of non-localised barium are present throughout the structure. SPM data indicates a level of ~1%.

(4) External stresses as morphology regulators - the role of membrane and filaments in the development of morphological form.

Acantharia

In acantharia, mineralisation of strontium sulphate occurs intracellularly within membrane bounded vesicles which are themselves subject to external stresses from cell membranes and filaments which are spatially organised with respect to the developing spicules, Figure 1. An idealised drawing showing the development of a single spicule is shown in Figure 13. The chemistry of the mineral phase is totally prescribed (there is only one crystalline allotrope of strontium sulphate) and the supply of material is largely a matter of transport e.g. Sr^{2+} and SO_4^{2-} and not of metabolism. We note again that the crystal habit is not that observed *in vitro* and the spicule morphology is species specific (Schewiakoff 1926). In trying to understand how such a morphology (20 'apparently' equivalent spicules radiating from a central point with D_{4h} symmetry) might arise, we have considered the competition between crystallochemical and biological controls on morphology (section 1) and will now consider the possible effects of membranes and filaments on the development of morphological features. The argument is presented in great detail in an article by Perry *et al.* (1988). A consideration of early growth stages in acantharia (Schewiakoff 1926) showed that single cell morphology, for these organisms may be decided quite early in growth if the spicule or filament growth rate is more rapid than the growth rate of the whole cell. The growth of crystals inside vesicles can only continue if the vesicle also continues to grow. If the growth rate of the vesicle and the developing spicular crystal is more rapid than general cell growth then at an early stage in development the vesicle will hit the cell membrane. Interestingly, the crystal continues growth with the same habit and it appears that (a) a shape is forced upon the cell, and (b) all further growth is of the system as a whole, "equilibrium growth" of all components. There must be an interactive balance between all components if 'shape' is to be maintained (Williams 1988) as growth of one component would result in the development of stress fields for the others, e.g. mineral growth could produce stresses on membrane and filament components or, membrane and filament positions may have an effect on crystal morphology. When cell growth, including membranes and filaments, terminates, the shape of the cell could remain fixed- as during the "equilibrium growth" stage. If the supply of ions, Sr^{2+} and SO_4^{2-}, to the mineralising site continues, then crystal growth would take place in regions of least resistance resulting in (a) curved mineral structures under the restraining cortical membrane and muscular myoneme structures Figure 14a, or (b) a rectilinear grid of mineral deposited under apparent "inorganic/crystallochemical" control

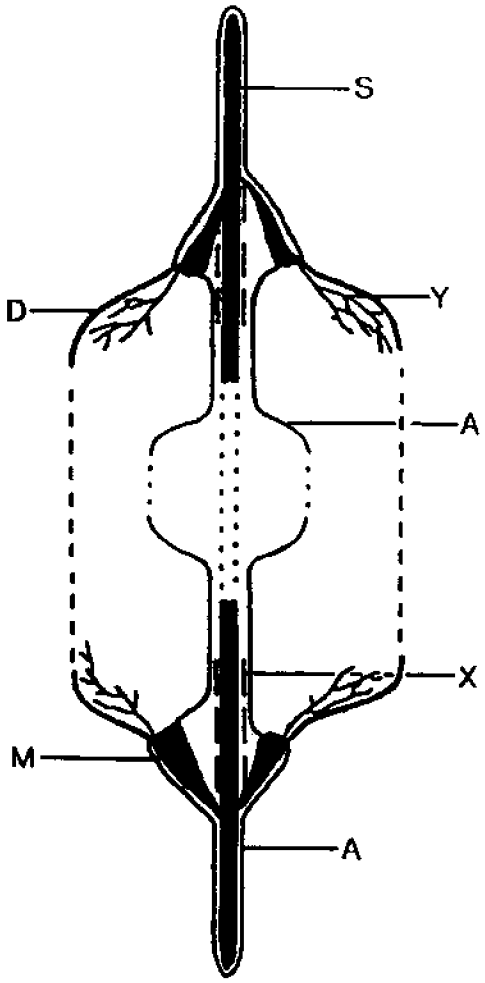

Figure 13. Schematic diagram showing the effects of cell filaments and membranes on spicule growth. S = spicule enclosed within a vesicle membrane. A = cytoplasmic membrane, D = cortex membrane, Y = cortex filaments, X = tubulin filaments and M = myoneme (muscular structure).

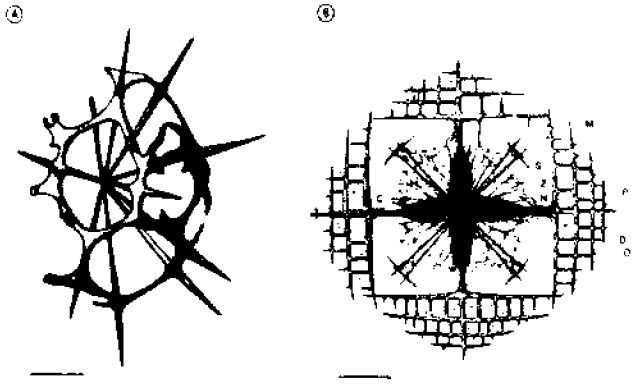

Figure 14. a) Part of an acantharian species with skeletal growth orthogonal to the spicule axes and curving under the restraining cortical membranes and muscular myoneme structure, which are not shown. Bar represents 50 μm. Reproduced with permission from Schewiakoff (1926). b) acantharian species with skeletal growth on a rectilinear grid just outside the muscular myonemes and external to the cortical membrane. M = myoneme, C = capsular membrane, P = pseudopodia, D = cortex membrane, O = axoneme, S = spicule, Z = zooxanthellae, N = nucleus. Adapted from Schewiakoff (1926). Bar represents 100 μm.

external to the muscular myoneme and cortical membrane system, Figure 14b.

The proposed argument is that the driving forces in the determination of cell morphology are chemical production and pumping (genetic control) ⟶ crystal growth in membrane bounded vesicle ⟶ membrane (filament) restraints on growth ⟶ molecule rearrangements (giving rise to lateral anisotropy) in membranes ⟶ new stress field ⟶ morphology.

It may then be that an initial action (the formation of a vesicle with a growing crystal inside it) can generate a morphology without further complex genetic instruction except in the supply of materials. We may suppose that as well as cell shape this morphology includes (a) filament lengths, (b) membrane curvature, and (c) disposition of proteins and other chemicals in the membrane. Our statement is then that biogenic crystal morphology can be used to follow the force fields in a cell.

Desmids

The relative contributions of physical (including crystallographic) and biological control over crystalline mineralisation processes can vary widely. An interesting comparison with the strontium sulphate acantharian skeleton are the crystals of isostructural barium sulphate found in the vacuoles of desmids. In desmids, filaments and microtubules are absent from the site of mineralisation (Pickett-Heaps 1983) and the crystal morphology is similar to that observed *in vitro*. The level of biological control is minimal and the crystal form appears to be principally controlled by inorganic/physical crystallochemical stresses. The barium sulphate crystals so formed bear no morphological relationship to the cell in which they grow. This substantiates the idea that filaments and microtubules must play a major role in determining mineral morphology in species such as acantharia.

General Conclusions

In this article we have attempted to show that in general, the development of morphological features at both the molecular and microscopic levels do not arise from genetic factors alone or indeed simply as a result of 'apparently' simple chemical (organic matrix or inorganic) interactions. In order to understand how the inorganic solid state, (including both crystalline and amorphous mineral forms) is regulated and organised by biology we must consider the relative importance of (1) inorganic crystal/structural chemistry, (2) organic matrices, (3) ionic environment and (4) membrane and filament effects at all stages of development of the mineral phase. The relative importance of each of the factors (1) through (4) at any specific point in mineral formation may be of vital importance in determining the mineral morphology which results.

Acknowledgements

The authors would like to thank Professor R.J.P. Williams F.R.S. (Inorganic Chemistry Laboratory, Oxford) for stimulating discussion of the subject matter presented in this article and Mr. N.P. Hughes for allowing us to publish Figures 8d and 8e. We wish to acknowledge the permission of the Radcliffe Science Library, Oxford to reproduce Figures 14a and 14b from the paper by Schewiakoff (1926). J.R.W. is in receipt of an SERC studentship.

References

Addadi, L. and S. Weiner. 1986. Interactions between acidic macromolecules and structured crystal surfaces. Stereochemistry and Biomineralisation. Mol. Cryst. Liq. Crystal. 137:305-322.

Hodson, M.J., A.G. Sangster and D.W. Parry. 1984. An ultrastructural study of the development of silicified tissues in the lemma of *Phalaris canariensis* L. Proc. Roy. Soc. Lond B222:413-425.

Hughes, N.P., C.C. Perry, R.J.P. Williams, F. Watt and G.W. Grime. 1988. A scanning proton microprobe study of stinging emergences from the leaf of the common stinging nettle *Urtica dioica* L. Nucl. Instr. Meth. B30:383-387.

Iler, R.K. 1979. The Chemistry of Silica. John Wiley, New York. 866 pp.

Lowenstam, H.A. 1981. Minerals formed by organisms. Science 211:1126-1131.

Lowenstam, H.A. and S. Weiner. 1983. Mineralisation by organisms and the evolution of biomineralisation. In: P. Westbroek and E.W. de Jong (eds.) Biomineralisation and Biological Metal Accumulation. Dordrect: Reidel. p. 191-203.

Mann, S. 1983. Mineralisation in biological systems. Struct. and Bond. 54:125-174.

Mann, S. 1987. High resolution structural and analytical studies of biominerals. Life Chem. Reports, 4:219-272.

Mann, S. and C.C. Perry. 1986. Structural aspects of biogenic silica. In: D. Evered and M. O'Connor (eds), CIBA Foundation Symp. 121, Silicon Biochemistry. John Wiley, p. 40-58.

Mann, S.; C.C. Perry, R.J.P. Williams, C.A. Fyfe, G.C. Gobbi and G.J. Kennedy. 1983. The characterisation of the nature of silica in biological organisms. J. Chem. Soc. Chem. Commun. 168-170.

Perry, C.C. and S. Mann. 1988. Aspects of biological silicification in the origin of ocean chemistry and its significance to biomineralisation. In: R.E. Crick. (ed.) 5th Int. Symp. Biomin., in press.

Perry, C.C., S. Mann and R.J.P. Williams. 1984a. Structural and analytical studies of the silicified macrohairs from the lemma of the grass *Phalaris canariensis* L. Proc. Roy. Soc. Lond. B222:427-438.

Perry, C.C., S. Mann, R.J.P. Williams, F. Watt, G.W. Grime and J. Takacs. 1984b. A scanning proton microprobe study of macrohairs from the lemma of the grass *Phalaris canariensis* L. Proc. Roy. Soc. Lond. B222:439-445.

Perry, C.C., J.R. Wilcock and R.J.P. Williams. 1988. A physicochemical approach to morphogenesis: the roles of inorganic ions and crystals. In: P.S. O'Shea (ed.) The Biophysical and Biochemical Basis of Morphogenesis, Birkhauser Verlag, Basle. 44:638-650.

Perry, C.C., R.J.P. Williams and S.C. Fry. 1987. Cell wall biosynthesis during silicification of grass hairs. J. Plant Physiol. 126:436-448.

Pickett-Heaps, J.D. 1983. Morphogenesis in desmids: our present state of ignorance. Modern Cell Biology 2:241-258.

Schewiakoff, W. 1926. Die acantharia des Golfes von Neapel. Fauna u. Flora, Neapel, 376, Monogr. Berlin. G. Berdi, Roma und Friedlander und Sohn, Berlin.

Simkiss, K. 1986. The process of biomineralisation in lower plants and animals-an overview. In: B.S.C. Leadbetter and R. Riding (eds.)Biomineralisation in lower plants and animals. Clarendon Press, Oxford. p. 17-37.

Watt, F. and G.W. Grime. 1987. Editors of Applications of high energy ion microbeams, Adam Hilger, Bristol. 399pp.

Wilcock, J.R., C.C. Perry, R.J.P. Williams and R.F.C. Mantoura. 1988. Crystallographic and morphological studies of the celestite skeleton of the acantharian species *Phyllostaurus siculus*. Proc. Roy. Soc. Lond. B, 233:393-405.

Wilcock, J.R., C.C. Perry, R.J.P. Williams and A.J. Brook. Structural and analytical studies on barium sulphate crystals in desmids. In preparation.

Williams, R.J.P. 1984. An introduction to biominerals and the role of organic molecules in their formation. Phil. Trans. R. Soc. Lond. B304:411-424.

Williams, R.J.P. 1989. The functional form of biominerals. In: S. Mann, J. Webb and R.J.P. Williams (eds.) Chemical Perspectives on Biological Mineralisation. ed. VCH, Weinheim, W. Germany. to be published.

Carole Perry is a Lecturer in chemistry at Brunel, the University of West London in England. She received the B.A. in 1982 and the Ph.D. in 1985, both in chemistry at Oxford. Her research has emphasized mechanisms of silicification, with a recent focus on the relationship between the organic and inorganic phases. Carole's interests also encompass mineralization phenomena in general, including environmental relationships, morphogenesis, and the nature of composite materials.

Chemical Aspects of Regulation of Mineralization. C.S. Sikes and A.P. Wheeler, editors, University of South Alabama Publication Services, Mobile, Alabama, 1988.

Covalent Binding of Aminopropanehydroxydiphosphonate to Prevent Cardiovascular Calcification

Catherine L. Webb, MD, Frederick J. Schoen, MD, Ph.D. and Robert J. Levy, MD.

Section of Cardiology, Department of Pediatrics, University of Michigan Medical Center, R-5014 Kresge II, Box 0576, Ann Arbor, Michigan 48109

ABSTRACT

Calcification of bioprosthetic heart valves (BPV) fabricated from either glutaraldehyde pretreated bovine pericardium or porcine aortic valves is the most frequent cause of their clinical failure. Aortic homografts have also been noted to undergo calcific degeneration after clinical implantation. Implant calcification occurs more rapidly in young children and adolescents. The pathophysiology of this disease process in BPV's involves calcium phosphate crystal growth within devitalized cells and collagen fibrils, and is accentuated by mechanical stress. In addition, aortic homograft calcification is also associated with elastin present in the aortic wall as well as collagen. Investigations in our laboratory have focused on methods of biomaterial pretreatment for preventing pathologic calcification. For this purpose, the use of the compound aminopropanehydroxydiphosphonate (APDP), which covalently binds to residual aldehyde groups, has shown promising results in preventing calcification in both pericardial bioprosthetic tissue and aortic homograft tissue.

Introduction

The general problem of cardiovascular calcification both of native and bioprosthetic heart valves, as well as vascular tissue and components of artificial hearts presents a major challenge for current research. Glutaraldehyde pretreated bioprosthetic heart valves (BPV) fabricated from either bovine pericardium or porcine aortic valves are in widespread use today. An estimated 500,000 have been implanted worldwide to date and an additional 100,000 will be implanted in the next year (Schoen 1987). Characteristics such as their non-thrombogenicity and central orifice flow dynamics make bioprosthetic valves preferable in these respects when compared to mechanical valves (Schoen 1987). However, the problem of calcification has limited the widespread use of bioprostheses to date.

Figures 1a and 1b illustrate unimplanted bioprosthetic heart valves fabricated from a glutaraldehyde pretreated porcine aortic valve which is sewn onto a stent and then mounted on a sewing ring which is covered with Dacron cloth. After surgical implant, stiffening of the valve cusps due to calcific deposits may cause valvular stenosis, while ulceration and tearing of the cusps leads to valvular regurgitation. In Figures 1c and 1d, calcium nodules can be seen in areas of maximal leaflet stress along with tissue tears which caused clinical failure of the explanted valve as illustrated.

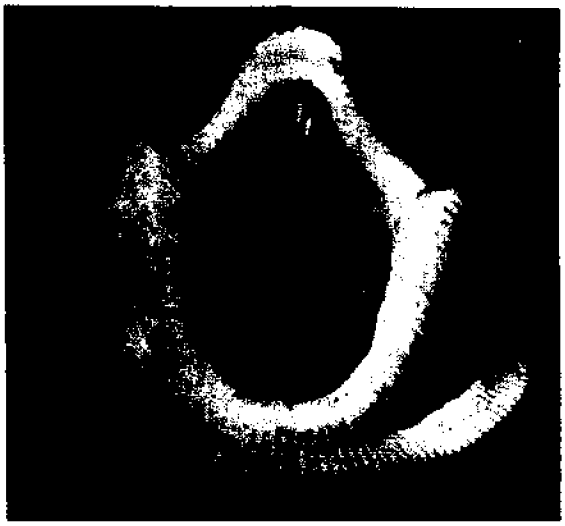

Figure 1a. Unimplanted, stent mounted porcine aortic valve prosthesis (reprinted with permission from Schoen and Levy 1984).

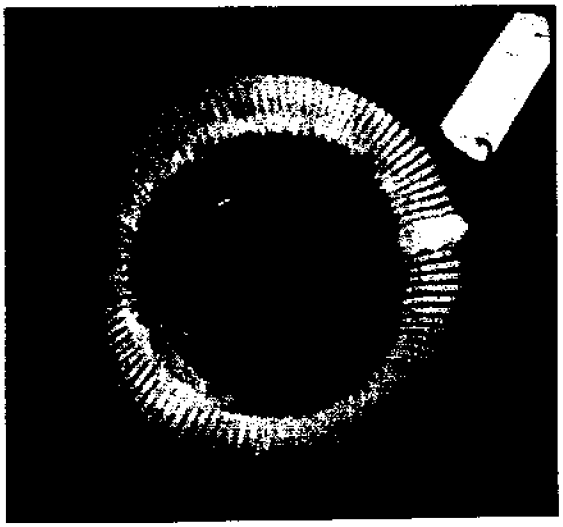

Figure 1b. Unimplanted, stent mounted porcine aortic valve prosthesis. View of the inflow side.

Figure 1c. Calcified explanted bioprosthesis with cuspal tear.

Figure 1d. Radiograph of valve specimen illustrated in Figure 1c. Calcium appears bright white. (Figures 1c and 1d reprinted with permission from Schoen and Hobson 1985).

Calcium deposition has been shown to occur more rapidly in BPV's implanted in young children and adolescents. Approximately 50% of BPV's implanted in young children required replacement for clinical degeneration within 5 years of implant, whereas less than half of BPV's implanted in adults required replacement after 10 years (Schoen 1987).

The flow diagram shown in Figure 2 depicts the pathophysiologic processes which lead to clinical valve failure. Glutaraldehyde pretreatment is necessary for tissue sterilization and *in vivo* stabilization as a result of structural protein crosslinking; however, glutaraldehyde is also an important prerequisite for the beginning of pathologic calcification in BPV. As Figure 2 illustrates, host factors such as young age, and implant factors - - the most important of which are glutaraldehyde pretreatment and mechanical stress - - interact to cause formation of calcium phosphate microcrystals in individual cells and on collagen fibrils. With time, these crystals grow in size and number, eventually coalescing into nodules which can cause stiffening of the valve and/or tears in the valvular tissue leading to valvular stenosis, regurgitation and eventual clinical failure.

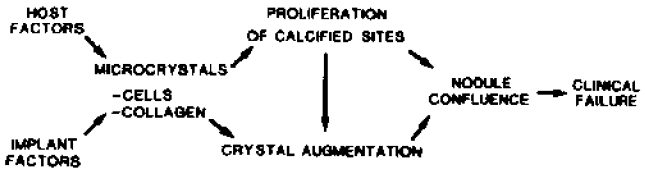

Figure 2. Schematic representation of the pathophysiology of bioprosthetic heart valve calcification (Reprinted with permission from Schoen *et al.* 1985).

Aminopropanehydroxydiphosphonate (APDP) (Figure 3), which is an analogue of pyrophosphoric acid, has been shown to be effective in inhibiting calcium deposition in BPV tissues (Levy *et al.* 1985; Webb *et al.* 1987). Its mechanism of action is related to glutaraldehyde induced structural protein crosslinks in the BPV tissue. Figure 3 shows a schematic drawing of a bioprosthetic heart valve illustrating our hypothesis of the method of APDP binding to residual aldehyde groups in glutaraldehyde pretreated tissue. Initially, the valve is treated with glutaraldehyde which covalently binds primarily to lysine and hydroxylysine residues of collagen, forming crosslinks which provide tissue stability and leaving residual aldehyde groups which are then available for binding to the APDP. The amino group of the aminodiphosphonate covalently binds to the residual aldehyde groups via a Schiff base type reaction illustrated in step 2. Deposition of calcium phosphate may then be sterically inhibited by the bulky, negatively charged tail of the bound APDP molecule.

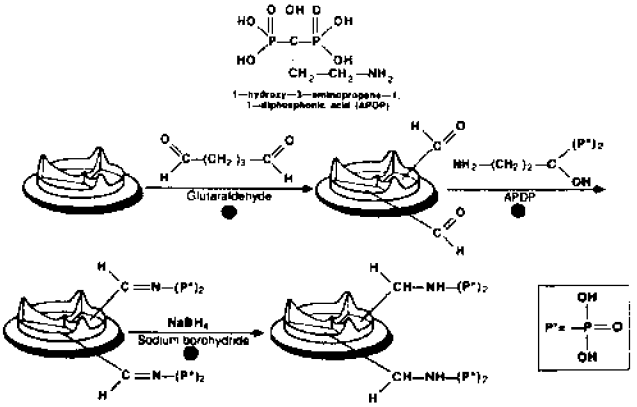

Figure 3. Schematic drawing illustrating the method of APDP binding to residual aldehyde groups in glutaraldehyde pretreated tissue. $NaBH_4$ subsequently stabilizes the APDP-glutaraldehyde bond. See text for details (modified from Webb *et al.* 1987).

Because of the tendency for the Schiff base to undergo hydrolysis to the aldehyde and primary amine, we further hypothesized that stabilization of this bond would occur with reduction by sodium borohydride, where the borohydride is the hydrogen donor. This is shown in step 3 of the sequence.

Using C-14 radiolabeled APDP, we explored the mechanism of APDP binding, its tissue stability and the effectiveness of BPV calcification prevention using the *in vivo* rat subdermal implant model. The ability of $NaBH_4$ to stabilize tissue bound APDP was studied in an *in vitro* system.

Survey of Methodology

Rat subdermal implantation of bioprosthetic tissue has provided a useful model to assess BPV calcification and the effect of APDP in the prevention of this pathologic process. This *in vivo* animal model has been shown to mimic the pathologic calcification found in failed circulatory implants. It also provides an accelerated example of calcification. BPV tissues implanted for twenty-one days in rats show approximately 100 μg/mg calcium which is comparable to the mean BPV tissue calcium levels found in explanted bioprosthetic valves removed for clinical failure (Schoen *et al.* 1987). When calcification characteristics of bovine pericardium and porcine aortic valve leaflets were compared, no difference in calcification between the two tissues was observed (Levy *et al.* 1983; Schoen *et al.* 1986). Therefore, we currently use bovine pericardium in our studies. In addition, due to a renewed interest in the clinical use of valved aortic homograft tissue, we have very recently begun to use the rat subdermal model to explore the calcification characteristics of rat aortic homograft tissue.

Specimens of bovine pericardium were initially incubated in 0.2% glutaraldehyde for 7 days at 25°C, then washed and incubated at 25°C at varied pH and incubation durations in

0.14 M C-14 APDP or 0.05M HEPES buffer for controls. Rat aortic homograft tissue was incubated only in 0.004M APDP for 30 minutes at 37°C. The methodology of the rat subdermal implantation has been previously described (Levy *et al.* 1985). Explanted tissue was analyzed for calcium by atomic absorption sprectroscopy (Schoen *et al.* 1986) and for C-14 APDP by liquid scintillation counting (Webb *et al.* 1987). To study homograft calcification, thoracic aortas were removed from large (300-400 gm) male CD rats, pretreated with APDP or control solution and implanted subdermally in weanling rats as previously described.

Studies exploring the stabilizing effect of $NaBH_4$ on the APDP-glutaraldehyde bond were carried out *in vitro* (Webb *et al.* 1988). Glutaraldehyde pretreated bovine pericardial tissue was incubated in C-14 APDP or control buffer and then placed in .05 M HEPES buffer at 25°C. Tissue was removed at various time points up to 6 months, and counted for C-14 radioactivity in a liquid scintillation counter (Webb *et al.* 1988).

Results and Discussion

In general, APDP pretreatment of both rat aortic homograft tissue and glutaraldehyde preserved bovine pericardium resulted in profound inhibition of tissue calcification (Table 1). In addition, $NaBH_4$ reduction stabilized the APDP-glutaraldehyde bond (Figure 4). Finally, no adverse effects on rat growth or bone morphology could be detected after subdermal implantation of tissue preincubated in APDP.

Table 1 Explanted Tissue Levels of Calcium (Ca++) and Aminodiphosphonate (APDP)

TISSUE	N	APDP(nM/mg)	Ca++(μg/mg)
Rat Aortic Homograft			
unimplanted	5	—	0.77 ± 0.11
control	10	—	76.7 ± 26.5
APDP pretreatment (0.004M)	10	2.48 ± 0.37	1.8 ± 0.3
Bioprosthetic Leaflet (Bovine Pericardium)			
unimplanted*	5	—	1.2 ± 0.1
control	10	—	93.64 ± 11.65
APDP pretreatment (0.14M)	10	15.33 ± 0.69	5.54 ± 2.08

*Data from Schoen *et al.* (1986).

Previous results of studies which assessed APDP binding to bovine pericardial tissue and its subsequent anticalcification effects showed that profound inhibition of calcification occurred when $\geq$ 30 nM APDP/mg was bound to the tissue. APDP binding was pH and incubation duration dependent, with greater amounts of APDP bound after longer incubation times and at higher pH. There was a concomitantly greater inhibition of calcification with increasing levels of bound APDP when compared to controls (Webb *et al.* 1987; 1988).

$NaBH_4$ reduction was found to stabilize the APDP-glutaraldehyde covalent bond in *in vitro* studies (Figure 4). There was a significantly greater tissue incorporation of APDP at each time point with $NaBH_4$ reduction. *In vitro* incubation at acidic

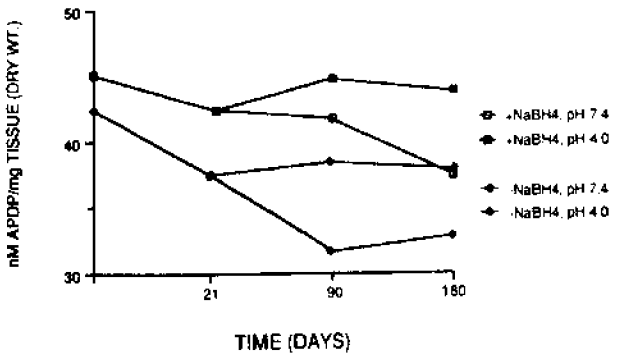

Figure 4. Effect of $NaBH_4$ on the stability of the APDP-glutaraldehyde bond (reprinted with permission from Webb *et al.* in press).

pH also favored greater APDP retention. Importantly, in both the borohydride and non-borohydride treated groups, the aminodiphosphonate appeared to leach out of the tissue with time, at physiologic pH (Webb *et al.* 1988).

Rat aortic homograft tissue preincubation in a very dilute solution of APDP (0.004M) was also found to prevent calcification. Table 1 compares the levels of APDP and calcium in explanted bovine pericardial and rat aortic homograft tissue. Of note is the profound inhibitory effect of APDP even at very low levels in explanted tissue as seen in the homograft tissue.

A common structural protein to both bovine pericardium and porcine aortic valves is collagen, which has few native crosslinks and requires glutaraldehyde stabilization before clinical implantation. Although the mechanism of APDP binding to glutaraldehyde crosslinked bovine pericardial tissue is thought to occur by APDP covalently binding to residual aldehyde groups bound to collagen, the method of binding to homograft tissue is not as well worked out. Aortic homograft tissue also contains collagen, and a unique feature of this tissue is the presence of the structural protein, elastin, a naturally highly crosslinked molecule. A preliminary hypothesis for the mechanism of APDP binding to non-glutaraldehyde treated homograft tissue involves these natural crosslinks in which semialdehydes may become available for binding APDP as a result of the intermediary action of lysyl oxidase (Lehninger 1982). The inherently high number of elastin crosslinks in aortic homograft tissue may therefore provide sufficient binding sites for APDP without glutaraldehyde stabilization. This concept was supported by our data on homograft tissue included in Table 1. Even though the homograft tissue was not treated with glutaraldehyde, a sufficient amount of APDP was bound to the tissue to profoundly inhibit calcification, compared to the severely calcified control group.

The data related to NaBH4 stabilization of the APDP-glutaraldehyde bond in bovine pericardium (Figure 4) is thought provoking in the sense that it showed a loss of tissue bound APDP with time. This would imply that the onset of calcification is only delayed by APDP and may not be prevented in the long term. Therefore, a method of sustained drug delivery may need to be developed to insure freedom from calcification in the long term. Current studies in our laboratory are focused on the combined approach of BPV tissue pretreatment with APDP and subsequent tissue implantation of controlled release matrices.

In conclusion, APDP effectively inhibited calcification of glutaraldehyde pretreated bovine pericardium as well as rat aortic homograft tissue. NaBH4 stabilized the APDP-glutaraldehyde tissue bond. No adverse effects were detected on rat growth or bone morphology after local delivery of APDP. Finally, because

APDP was noted to leach out of the BPV with time, a combined approach of APDP pretreatment and controlled release may be necessary for effective, long term inhibition of pathologic tissue calcification.

Acknowledgments

This work was supported in part by NHLBI grant #5 R01 HL36574-01A1 (Dr. Levy) and an American Heart Association of Michigan fellowship award 1986-88 (Dr. Webb). Dr. Levy is an Established Investigator of the American Heart Association. We gratefully acknowledge the expert secretarial assistance of Catherine M. Wongstrom and the expert technical assistance of James Boyd.

References

Lehninger, A.L. 1982. Principles of Biochemistry. Worth Publishers, Inc., New York.

Levy, R.J., F.J. Schoen, J.T. Levy, A.C. Nelson, S.L. Howard, and L.J. Oshry. 1983. Biologic determinants of dystrophic calcification and osteocalcin deposition in glutaraldehyde preserved porcine aortic valve leaflets implanted subcutaneously in rats. Am. J. Pathol. 113:143-155.

Levy, R.J., M.A. Hawley, F.J. Schoen, S.A. Lund, and P.Y. Liu. 1985. Inhibition of diphosphonate compounds of calcification of porcine bioprosthetic heart valve cusps implanted subcutaneously in rats. Circulation 71(2):349-356.

Schoen, F.J. 1987. Cardiac valve prostheses: review of clinical status and contemporary biomaterials issues. Jour. Biomed. Mat. Res. Applied Biomaterials 21 (A1): 91-117.

Schoen, F.J. and C.E. Hobson. 1985. Anatomic analysis of removed prosthetic heart valves: Causes of failure of 33 mechanical valves and 58 bioprostheses, 1980 to 1983. Human Pathology 16(6):553.

Schoen, F.J. and R.J. Levy. 1984. Bioprosthetic heart valve failure: Pathology and pathogenesis. Cardiology Clinics 2(4):719.

Schoen, F.J., R.J. Levy, A.C. Nelson, W.F. Bernhard, A. Nashef and M. Hawley. 1985. Onset of progression of experimental bioprosthetic heart valve calcification. Lab. Investigation 8(5):531.

Schoen, F.J., J.W. Tsao, and R.J. Levy. 1986. Calcification of bovine pericardium used in cardiac valve bioprostheses. Implications for the mechanisms of bioprosthetic tissue mineralization. Am. J. Pathol. 123(1):134-145.

Schoen, F.J., J.L. Kujovich, C.L. Webb, and R.J. Levy. 1987. Chemically determined mineral content of explanted porcine aortic valve bioprostheses: correlation with radiographic assessment of calcification and clinical data. Circulation 76(5):1061-1066.

Webb, C.L., J.J. Benedict, F.J. Schoen, J.A. Linden, and R.J. Levy. 1987. Inhibition of bioprosthetic heart valve calcification with covalently bound aminopropanehydroxydiphosphonate. Transaction Am. Soc. Artif. Internal Organs 10(3):592-595.

Webb, C.L., J.J. Benedict, F.J. Schoen, J.A. Linden, and R.J. Levy. 1988. Inhibition of bioprosthetic heart valve calcification with aminodiphosphonate covalently bound to aldehyde groups. Ann. Thorac. Surg., 46(3):309-316.

Dr. Webb is a staff pediatric cardiologist in the Section of Cardiology, Department of Pediatrics, University of Michigan Medical Center, Ann Arbor, Mich. She received her undergraduate degree from Smith College, Northampton, Mass., and her M.D. from the Medical College of Ohio, Toledo, OH. Her clinical training in pediatrics and cardiology was completed at the University of Michigan. She is currently conducting research on prevention of bioprosthetic heart valve calcification in the laboratory of Robert J. Levy, MD.

Chemical Aspects of Regulation of Mineralization. C.S. Sikes and A.P. Wheeler, editors, University of South Alabama Publication Services, Mobile, Alabama, 1988.

Use of Polymers to Control Scale in Industrial Cooling Water and Boiler Water Systems

Claudia C. Pierce and John E. Hoots

Nalco Chemical Company, One Nalco Center
Naperville, IL 60566

ABSTRACT

Although cooling water and boiler water systems represent two totally different industrial environments, both systems use water soluble polymers in their treatment programs. A better understanding of how the system components interact chemically and physically is essential to optimize polymer treatment programs for both applications. Water soluble polymers should prevent precipitation of scaling salts and allow the formation of very thin, protective films on heat transfer surfaces. Factors controlling the performance of polymers in these two different environments are presented and discussed. The importance of particulate dispersion, polymer complexation and threshold inhibition on minimizing deposition of scaling salts is described. The effects of molecular weight, chemical composition and thermal stability on polymer performance are examined.

Introduction

Naturally occurring polymers, such as starch and tannins, were discovered more than a century ago to be effective sludge conditioners for boiler applications. Other natural products such as lignosulfonates and humates are still used today as dispersants and crystal modifiers. In the 1950's, synthetic polymers were introduced in the market and were used to replace the naturally occurring products. The switch was due in large part to the greater thermal stability of synthetic polymers and to their higher activity in conditioning deposit-forming precipitates. In the 1970's, the use of natural and synthetic polymers in cooling water applications as scale inhibitors and particulate dispersants had paralleled the boiler applications. However, early versions of homopolymers and copolymers were limited in their ability to handle wide-ranging conditions or a variety of foulants at the same time. Reviews of cooling and boiler water systems are available (McCoy 1981; Strauss and Puckorius 1984).

In today's non-chromate cooling water programs, polymers usually serve to minimize formation of bulk deposits, while still allowing the corrosion inhibitors to form very thin protective films on metal surfaces (Dubin 1982; Strauss and Puckorius 1984; Hoots and Crucil 1987; Smyk *et al.* 1988). Stabilized phosphate programs, for example, use inorganic phosphate to help prevent corrosion with a polymer to help control calcium phosphate precipitation. The polymer is a key element in the proper functioning of this product, because phosphate containing deposits would form otherwise. In order to choose polymers which provide this desired performance balance, it is necessary to characterize the processes leading to deposit formation and examine the effect that critical operating conditions have on polymer performance.

In boiler water applications, synthetic polymers are not only used in conjunction with carbonate, phosphate and chelant programs, but are also used alone as an all-polymer internal boiler treatment. The advantage of an all-polymer program is that it helps provide chelant equivalent clean boilers while having non-corrosive characteristics normally associated with phosphate treatments. In addition to preventing precipitation of scaling salts, an all-polymer treatment enhances the formation of a very thin, protective oxide film on the internal boiler heat transfer surfaces. Polymer performance in this program is strongly dependent on several critical parameters (molecular weight, for example) which have to be optimized in order for the program to be effective in boiler operations.

Boiler water systems operate at much higher temperatures and generally have better water quality than cooling water systems. Although these environments are very different, polymers are used in both systems to achieve the common goal of helping to maintain heat transfer surfaces clean of deposits and corrosion products. The objective of this paper is to describe in detail several factors which strongly affect polymer performance in cooling and boiler water applications, and to identify which of these factors are critical to both systems.

Methods

The specific polymer systems examined in this paper are polyacrylic acid (PAc), polyacrylamide (PAm), acrylic acid/acrylamide copolymers (Ac/Am) of different monomer ratios and physical blends of polyacrylic acid and polyacrylamide homopolymers.

Benchtop Cooling Water Activity Tests

These tests allow rapid evaluation of the performance of new materials as compared to known inhibitors. The benchtop activity tests can be carried out in a matter of hours and several tests can be conducted concurrently (Hoots and Crucil 1987; Smyk *et al.* 1988).

Calcium Phosphate Inhibition: Water containing hardness (250 ppm Ca^{+2} and 125 ppm Mg^{+2}), inhibitor (10 ppm), and orthophosphate (10 ppm) is heated to 70°C and stirred continuously. The pH is raised to 8.5 and maintained for 4 hours. The test solution is passed through a Millipore cellulose nitrate/acetate filter (refer to Figures 1-4 and Table I for pore sizes). The initial and final filtered test solutions are analyzed for orthophosphate. Performance is expressed as "Percent Inhibition" or ppm of orthophosphate in the filtered solution. Stress testing of a polymer's ability to inhibit formation and agglomeration of particulates containing phosphate salts is accomplished by changing the operating parameters (e.g. increasing temperature).

Experimental Scale Boilers

Polymer testing in boiler conditions is done in experimental scale boilers (Kelly *et al.* 1983a). Typical boiler conditions are the following:

Feedwater:	1 ppm Ca (as $CaCO_3$) 0.5 ppm Mg (as $CaCO_3$) 0.5 ppm SiO_2 (as SiO_2) 0.5-10 ppm polymer active
Boiler Water:	pH 11.0 10 ppm residual sulfite
Boiler Conditions:	1000 psig 110,000 Btu/ft^2 hr 10 concentration cycles

Percent Transport of a component C is defined as:

$$\%\text{Transport} = ([C]_{BD}/[C]_{FW}) \bullet (1/\#\ \text{cycles}) \bullet (100)$$

BD = Blowdown

FW = Feedwater

100% transport of a component means that this component is removed via blowdown, i.e., no deposition occurs on the boiler heat transfer area.

Results and Discussion

Cooling Water Applications: Polymer Optimization Studies for Calcium Phosphate Inhibition

Polymer Composition

When treating cooling waters, in which the water quality ranges from 50 to 2000 ppm total hardness expressed as calcium carbonate, the chemical composition of a polymer has a very significant effect on its ability to limit growth of particulates containing calcium and magnesium phosphates (Figure 1).

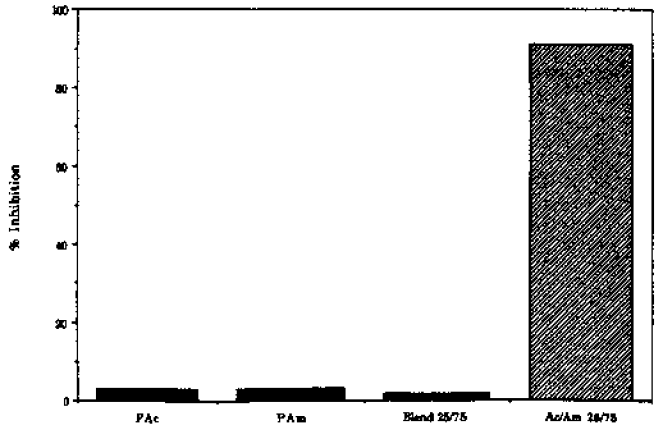

Figure 1 - % Calcium Phosphate Inhibition versus Polymer Composition (0.45 micron filter)

Homopolymers of acrylic acid (PAc) and acrylamide (PAm) were not able, to any measurable extent, to limit the growth of those particulates to less than 0.45 microns. In addition, a physical blend of polyacrylic acid and polyacrylamide (7.5 ppm and 2.5 ppm actives, respectively) performed as poorly as the individual homopolymers (PAc and PAm). However, an acrylic acid/acrylamide copolymer [Ac/Am (25/75 mole %)] shows a high level of activity for inhibiting the growth of calcium phosphate particulates to < 0.45 microns.

Within the acrylic acid / acrylamide copolymer (Ac/Am) system, the mole ratio of the mer units also has a significant effect on inhibiting the growth of phosphate salt particulates (Figure 2).

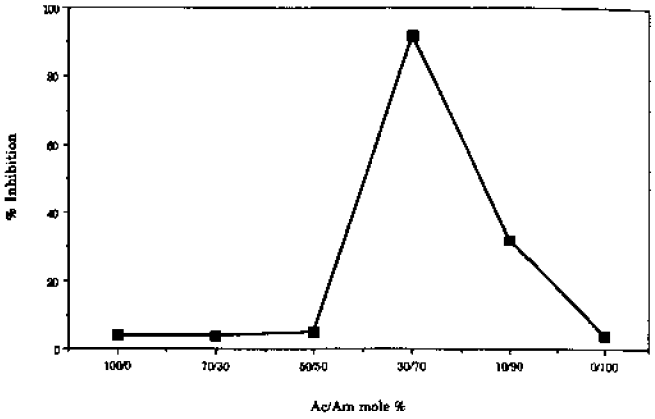

Figure 2 - Effect of Ac/Am ratio on Calcium Phosphate Inhibition (0.45 micron filter)

A high level of inhibition (≈100%) is observed with copolymers containing ≈30/70 mole % Ac/Am. As the acrylic acid/acrylamide ratio increases or decreases on either side of that optimal ratio, polymer performance drops sharply. It is clear that the chemical combination of organic functional groups within a molecule, in addition to the overall concentration and ratio of those functional groups, is essential in determining polymer performance. It is believed that polymers exhibiting "dual character" are essential in limiting particulate growth in certain scaling salts (e.g. calcium/magnesium phosphates). The dual character arises from the necessity of the polymer to adsorb onto the surface of a growing particulate and for the adsorbed polymer to help prevent agglomeration of microparticulates by interacting with the bulk solution and repelling other particulates (Tadros 1983).

Particle Size Control

The particle formation process and ability of certain Ac/Am copolymers to limit the growth of phosphate salts is exemplified in Figure 3. A decrease in percent inhibition indicates that larger amounts of particulates are being trapped by the filter. Large amounts of microparticles (<0.1 microns) are formed in the

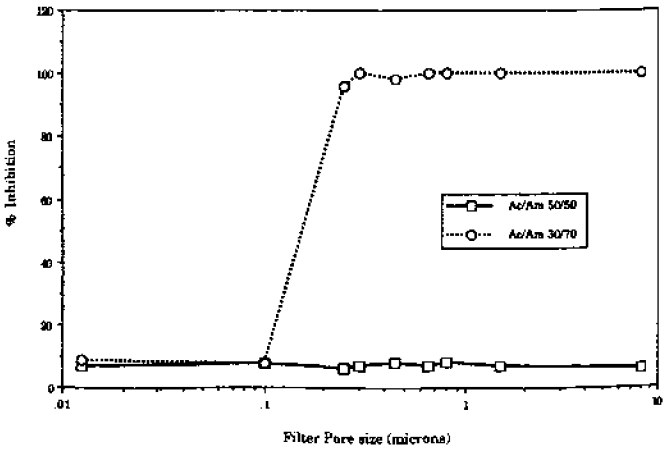

Figure 3 - Effect of Polymer Composition on Calcium Phosphate Particle Size

presence of all polymers examined to date. The effectiveness of a polymer is determined by its ability to prevent agglomeration of those microparticles. The 50/50 mole % Ac/Am copolymer exhibits no significant inhibition of particulate agglomeration as > 90% of the phosphate is incorporated into large particulates (> 8 microns diameter). In contrast, the 30/70 mole % Ac/Am copolymer limits virtually 100% of the particulates to a range between 0.1-0.22 microns. The drastic change in the ability of a polymer to prevent agglomeration of microparticulates is observed with seemingly minor changes in polymer composition.

Effect of Polymer Molecular Weight

In addition to chemical composition, the molecular weight of a polymer has a significant role in determining whether a polymer provides effective inhibition of particulate growth (Table 1). The

Table 1 Effect of Molecular Weight On Calcium Phosphate Inhibition

[Ac/Am copolymers (25/75 mole %)]

Polymer Mw	% Inhibition (0.45 micron filter)
6,000	4
19,000	91
88,000	95

polymer's molecular weight typically needs to be within an optimum range, large enough for the polymer adsorbed on the particle surface to provide an effective barrier to agglomeration and below a value which would promote flocculation processes (Tadros 1983). In the Ac/Am (25/75 mole %) copolymer system, a weight average molecular weight (Mw) of 6000 was insufficient to prevent particle agglomeration. As the Mw increases to 19,000 and 88,000 very effective inhibition of particle growth was observed. Although higher molecular weight samples of Ac/Am copolymers were not available, it is expected that flocculation will lead to a decrease in particulate growth inhibition as the molecular weight of the Ac/Am copolymer continues to increase. Polymers having a Mw higher than 50,000 are unsuitable for boiler applications due to their tendency to form insoluble calcium polyacrylate salts.

Effect of Temperature

Temperature (bulk recirculating water and heat-exchanger surface) are critical operating parameters in industrial cooling water systems. As operating temperatures increase, the ability of a polymer to inhibit particulate growth eventually decreases and the decrease in performance can be very sharp. Without a polymer present, particle formation and growth of phosphate salts occurs rapidly as temperature increases above 20°C (Figure 4). The addition of a low performance copolymer (50/50 mole % Ac/Am) does provide modest control of particle formation and agglomeration near ambient temperature, but a sharp decrease in performance is observed as the temperature exceeds 40°C. The 30/70 mole % Ac/Am copolymer provides a significant increase in the temperature range over which particle agglomeration is controlled, although performance ultimately starts to decrease as the temperature increases above 80°C. Due to its higher temperature and performance limit, the 30/70 mole % Ac/Am copolymer is viewed as being much more useful than the corresponding 50/50 mole % copolymer in industrial cooling water systems.

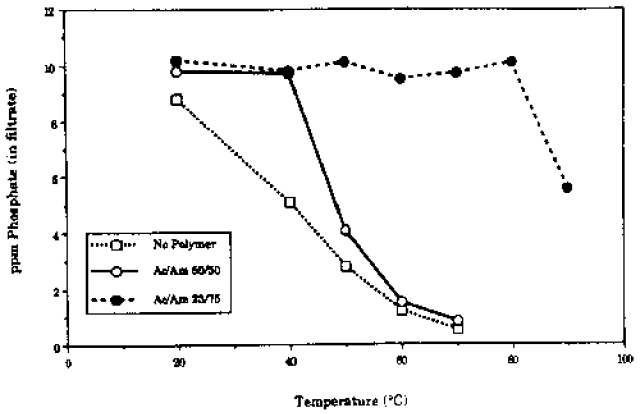

Figure 4 - Effect of Temperature on Copolymer Inhibition of Calcium Phosphate (0.45 micron filter)

Boiler Water Applications: Polymer Optimization Studies for All-polymer Treatment Program

The feasibility and effectiveness of the all-polymer treatment program for boiler applications have been demonstrated and documented (Kelly *et al.* 1983a, 1983b; Kelly 1984; Lorenc *et al.* 1984). The following sections describe in detail the parameters which have to be taken into consideration in order for an all-polymer treatment to be effective.

Polymer Thermal Stability

In contrast to cooling water systems where thermal decomposition of a polymer is usually not a problem, polymers used for internal boiler treatment should be able to maintain high performance in the high temperature and high pressure environments normally associated with boiler operations and experience a minimum amount of thermal decomposition. Polymer thermal stability was previously determined by thermogravimetric analysis in which weight loss is monitored as a function of temperature (Kelly 1984). Synthetic polymers are generally more thermally stable than naturally occurring products (Denman and Salutsky 1967) and the superior thermal stability of polyacrylic and polymethacrylic acid compared to polymaleic acid has been reported (Masler 1982).

Figure 5 shows the hydrolytic thermal stability of a synthetic acrylic acid/acrylamide copolymer as determined in a laboratory autoclave. The half-life at 252 and 285°C were found to be 8.5 days and 2.7 days, respectively. Tests performed in experimental boilers (Kelly *et al.* 1983a) have demonstrated that this copolymer has sufficient thermal stability to be practical for use in high pressure boiler systems.

Polymer Complexing Ability

Polymers containing carboxylate functionalities are not only able to disperse particulates arising from boiler contaminants, but they can also complex hardness and maintain it in a soluble

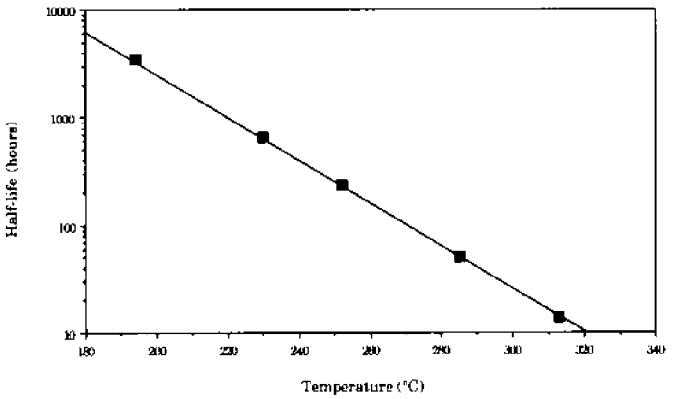

Figure 5 - Hydrolytic Thermal Stability of Acrylic Acid/Acrylamide Copolymer

form. These two different mechanisms are graphically illustrated in Figure 6 where percent calcium and magnesium transport in a boiler operating at 1000 psig is reported as a function of the polymer dosage. The hardness transport increases first at a threshold level at which the polymer acts as a dispersant and a crystal modifier. At the most preferred dosage (5-15 ppm polymer active/ppm hardness), all the hardness is complexed, transported through the boiler and eventually removed via blowdown. In the all-polymer treatment program, the polymer dosage is chosen in such a way to insure that all the hardness present in the feedwater is complexed and maintained in a soluble form (Lorenc *et al.* 1984). The complexing ability of a polymer in boiler water systems is of much greater significance than in cooling water systems in which, because of the much higher hardness content, polymers are mostly used as threshold inhibitors.

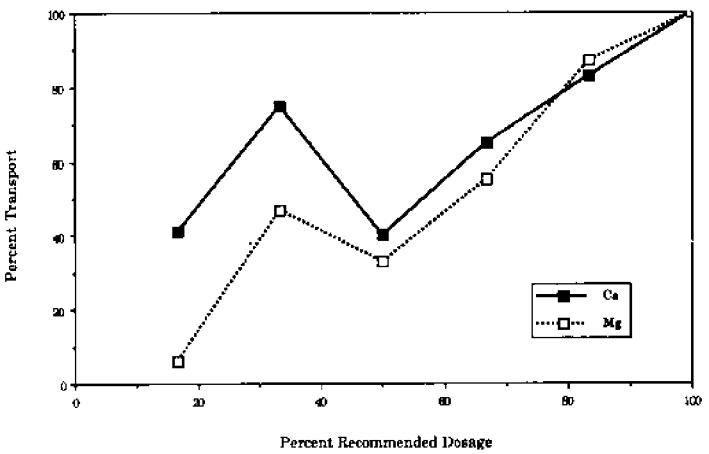

Figure 6 - Hardness Transport with Ac/Am Copolymer (All-Polymer Treatment)

Polymer Molecular Weight

As in cooling water systems, polymer performance in boiler applications can be strongly affected by the polymer molecular weight distribution (Mw). The Mw affects the polymer complexing ability and the solubility of the resulting calcium polymer salt. Increasing the polymer Mw increases the polymer's calcium binding ability (Pierce and Grattan 1988). This is due to the fact that higher molecular weight anionic polymers have a higher negative charge per molecule than lower molecular weight ones. Those characteristics are common to most carboxylate containing polymers which have been tested to date. Accordingly, one would expect that a very high Mw polymer would exhibit the highest performance because of its enhanced ability to complex hardness in the boiler. However, high Mw polymers able to complex hardness can also, if not properly dosed, form insoluble calcium polymer salts which exhibit inverse solubility. Table 2 shows how polyacrylic acid Mw influences the solubility of the corresponding calcium saturated polymer salt. Polyacrylate calcium salts, of respective Mw values of 4,000 and 100,000, were prepared in the laboratory and the relative solubility of each was measured at room temperature. Increasing the Mw of the calcium polyacrylate salt leads to a decrease in the salt solubility. Both salts also exhibit inverse solubility behavior, with their solubility decreasing as temperature increases.

Table 2 Solubility of Calcium Polyacrylate Salts

Polymer Mw	Solubility (22°C) g/l
4,000	1.84
100,000	0.80

Through extensive testings in our experimental boilers, the molecular weight of the all-polymer treatment program is optimized to maximize its calcium complexing ability and minimize calcium polymer deposition in the event that polymer underdosing occurs due to severe hardness upset conditions.

Polymer Composition

In order for an all-polymer treatment to be effective, the polymer must provide good hardness control, offer good corrosion protection of the internal boiler surface and help prevent iron oxide deposition on the heat transfer surface. Although homopolymers are able to complex hardness in boiler conditions, they are less effective in dispersing iron oxide particles, another major component in boiler water contaminants.

Iron oxide particles are returned to the boiler as corrosion products from the condensate system and, if not properly treated, can cause deposition on the internal boiler surface. For this reason polymer treatment is necessary to disperse the iron oxide particles. Dispersion occurs when polymer molecules are adsorbed on the iron oxide particles, thereby minimizing agglomeration. The level of polymer adsorption is affected by various operating conditions such as pH, temperature, hardness and competing anions (e.g. orthophosphate).

The iron dispersion ability of different polymers was evaluated using a once-through simulator for high pressure/high temperature operations. Figure 7 shows the iron transport abilities of polymers compared to a blank (no polymer treatment). All polymers are superior to the blank and polyacrylic acid is superior to polyacrylamide. However, a 90/10 mole % Ac/Am copolymer is superior to both homopolymers as well as to their physical blends.

The superior performance of certain Ac/Am copolymers as compared to polyacrylic acid, polyacrylamide and physical blends of these homopolymers is consistent with the results obtained in cooling water systems. However, as we have demonstrated, the preferred ratio of acrylic acid to acrylamide in the copolymer is dependent on the application.

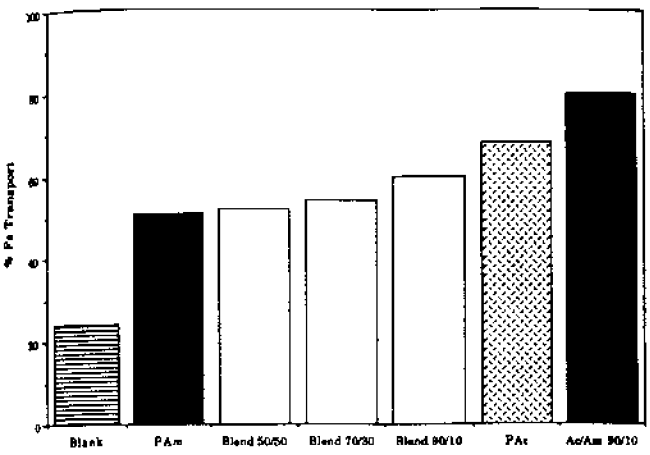

Figure 7 - % Iron Transport versus Polymer Composition

Conclusions

Many parameters control polymer performance in cooling and boiler water applications and all of them appear to be temperature dependent. In the systems tested, the Ac/Am copolymers are superior to polyacrylic acid, polyacrylamide and physical blends of these homopolymers. Other parameters which can be crucial to both applications are temperature, the polymer average molecular weight and monomer ratio. All these parameters need to be evaluated and analyzed in detail in order to optimize polymer performance in either cooling or boiler water applications.

References

Denman, W.L. and M.J. Salutsky. 1967. Boiler Scale Control with Polyacrylates and Polymethacrylates. 28th International Water Conference, Pittsburgh, Pennsylvania.

Dubin, L.D.1982. The Effect of Organophosphorous Compounds and Polymers on $CaCO_3$ Crystal Morphology. Journal of Cooling Tower Institute, 3:17.

Hoots, J.E. and G.A. Crucil. 1987. The Mechanisms of Polymers in Alkaline Cooling Water Programs. Materials Performance, 26(4):17.

Kelly, J.A., M.L. Lin, and G.W. Flasch. 1983a. Improved Control of Boiler Scaling and Corrosion with an All-Polymer Treatment Program. 44th International Water Conference, Pittsburgh, Pennsylvania.

Kelly, J.A., B.N. Nimry, and G.W. Flasch. 1983b. The Development of a New Concept in Boiler Treatment Technology. Corrosion/83, Paper No. 1, National Association of Corrosion Engineers, Houston, Texas.

Kelly, J.A. 1984. The Chemistry of Polyelectrolyte Interactions in Boiler Water Applications. Proceedings of the 10th International Conference on the Properties of Steam, Moscow, USSR, 3-7 September.

Lorenc, W.F., J.A. Kelly, and F.S. Mandel. 1984. US Patent 4,457,848.

McCoy, J.W. 1981. The Chemical Treatment of Boiler Water. Chemical Publishing Co.

Masler, W.F. 1982. Characterization and Thermal Stability of Polymers for Boiler Treatment. 43rd International Water Conference, Pittsburgh, Pennsylvania.

Pierce, C.C. and D.A. Grattan. 1988. Chemical and Physical Parameters Controlling Polymer Performance in Boiler Systems. Corrosion/88, Paper No. 205, National Association of Corrosion Engineers, St. Louis, Missouri.

Smyk, E.B. *et al.* 1988. The Design and Applications of Polymers in Cooling Water Programs. Corrosion/88, Paper No. 14, National Association of Corrosion Engineers, St. Louis, Missouri.

Strauss, S.D. and P.R. Puckorius. 1984. Cooling Water Treatments for Control of Scaling, Fouling, Corrosion. Power, 128(6):S-1.

Tadros, T.F. 1983. Solid/Liquid Dispersions. Academic Press, New York.

Claudia Pierce is a Senior Research Chemist at Nalco Chemical Company. She received the doctorate in organic chemistry at the University of Rome in Italy in 1979. She next spent one year in research with the National Committee on Nuclear Energy in Italy and then went to Argonne National Laboratory for 3 years of postdoctoral work in separation of transuranic elements before assuming her present position. Her present research deals with interactions of polyelectrolytes and metals in boiler water environments.

John Hoots also is a Senior Research Chemist at Nalco. He received the Ph.D. in inorganic chemistry at the University of Illinois in 1983. John's work centers on interactions of polyelectrolytes and metals in cooling water environments.

The following presentations were also made at the symposium. Published versions of the complete papers are available in other sources from the authors.

Mechanisms of Diphosphonate Control of Mineral Formation and Resorption

Marion D. Francis

Woods Corners Laboratories,
Norwich Eaton Pharmaceuticals, Inc.,
P.O. Box 191,
Norwich, NY 13815-0191

ABSTRACT

Endogenous substances such as pyrophosphate and osteocalcin exert a controlling influence on mineral formation in bone. This is primarily accomplished by their properties of adsorption on existing bone. Administered orally or parenterally, the geminal diphosphonates are hydrolytically stable, have strong adsorption (chemisorption) on calcium phosphate of bone, and can have profound effects on mineral resorption and accretion depending on structure and systemic load administered. To understand their biological effect on mineral resorption and formation, we studied their desorption rates from synthetic hydroxyapatite (HA) in saline and serum. Using a calculated ratio of surface adsorption area to volume of surrounding fluid or osteoid matrix, we designed a model system of HA and fluid in which both the rate of desorption and concentration of desorbed diphosphonates in the peripheral fluid could be determined. These data are presented. Perspective is given to the selective effects of various diphosphonates on bone resorption, heterotopic calcification and ossification.

Biological Inhibitors of Apatitic Crystal Growth

E.C. Moreno

Physical Chemistry Department,
Forsyth Dental Center,
Boston, MA 02115

ABSTRACT

Inhibitors of biomineralization range from very small and ubiquitous molecules such as pyrophosphate (PPi) to relatively large and unusual moieties such as the salivary acidic proline-rich proteins (PRP). The present paper shows that, in most cases, it is possible to relate parameters derived from adsorption isotherms onto hydroxyapatite to the inhibitory activity of a given molecule. In the case of pyrophosphate, such a relationship is complicated because a) a slow hydrolysis of the adsorbate takes place in the condensed state and b) there are two adsorption sites only one of which is involved in the crystal growth inhibition. Coverages, calculated from the adsorption isotherm, correlate well with the fractional decrease in the initial precipitation rates. The adsorption of PRP and synthetic polymers onto apatite is well described by a Langmuir adsorption isotherm. Inhibitor coverages correlate very well with the crystal growth inhibition of apatite by those macromolecules. It is shown that small inhibitory molecules are buried during crystal growth whereas the proteins and polymers display a different behavior. This investigation was supported by NIDR Grant DE3187.

Extracellular Matrix and Mineralization in Developing Enamel and Bone

John D. Termine

National Institute of Dental Research,
National Institutes of Health,
Bethesda, Maryland 20892

ABSTRACT

The enamel layer of developing teeth presents a hydrophobic environment in which forming hydroxyapatite crystallites grow and coalesce in a highly co-oriented manner. Acidic glycoproteins, enamelins, coat the forming crystallite surfaces and are thought to regulate lateral mineral growth. A hydrophobic intercrystalline milieu is provided by the amelogenin proteins, the major secretory product of enamel-forming cells, ameloblasts. The amelogenins comprise a heterogeneous set of molecules, rich in proline and glutamine, that arise from a single gene by alternate splicing mechanisms. The hydroxyapatite mineral of bone forms on and within collagen protein fibers that also contain a number of noncollagenous, calcium-binding proteins thought to mediate bone mineral formation and/or secondary crystal growth. One such molecule, osteonectin, is a phosphorylated glycoprotein that seems to be polyfunctional in growing body tissues.

Silicification in Siliceous Organisms and Plants: An Overview

B.E. Volcani

Scripps Institution of Oceanography,
University of California,
San Diego, LaJolla, California 92093

ABSTRACT

A condensed overview of the biological mineralization of silicon will be presented: Siliceous structures of diverse forms and architectural complexities in chrysophytes, silicoflagellates, diatoms, choanoflagellates, radiolarians, sponges, and vascular plants will be briefly described. The systems involved in the origin of the structures, and the possible mechanisms of silification will be discussed.